NASA TECHNICAL NOTE

NASA TN D-2611

A CRITICAL EVALUATION OF METHODS FOR CALCULATING TRANSPORT COEFFICIENTS OF PARTIALLY AND FULLY IONIZED GASES

by Warren F. Ahtye

Ames Research Center
Moffett Field, Calif.

NATIONAL AERONAUTICS AND SPACE ADMINISTRATION • WASHINGTON, D. C. • JANUARY 1965

A CRITICAL EVALUATION OF METHODS FOR CALCULATING TRANSPORT COEFFICIENTS OF PARTIALLY AND FULLY IONIZED GASES

By Warren F. Ahtye

Ames Research Center
Moffett Field, Calif.

NATIONAL AERONAUTICS AND SPACE ADMINISTRATION

For sale by the Office of Technical Services, Department of Commerce,
Washington, D.C. 20230 -- Price $4.00

TABLE OF CONTENTS

	Page
SUMMARY	1
INTRODUCTION	2
SYMBOLS	3
CALCULATION OF SECOND-ORDER BASIC TRANSPORT COEFFICIENTS	7
Physical Model	7
Outline of Derivation of Transport Coefficients	8
Interparticle Potentials	12
Expressions for Second-Order Basic Transport Coefficients	18
DISCUSSION OF RESULTS AND COMPARISONS	25
Basic Transport Coefficients for Partially Ionized Gases	25
Basic Transport Coefficients for Fully Ionized Gases	34
Reactive and Thermal Diffusive Components of Thermal Conductivity	38
CONCLUDING REMARKS	43
APPENDIX A - THERMODYNAMIC PROPERTIES OF PARTIALLY IONIZED ARGON	45
APPENDIX B - SHOCK-WAVE VARIABLES FOR PARTIALLY IONIZED ARGON	49
APPENDIX C - SECOND-ORDER EXPRESSIONS FOR VISCOSITY AND MULTICOMPONENT DIFFUSION COEFFICIENTS	53
REFERENCES	57
TABLE	61
FIGURES	63

A CRITICAL EVALUATION OF METHODS FOR CALCULATING TRANSPORT COEFFICIENTS OF PARTIALLY AND FULLY IONIZED GASES

By Warren F. Ahtye

Ames Research Center
Moffett Field, Calif.

SUMMARY

The basic transport coefficients of partially ionized argon have been calculated by the rigorous second-order Chapman-Enskog formulation. Comparisons were made between these values and the ones calculated by existing methods of less accuracy. The latter values for the viscosity agree with those for the second-order expression within a few percent. However, values of the second order expression for the translational thermal conductivity and for certain multicomponent diffusion coefficients are larger by 25 to 50 percent at large degrees of ionization. Values of the second order expression for the electrical conductivity are smaller by an order of magnitude at small degrees of ionization.

A comparison of the electrical conductivity values calculated by the rigorous second-order Chapman-Enskog formulation with experimental values indicates that this approach is valid for calculating electrical conductivity and further suggests that the same approach is reasonable for calculating the translational thermal conductivity.

The existing methods yield zero values for the thermal diffusion coefficients. The more exact theory used in the paper predicts appreciable effects of thermal diffusion. Comparisons of the thermal diffusion coefficients for the various species indicate that the diffusive motion of the atom and ion are strongly coupled, and are almost independent of the diffusive motion of the electron up to high degrees of ionization.

The existing method for predicting the reactive and thermal diffusive components of the thermal conductivity is inexact in many areas, the main defect being the neglect of the charge separation field. A cursory examination of the problem indicates that these two components would not be a constant for a specified temperature, but would vary in the direction of the temperature gradient, thereby increasing the complexity of the solution. Until the difficulty is resolved, accurate predictions of the last two components of the thermal conductivity for a partially ionized gas will not be possible.

The second-order values of the electrical conductivity and translational thermal conductivity for fully ionized argon are compared with those calculated by the simultaneous collision approach of Spitzer. The Spitzer approach yields thermal conductivity values which are larger by a factor of three, due to its neglect of ion-ion interactions.

INTRODUCTION

An object traveling through an atmospheric medium at low speeds has almost none of its kinetic energy converted into internal excitation of the surrounding gas molecules. As the speed is increased, the molecules undergo rotational and vibrational excitations, along with electronic excitation, then dissociation, and finally various stages of ionization. Existing methods (refs. 1 to 6) for calculating transport properties of gases at increasingly higher temperatures have undergone an analogous evolution. The basis for the calculation of transport properties is the Chapman-Enskog approach which was derived for a nonreactive mixture of monatomic gases (i.e., no internal excitation) at relatively low temperatures (refs. 7 and 8). A great amount of foresight was used in the complete formulation of the problem, for there exist terms which become appreciable only for reactive and/or ionized gases. Unfortunately, order of magnitude examinations of these terms for the case of monatomic gases near room temperature resulted in many approximations which have been retained for dissociating and ionizing gases. For polyatomic molecules the thermal conductivity was modified by the Eucken correction (ref. 8) to account for the energy exchange between the translational and internal (i.e., vibrational and rotational) modes. At higher temperatures, dissociation of the polyatomic molecules becomes a predominant effect. Butler and Brokaw (ref. 9) re-examined the Chapman-Enskog formulation for a dissociating gas, and concluded that the reaction energy must be added to the energy diffusion term. Consequently, they derived a simple expression to account for this reaction energy in the thermal conductivity. The existing methods in references 1 through 6 for calculating transport properties of a partially ionized gas contain nothing conceptually different. For example, the Butler and Brokaw expression for the reactive thermal conductivity was retained, with the ionization potential used in place of the dissociation energy.

To assess the validity of these approximate methods, the experimental and theoretical thermal conductivity of nitrogen are compared in figure 1. The experimental data were obtained from measurements in a cylindrical cascade arc by Maecker (ref. 10); the experiment was performed at atmospheric pressure for temperatures ranging as high as 15,000° K (corresponding to 50-percent ionization). A wide range of arc currents was also used. The theoretical values were calculated by the existing methods and are based on what is believed to be the most accurate intermolecular potential data. For example, the N^+-N charge-exchange cross section, recently calculated by Knof, Mason, and Vanderslice (ref. 11), is used. The arc data show fairly good agreement in the region of dissociation. This is substantiated by the shock tube experiments described in references 4 and 12, where heat transfer was measured with a thin film gage. At the point where ionization is initiated, the experimental arc values increase more rapidly than the predicted values and show no signs of peaking as predicted by the theory. At the highest temperature attained the experimental values are higher by almost an order of magnitude. However, it should be pointed out that there may be either an experimentally induced error or an unpredicted phenomenon, for the experimental values of the total thermal conductivity at a given temperature increase as the arc current is increased.

Consequently, the comparison in figure 1 should be considered as only a rough indication of the accuracy of the approximate methods for calculating transport coefficients.

These comparisons indicate that the assumptions and approximations being used for most calculations should be re-evaluated for partially and fully ionized gases. A discrepancy may be attributed to the following differences in the system: (1) The magnitude and range of intermolecular forces between charged particles are orders of magnitude greater than those between neutral particles; and (2) a much greater mass disparity exists for the interacting species due to the presence of free electrons. The results of figure 1 also point out the need for more accurate experimental data in the region of 50-percent ionization (15,000° K) where a peak is predicted, and in regions of even higher degrees of ionization where such effects as thermal diffusion of electrons may become important. Development of a cascade arc producing much higher temperatures does not appear too promising (ref. 13). However, arc-driven shock tubes operating at much lower pressures are capable of producing much higher temperatures and degrees of ionization (ref. 14).

The primary purpose of this paper is to determine whether the transport coefficients of partially and fully ionized gas can be more accurately determined by the second-order Chapman-Enskog formulation. The approach used is to start from the basic equation, the Boltzmann equation, and obtain as accurate a calculation of transport coefficients as possible. These values are then compared with those calculated by existing methods, in order to point out the magnitude of the errors incurred by the use of these methods. Numerical values are obtained by using the atomic properties of argon. The choice of argon is based on the availability of intermolecular potentials and the relative ease required for the calculation of its transport coefficients. For the transport coefficients where the quantitative theory is still wanting, a qualitative discussion will be made.

Equilibrium thermodynamic properties are essential ingredients in any experimental or theoretical investigation of transport coefficients. The calculation of the thermodynamic properties of partially ionized argon is briefly described in appendix A. Shock-wave properties can be useful for any anticipated shock-tube determination of the transport properties of partially ionized argon. The calculation of these properties is briefly described in appendix B.

SYMBOLS

a	speed of sound at zero frequency
$a_i, b_i, \ldots$	stoichiometric coefficients for components $A_i, B_i, \ldots$
A	argon atom
A^+	argon ion

b	impact parameter
c_p	specific heat per mol at constant pressure
c_v	specific heat per mol at constant density
D_{ij}	multicomponent diffusion coefficient
D_s	ambipolar diffusion coefficient
D_i^T	coefficient of thermal diffusion
$\mathscr{D}_{ij}$	coefficient of diffusion for binary mixture
e	base of natural logarithms, also electron charge
e^-	electron
E	energy per mol
E_I	first ionization potential
$\underline{E}_s$	charge separation field
f_i	velocity distribution function for single particle
f_{o_i}	Maxwellian velocity distribution function
g_i	degeneracy of ith state
g_{ij}	initial relative speed in binary system
h	Planck's constant, also Debye shielding length
h_i	enthalpy per unit mass
H	enthalpy per mol
$\tilde{H}_{ij}^{oo}$	element of viscosity determinant
I	ion
$\underline{j}$	current density
k	Boltzmann's constant
K_p	chemical equilibrium constant for pressure units
l_i	mean free path

m_i	mass of particle
M	Mach number
M_i	molecular weight per mol
n	electron quantum number, also concentration in particles per unit volume
p	pressure
p_o	reference pressure, 1 atm
p_i	partial pressure
$\underline{P}_i$	momentum flux vector
$\underline{q}$	energy flux vector
q_{ij}^{mm}	element of thermal conductivity determinant
Q	total partition function
$\tilde{Q}_{ij}^{mm'}$	element of thermal diffusion determinant
Q_p	total partition function for a standard state of unit pressure, pQ
r	distance between particles
R	universal gas constant, energy per mol per deg
S	entropy per mol
S_{i_o}	entropy per mol of component i at 1 atm pressure
T	absolute temperature
u	velocity with reference to incident shock wave
$\mathbb{U}$	unit tensor
$\underline{v}_i$	molecular velocity
V	volume
$\underline{\overline{V}}_i$	diffusion velocity
w	velocity with reference to reflected shock wave
$\underline{W}_i$	reduced velocity

x_i	mol fraction
$\underline{X}_i$	total force
Z	compressibility
γ	ratio of specific heats, $\frac{c_p}{c_v}$
γ_{ij}	reduced initial relative speed of colliding particles in binary system
ϵ	fraction of atoms which have become ionized, also constant in Lennard-Jones potential
ϵ_i	energy of the ith state
η	coefficient of viscosity
λ	total coefficient of thermal conductivity
λ_d	coefficient of thermal conductivity due to thermal diffusive effect
λ_r	coefficient of thermal conductivity due to chemical reaction
λ_t	coefficient of thermal conductivity due to atomic collision
μ	mobility
μ_{ij}	reduced mass for binary system
ν	number of species
ν_c	collision frequency
Π	consecutive product
ρ	density
σ	electrical conductivity
σ_{ij}	collision diameter
φ	intermolecular potential
χ	deflection angle
$\Omega_{ij}^{(l,s)}$	collision integral of order l,s

$\bar{\Omega}_{ij}^{(1,1)}$ diffusion cross section

$\bar{\Omega}_{ij}^{(2,2)}$ viscosity cross section

Subscripts

A	atom
e	electron
ij	binary interaction between particles i and j
i,j,. . .	particles of type i, j, . . .
I	ion
m	degree of Sonine polynomial
p	constant pressure process
ρ	constant density process
1	argon atom also initial conditions in gas medium
2	argon ion also conditions behind incident shock wave
3	electron also conditions behind reflected shock wave

CALCULATION OF SECOND-ORDER BASIC TRANSPORT COEFFICIENTS

Physical Model

Argon is a monatomic gas whose thermodynamic and transport properties are essentially determined by the effects of its 18 orbital electrons, exclusive of mass effects. In principle, excitation of any degree of ionization of these electrons can occur. For the range of temperatures and pressures described in this paper, it will be assumed that only single ionization occurs. A general study of argon plasma was made in reference 15, where it was assumed that all degrees of ionization can occur simultaneously. The analysis showed that single ionization is essentially completed before double ionization becomes appreciable. As a result, the use of the thermodynamic and transport properties in this paper should be limited, for a given pressure, to the temperature at which argon approaches the fully ionized state ($Z \leq 2.00$).

The ideal gas law

$$pV = NRT = [N(e^-) + N(A) + N(A^+)]RT \tag{1}$$

is used, where N, the number of mols, is a function of the additional particles produced by the single ionization. Equation (1) implies that the particles spend the greatest part of their time in field-free space, but that short-range interactions can occur. This assumption is violated by the existence of Coulomb forces. However, equation (1) is used throughout because the corrections are believed to be relatively small (see appendix A), and its use greatly simplifies the calculations.

Outline of Derivation of Transport Coefficients

The Boltzmann integro-differential equation is assumed to be the basis for calculating transport coefficients of a partially ionized gas. This equation specifies f_i, the distribution function for a single particle of species i. The assumption of the single particle distribution function implies that only binary collisions are considered. This assumption restricts the theory to low-density gases and also imposes a restriction that the range of intermolecular forces must be smaller than the interparticle spacing.

For equilibrium situations the distribution function is given by the well-known Maxwell-Boltzmann distribution

$$f_{o_i} = n_i \left(\frac{m_i}{2\pi kT}\right)^{3/2} \exp\left(-\frac{m_i V_i^2}{2kT}\right) \tag{2}$$

Any deviation from equilibrium (i.e., the distribution of eq. (2)) results in transport phenomena. The Boltzmann equation in its most general form is given as

$$\frac{\partial f_i}{\partial t} + \underline{v}_i \cdot \frac{\partial f_i}{\partial \underline{r}} + \frac{1}{m_i}\left(\underline{X}_i \cdot \frac{\partial f_i}{\partial \underline{v}_i}\right) = \left[\Gamma_{ij}^{(+)} - \Gamma_{ij}^{(-)}\right] \tag{3}$$

The quantity $\underline{X}_i$, the total force acting on the particle, includes any macroscopic force fields stemming from the particles in the system. One example of the latter is the electromagnetic forces due to a charge separation field. This field, in turn, is attributed to the difference in the ion and electron concentration gradients. The quantities $\Gamma_{ij}^{(+)}$ and $\Gamma_{ij}^{(-)}$ are the rates at which particles are added and removed by binary collisions from unit volume of phase space. These terms account for both elastic and inelastic collisions. Furthermore, the total macroscopic force is assumed to be much smaller than the intermolecular forces. As a result of this last assumption, charge separation effects do not enter into the expressions for the basic transport coefficients (i.e., those prescribed only by collisional processes) such as the viscosity, translational thermal conductivity, multicomponent diffusion coefficients, thermal diffusion coefficients, and the electrical conductivity. However, charge separation effects should affect macroscopic quantities such as the concentration gradients of the ions and electrons.

At this point two important simplifications are made. First, it is assumed that all collisions are elastic (i.e., no internal excitations or chemical reactions). The resulting expression for the Boltzmann equation is

$$\frac{\partial f_i}{\partial t} + \underline{v}_i \cdot \frac{\partial f_i}{\partial \underline{r}} + \frac{1}{m_i}\left(\underline{X}_i \cdot \frac{\partial f_i}{\partial \underline{v}_i}\right) = \sum \iiint (f_i' f_j' - f_i f_j) g_{ij} b \; db \; d\underline{v}_j \; d\epsilon \tag{4}$$

where the primes denote quantities after a collision. The approximate solution of this equation is vastly simplified if the force term is assumed to arise from an external source only, and is a given function of space and time.

The next step is to expand the distribution function in a perturbation series about the Maxwell-Boltzmann distribution, f_{o_i}. The expansion is given as

$$f_i = f_{o_i}(1 + \varphi + \ldots) \tag{5}$$

It can be seen from equation (2) that the first term in equation (5) is proportional to n^1. Chapman and Cowling (ref. 7) have shown that the second term, $f_{o_i}\varphi$, is proportional to n^0, and any third term is proportional to n^{-1}. Since we are dealing with number densities of the order of 10^{15} to 10^{20} particles per cm^3, then two terms should be sufficient to describe the nonequilibrium distribution. This form is substituted back into the Boltzmann equation (eq. (4)). One of the results of this substitution is that the perturbation function φ is linear in the derivatives $\partial T/\partial \underline{r}$, the temperature gradient, $\partial x_i/\partial \underline{r}$, the concentration gradient, and $\partial \underline{v}/\partial \underline{r}$, the gradient of the mass average velocity. The linearity implies that these gradients be small over a distance of one mean free path. For example,

$$\frac{l}{T}\frac{\partial T}{\partial x} \ll 1 \tag{6}$$

must be satisfied for the thermal conductivity to have any meaning, where l is the mean free path.

The steps leading from the Boltzmann equation to the final expressions for the transport coefficients are quite complex. The main steps can be found in reference 8. The result is that the perturbation function, φ, is expressed as a sum of integrals, where the integrands contain infinite series of Sonine polynomials. The mth Sonine polynomial of order n is defined as

$$S_n^{(m)}(x) = \frac{(-1)^j (m + n)!}{(n + j)!(m - j)!j!} x_j \tag{7}$$

where j is a dummy index, and the variable x is the square of a reduced particle velocity, $\underline{W}_i^2$, defined as

$$\underline{W}_i^2 = \frac{m_i}{2kT} \underline{V}_i^2 \tag{8}$$

The first two Sonine polynomials are

$$S_n^{(0)}(x) = 1 \tag{9a}$$

$$S_n^{(1)}(x) = n + 1 - x \tag{9b}$$

The transport coefficients are then obtained when the distribution function, which is now expressed in terms of infinite series of Sonine polynomials, is substituted into the expressions for the flux vectors and the diffusion vectors. These expressions are:

Transport of momentum $$p_{x_i} = m_i \int V_{x_i} \underline{V}_i f_i \, d\underline{V}_i \tag{10}$$

Transport of kinetic energy $$\underline{q}_i = \frac{1}{2} m_i \int \underline{V}_i^2 \underline{V}_i f_i \, d\underline{V}_i \tag{11}$$

Diffusion velocity $$\overline{\underline{V}}_i = \frac{1}{n_i} \int \underline{V}_i f_i \, d\underline{V}_i \tag{12}$$

There are also flux vectors that correspond to equation (10), transport of momentum in the y and z directions. The nine components of the three momentum flux vectors form the partial pressure tensor of the ith species. The sum of these tensors over all species gives the pressure tensor for the multicomponent mixture. Similarly, the sum of the heat flux vector (eq. (11)) over all species, gives the heat flux vector for the multicomponent mixture.

The integral in equation (12) and the sum of the integrals over species of equations (10) and (11) can be regrouped in the familiar basic transport coefficients. For example, a component of the pressure tensor of the mixture

$$\mathbb{P} = p\mathbb{U} - 2\eta\mathbb{S} \tag{13}$$

is expressed as a product of the viscosity, η, and the rate of shear tensor, $\mathbb{S}$. The diffusion velocity vector for species i

$$\overline{\underline{V}}_i = \left(\frac{n^2}{n_i \rho}\right) \sum m_j D_{ij} \, \underline{d}_j - \frac{1}{n_i m_i T} D_i^T \frac{\partial T}{\partial \underline{r}} \tag{14}$$

is expressed in terms of the multicomponent diffusion coefficients, D_{ij}, the thermal diffusion coefficients, D_i^T, and a macroscopic gradient vector defined as

$$\underline{d}_i = \frac{\partial x_i}{\partial \underline{r}} + \left(x_i - \frac{n_i m_i}{\rho}\right) \frac{\partial \ln p}{\partial \underline{r}} - \left(\frac{n_i m_i}{p\rho}\right) \left(\frac{\rho}{m_i} \underline{X}_i - \sum n_j \underline{X}_j\right) \tag{15}$$

In the last term in equation (15), the summation over species j includes the ith species. The coefficients D_{ij} and D_i^T are analogous quantities

describing the relative transfer of the different species in a multicomponent gas. The main difference is that the driving potential for D_{ij} is the concentration gradient, and the driving potential for D_i^T is the temperature gradient.

The expression for the heat flux vector of a multicomponent mixture

$$\underline{q} = -\lambda_t \frac{\partial T}{\partial \underline{r}} + \sum_i n_i h_i \underline{V}_i - nkT \sum \frac{1}{n_i m_i} D_i^T \underline{d}_i \tag{16}$$

can be expressed as the sum of three components. In turn, each of these components can be expressed as the product of an effective thermal conductivity and the temperature gradient. The first component contains the translational thermal conductivity, λ_t, and is the only component explained by simple kinetic theory (ref. 8). The second component contains the reactive thermal conductivity, λ_r, and derives its name because of the addition of the reaction energy to the enthalpy (ref. 9). This mode of heat transfer can be described in terms of a diffusion cycle. In the higher temperature region, an atom is ionized, thereby gaining the energy of ionization. Since the derivative of ion concentration with temperature is positive, the ions diffuse toward the lower temperature region. In this region, the ion recombines with an electron, thereby releasing the energy of ionization (i.e., transport of energy). The cycle is completed when the atom is forced by the atomic concentration gradient to diffuse toward the higher temperature region where the ionization process is repeated. For obvious reasons, the third component of the thermal conductivity, λ_d, is called the thermal diffusive component. Unfortunately, no simple physical picture can describe this mode of heat transport.

There are some fundamental differences between the first component and the last two components, λ_r and λ_d. Translational thermal conductivity is a phenomenon which occurs for both a pure gas and a multicomponent mixture. The last two components of thermal conductivity are observed only for a multicomponent mixture. Another distinction is that the translational thermal conductivity is completely described by binary collision effects (i.e., is a basic transport coefficient) whereas the reactive and thermal diffusive components of the thermal conductivity depend on the macroscopic quantity $\partial x_i/\partial \underline{r}$ as well.

Infinite series of Sonine polynomials are used in evaluating the basic transport coefficients for a multicomponent mixture, such as the components of the viscosity, η_i, the translational thermal conductivity, λ_t, the multicomponent diffusion coefficients, D_{ij}, and the thermal diffusion coefficients, D_i^T; hence these coefficients are all expressed in terms of ratios of infinite determinants. Since the convergence of these ratios is fairly rapid, it is necessary to consider only the first few Sonine polynomials. The expressions "first-order approximation" and "second-order approximation" stem from the fact that either the first one (eq. (9a)) or the first two (eqs. (9a) and (9b)) in the series of Sonine polynomials have been used. These two expressions will be used quite extensively in the following section.

At a point in the derivation of the basic transport coefficients, Chapman and Cowling (ref. 7) expressed the integrals containing Sonine polynomials as a linear combination of the collision integrals

$$\Omega_{ij}^{(l,s)} = \frac{2\pi kT}{\mu_{ij}} \int_0^\infty \int_0^\infty \exp(-\gamma_{ij}^2)\gamma_{ij}^{2s+3}(1 - \cos^l \chi)b \, db \, d\gamma_{ij} \tag{17}$$

where γ_{ij} is the dimensionless form of the initial relative speed, v_{ij}, between particles i and j with reduced mass μ_{ij}. The relationship between these quantities is

$$\gamma_{ij} = \sqrt{\frac{\mu_{ij}}{2kT}} v_{ij} \tag{18}$$

The other variables in equation (17) are b, the impact parameter, and χ, the angle in the center of mass coordinate system between the relative velocity vectors before and after collision. Since the quantity χ is an explicit expression of the type of intermolecular force involved (ref. 8), it is obvious that the collision integrals are also expressions of the intermolecular force effects in the Chapman-Enskog formulation.

Interparticle Potentials

This section will describe the source of the various potentials used in this calculation. The transport coefficients of argon can be calculated with a greater degree of confidence than most gases because of the availability of molecular beam scattering data for all high-temperature interactions, with the exception of those between two charged particles. These experimental scattering cross sections, in turn, are converted to interparticle potentials, $\varphi(r)$. It should be emphasized that these potentials cannot be arbitrarily used at all temperatures of interest. The criterion proposed by Amdur (ref. 16) for non-Coulombic interactions, is that the range of validity of temperatures is determined by the range of the potential energy corresponding to the measured scattering. The expression relating the potential energy and temperature is

$$\varphi(r) = kT \tag{19}$$

In fact, the validity of equation (19) can be determined in the following manner. For a given potential $\varphi = \varphi(r)$, equation (19) can be solved for the quantity $r = \sigma_{ij}$, the equivalent hard sphere diameter. The quantity σ_{ij} then will be used in the simple kinetic theory for hard sphere molecules to obtain approximate values of the viscosity and the translational thermal conductivity.[1] Comparison of these approximate values with the corresponding quantities calculated by the Chapman-Enskog formulation will determine the regime of validity of equation (19). This approach is discussed in a subsequent section of this paper.

[1]This approximation does not account for the thermal conductivity due to thermal diffusion and chemical reaction.

At temperatures below 2000° K, the only species present is neutral argon. The molecular beam apparatus cannot supply a beam of neutral argon with sufficient velocity resolution at beam velocities corresponding to this lower range of temperatures. For this reason the Lennard-Jones potential

$$\varphi_{11}(r) = 4\epsilon \left[\left(\frac{\sigma}{r} \right)^{12} - \left(\frac{\sigma}{r} \right)^{6} \right] \tag{20}$$

is used for atom-atom collisions where the constants, $\epsilon/k = 124.0^{\circ}$ K and $\sigma = 3.418$ Å, were determined from viscosity measurements ranging from 80° K to 1500° K (ref. 8). The collision integral corresponding to this form of the potential is derived in reference 8, and the result is shown in figure 2(a). For a pure substance the coefficients of viscosity and thermal conductivity are given in reference 8 as

$$\eta = \frac{5}{8} \frac{kT}{\Omega_{11}^{(2,2)}} \tag{21}$$

$$\lambda = \frac{5}{2} \frac{c_v}{m} \eta \tag{22}$$

where c_v is the specific heat at constant density for a single particle.

At temperatures between 1,500° and 5,000° K equilibrium argon has not undergone appreciable ionization, so that the transport coefficients can still be specified by equations (21) and (22). For the upper part of this temperature range, the atom-atom potential is taken from the results of a molecular beam experiment by Amdur and Mason (ref. 17). This potential is given as

$$\varphi_{11}(r) = 3.120 \times 10^{-76} r^{-8.33} \tag{23}$$

where $\varphi(r)$ is the potential energy in ergs and r is the interparticle distance in centimeters. The range of r extended from 2.18 to 2.69 Å, which corresponds to a temperature range of 21,400° to 2,600° K according to the criterion of equation (19). The form of equation (23) is the well-known inverse-power repulsive potential. The calculation of the corresponding collision integral is described in reference 18, and the results of this calculation are shown in figure 2(a). A gap in the potential data exists between 1,500° and 2,600° K. The dotted line in figure 2(a) shows the interpolated value of $\Omega_{11}^{(2,2)}$ which was used.

For temperatures higher than 5000° K ionization effects become important. The following collisions must be accounted for: atom-atom (subscript 11), ion-ion (22), electron-electron (33), atom-ion (12), atom-electron (13), and ion-electron (23). In addition to the "viscosity" type of collision integrals

of order (l,s) equal to (2,2), as defined by equation (17), the Chapman-Enskog formulation requires the "diffusion" type of collision integrals, $\Omega^{(l,s)}$, of order (l,s) equal to (1,1), (1,2), and (1,3).

The collision integrals corresponding to the potential of equation (23) are used for temperatures up to 30,000° K although the range of the data extends only to 21,400° K. The extrapolation can be justified because the amount of atomic argon in this region approaches zero for pressures as high as 100 atmospheres.

Two mechanisms are possible for atom-ion interactions. These are elastic scattering and charge exchange. Mason, Vanderslice, and Yos pointed out in reference 19 that "diffusion" type collision integrals (e.g., $\Omega_{12}^{(1,1)}$, $\Omega_{12}^{(1,2)}$, and $\Omega_{12}^{(1,3)}$) for high-temperature gases are governed by the charge exchange mechanism. They also showed that the charge exchange effects cancelled out for the "viscosity" type collision integral $\Omega_{12}^{(2,2)}$. This predominance of charge exchange seems to be substantiated by the experimental data of reference 20 where the charge-exchange cross section is larger than the elastic cross section. Consequently, the "diffusion" type collision integrals $\Omega_{12}^{(1,1)}$, $\Omega_{12}^{(1,2)}$, and $\Omega_{12}^{(1,3)}$ are derived from charge-exchange cross sections, while the "viscosity" type collision integral $\Omega_{12}^{(2,2)}$ is computed on the basis of elastic collisions.

The atom-ion potential for elastic scattering is based on the results of reference 21 and is given as

$$\varphi_{12}(r) = 8.549\times10^{-6}\exp(-r/1.968\times10^{-9}) \tag{24}$$

where $\varphi_{12}(r)$ is the potential in ergs and r the interparticle distance in centimeters. The range of r extended from 2.47 to 3.39 Å, which corresponds to a temperature range of 213,000° to 2,000° K. The calculation of the corresponding collision integral is described in reference 22, and the results of this calculation are shown in figure 2(b).

The charge-exchange collision integrals are based on the experimental charge cross sections given by Cloney, Mason, and Vanderslice in reference 21. In this particular instance the collision integral can be expressed directly in terms of cross-section data as a result of the following conclusion reached by Mason, Vanderslice, and Yos in reference 19. The "diffusion" cross section,

$$Q^{(1)} = 2\pi\int_0^\infty (1 - \cos\chi)b\ db \tag{25}$$

approaches a value of twice the charge-exchange cross section at high temperatures. For cross-section data that can be fitted to an expression of the form

$$Q_{12} = (A - B\log_{10} v)^2 \tag{26}$$

where Q_{12} is the charge-exchange cross section (cm^2) for a velocity v (cm/sec), the relation between the collision integrals and the constants A and B is

$$\Omega^{(1,1)} = \frac{kT}{2\pi\mu}\left[(39.84B^2 - 17.85AB + 2A^2) + (8.923B^2 - 2AB)\log_{10}\frac{T}{M} + \frac{1}{2}B^2\left(\log_{10}\frac{T}{M}\right)^2\right] \quad (27)$$

$$\Omega^{(1,2)} = 3\,\frac{kT}{2\pi\mu}\left[(41.14B^2 - 18.13AB + 2A^2) + (9.067B^2 - 2AB)\log_{10}\frac{T}{M} + \frac{1}{2}B^2\left(\log_{10}\frac{T}{M}\right)^2\right] \quad (28)$$

$$\Omega^{(1,3)} = 12\,\frac{kT}{2\pi\mu}\left[(42.12B^2 - 18.35AB + 2A^2) + (9.176B^2 - 2AB)\log_{10}\frac{T}{M} + \frac{1}{2}B^2\left(\log_{10}\frac{T}{M}\right)^2\right] \quad (29)$$

These expressions were derived by Dr. Gerrold Yos of the Avco Corporation, but have not been published. For argon the constants $A = 1.564\times10^{-7}$ cm and $B = 1.660\times10^{-8}$ cm were obtained from reference 21. The resulting values of the "diffusion" integrals are shown in figure 2(b).

The interaction between a free electron and a neutral atom can be described approximately as the sum of three effects. The first effect is the electrostatic interaction of the free electron with the nucleus and the unperturbed charge distribution of the orbital electrons acting as a whole. An approximate orbital electron charge distribution obtained by Hartree (ref. 23) is used in this paper. The second effect is the net polarization, or charge displacement, of each orbital electron with respect to the nucleus, due to the electrostatic force of the free electron. The third effect is the exchange effect which is a manifestation of the Pauli exclusion principle for orbital electrons of like spins These last two effects are discussed in detail in reference 24. Kivel correlated the theoretical potential and experimental data for elastic electron-atom scattering (ref. 25) by assigning constants of proportionality to the calculated polarization and exchange terms. To obtain collision integrals of various orders, the resulting potential was converted to the more familiar form

$$\varphi_{13} = 2.242\times10^{-40}r^{-3.65} \quad (30)$$

where $\varphi(r)$ is the potential in ergs and r the interparticle distance in centimeters. The conversion of this type of potential to collision integrals of various orders is described in reference 18. The resulting values are shown in figure 2(c).

A percentage of atoms in a high-temperature equilibrium mixture exists in electronic excited states, whereas atoms used in scattering measurements

are in the ground or near-ground states. This poses the question of whether the potentials obtained from scattering measurements can represent those for the high temperature atoms. No generalizations can be made for the following reasons: (1) The amount of excitation imparted to the impinging atom or ion in the scattering experiments can vary because of the many available techniques for obtaining these particles, and (2) the levels of the first few excited states for these impinging particles and their corresponding selection rules (i.e., lifetimes of these states) vary from atom to atom.

The distribution of states for the argon particles used in the scattering measurements can be deduced by examining the experimental technique, then correlating it with the available excited states. The argon potentials in equations (23), (24), and (30) were obtained by essentially the same experimental technique. The impinging ions were obtained by the following steps: (1) Thermal electrons emanating from a filament were accelerated through a potential greater than the first ionization potential of argon (15.76 ev), and (2) the electrons were impacted against neutral argon atoms which are near room temperature, thereby creating argon ions. These ions are, in turn, accelerated and directed into the collision chamber. When the impinging particles were required to be neutral argon atoms, then they were obtained by the additional step of neutralization of the high velocity ions by charge exchange just before the collision chamber.

The first excited state for singly ionized argon is a relatively low one (0.18 ev). The collision of the electrons with the argon atoms should cause the formation of argon ions in both the ground and first excited states, with the populations in proportion to their statistical weight (g_i in eq. (2)). In other words, two thirds of the impinging ions are in the ground state and one third of the ions are in the first excited state. Because the excited state is metastable according to quantum-mechanical selection rules, the population of states of the impinging ions will remain in the same proportion.

If a beam of neutral argon atoms is required for the scattering experiment, then the distribution of states is quite different because of the absence of any low lying excited states for neutral argon. As a result, neutralization by charge exchange causes a beam of neutral atoms to exist in the ground state only.

The distribution of states in an equilibrium mixture of ions and atoms is different. For example, the percentage of argon atoms and ions in excited states is given in the following table.

T, °K	Percent atoms in excited state	Percent ions in first excited state	Percent ions in higher excited state
300	0	0.5	0
5,000	0	24.9	0
10,000	0	28.9	0
15,000	1.0	30.4	0
20,000	12.6	31.0	.2
25,000	43.7	31.3	.8
30,000	70.6	30.7	3.5

The percentage of equilibrium atoms in excited states is not large below 20,000° K. Above this temperature, the number of atoms as compared to ions is small (appendix A). As a result, the potential of equations (23) and (30), obtained from scattering of ground state atoms, is a good approximation throughout the specified range of temperatures and pressures. The 33-1/3-percent population of ions in the first excited state obtained in the scattering experiments is fortuitously close to the population found in a high-temperature equilibrium mixture. Accordingly, the potential of equation (24) is a good approximation for the range of temperatures and pressures where ion-atom interactions are important.

Ions do not exist in equilibrium mixtures at temperatures as low as 300° K. However, the population figure at this temperature serves to illustrate a point. Had the transition from the first excited state to the ground state been allowed, then the population of ions in the first excited state for the scattering measurements would have been 0.5 percent rather than 33-1/3 percent. This would have caused a large error in the potential of equation (24).

Interactions between charged particles are described by the shielded Coulomb potential

$$\varphi_{22}(r) = \varphi_{33}(r) = \varphi_{23}(r) = \frac{e^2}{r} \exp\left(-\frac{r}{h}\right) \tag{31}$$

The quantity h is the Debye shielding distance and is defined[2] as

$$h = \left(\frac{kT}{8\pi n_3 e^2}\right)^{1/2} \tag{32}$$

for singly ionized gases, where e is the electron charge. The physical significance of h can be described as follows. In a plasma, a given ion will have an excess of negatively charged particles in its vicinity, and vice versa, as a result of the attractive-repulsive nature of Coulomb forces. Consequently, the potential is exponentially attenuated by the screening effect of the electrons so that it decreases from e/r in the immediate vicinity of the given particle to negligible values at distances large compared to h. Therefore, h may be viewed as a correlation distance proportional to the effective range of a given charged particle. The collision integrals corresponding to the shielded Coulomb potential were derived by Liboff in reference 27. The values of these collision integrals are shown in figures 2(d) through 2(f).

---

[2]Spitzer (ref. 26) defines the Debye shielding distance as $h = (kT/4\pi n_3 e^2)^{1/2}$. However, equation (32) is used in this paper since all of the charge-charge collision integrals are based on this definition.

Expressions for Second-Order Basic Transport Coefficients

The derivation of the second-order expressions for the basic transport coefficients was outlined by Hirschfelder, Curtiss, and Bird in reference 8. However, second-order expressions were given only for the translational thermal conductivity and the thermal diffusion coefficients. Hirschfelder et al. expressed the viscosity and multicomponent diffusion coefficients in terms of the first-order approximation (i.e., only the first term in the series expansion of Sonine polynomials), since the first approximation is the predominant contribution for neutral gases. This order of approximation may not be sufficiently accurate for a partially ionized gas. Since a set of basic transport coefficients is required for a standard in this paper, the accuracies of the coefficients in this set must be consistent. Consequently, the second-order expressions[3] for λ_t, D_i^T, η, and D_{ij} will be given in the next few paragraphs.

The first component of thermal conductivity in equation (16), λ_t, is the only component predicted by collision effects alone. This component is described by Muckenfuss and Curtiss (ref. 30) in terms of a hypothetical isolated gaseous system, as "the thermal conductivity of a multicomponent system in which the diffusion forces vanish. If an initially uniform gas mixture is placed in a uniform temperature gradient, a thermal conductivity measurement, before any thermal diffusion takes place, would give λ_t. In the course of time, however, concentration gradients appear and the diffusion forces build up until the diffusion velocities vanish (the stationary state)." The second-order expression for this component is given in reference 8 as

[3]The selection of the second-order expressions should not give the connotation that it is the most accurate formulation of the Chapman-Enskog approach. An analysis by Landshoff (refs. 28 and 29) for an electron gas (infinitely heavy atoms) shows that third-order λ_t are 18 percent higher than second-order values, whereas fourth-order λ_t are higher than third-order values by less than 1 percent.

$$\lambda_t(2) = -\frac{75}{8} k^2 T \frac{\begin{array}{|ccc:ccc:c|}
\multicolumn{3}{c:}{\text{00 SUBDETERMINANT}} & \multicolumn{3}{c:}{\text{01 SUBDETERMINANT}} & \\
q_{11}^{00} & q_{12}^{00} & q_{13}^{00} & q_{11}^{01} & q_{12}^{01} & q_{13}^{01} & 0 \\
q_{21}^{00} & q_{22}^{00} & q_{23}^{00} & q_{21}^{01} & q_{22}^{01} & q_{23}^{01} & 0 \\
q_{31}^{00} & q_{32}^{00} & q_{33}^{00} & q_{31}^{01} & q_{32}^{01} & q_{33}^{01} & 0 \\
\hdashline
\multicolumn{3}{c:}{\text{10 SUBDETERMINANT}} & \multicolumn{3}{c:}{\text{11 SUBDETERMINANT}} & \\
q_{11}^{10} & q_{12}^{10} & q_{13}^{10} & q_{11}^{11} & q_{12}^{11} & q_{13}^{11} & 1 \\
q_{21}^{10} & q_{22}^{10} & q_{23}^{10} & q_{21}^{11} & q_{22}^{11} & q_{23}^{11} & 1 \\
q_{31}^{10} & q_{32}^{10} & q_{33}^{10} & q_{31}^{11} & q_{32}^{11} & q_{33}^{11} & 1 \\
\hdashline
0 & 0 & 0 & 1 & 1 & 1 & 0
\end{array}}{\begin{array}{|ccc:ccc|}
\multicolumn{3}{c:}{\text{00 SUBDETERMINANT}} & \multicolumn{3}{c|}{\text{01 SUBDETERMINANT}} \\
q_{11}^{00} & q_{12}^{00} & q_{13}^{00} & q_{11}^{01} & q_{12}^{01} & q_{13}^{01} \\
q_{21}^{00} & q_{22}^{00} & q_{23}^{00} & q_{21}^{01} & q_{22}^{01} & q_{23}^{01} \\
q_{31}^{00} & q_{32}^{00} & q_{33}^{00} & q_{31}^{01} & q_{32}^{01} & q_{33}^{01} \\
\hdashline
\multicolumn{3}{c:}{\text{10 SUBDETERMINANT}} & \multicolumn{3}{c|}{\text{11 SUBDETERMINANT}} \\
q_{11}^{10} & q_{12}^{10} & q_{13}^{10} & q_{11}^{11} & q_{12}^{11} & q_{13}^{11} \\
q_{21}^{10} & q_{22}^{10} & q_{23}^{10} & q_{21}^{11} & q_{22}^{11} & q_{23}^{11} \\
q_{31}^{10} & q_{32}^{10} & q_{33}^{10} & q_{31}^{11} & q_{32}^{11} & q_{33}^{11}
\end{array}} \qquad (33)$$

Note that the determinants in both the numerator and denominator contain subdeterminants whose elements are designated by the superscripts 00, 01, 10, and 11. These superscripts correspond to the combination of Sonine polynomials used in a particular subdeterminant. For example, the first Sonine polynomial (m = 0) and the second Sonine polynomial (m = 1) are implicit in the 01 subdeterminant. The elements q_{ij}^{mm} are related to the elements $\tilde{Q}_{ij}^{mm'}$ by

$$q_{ij}^{mm'} = \frac{\sqrt{m_i m_j}}{n_i n_j} \tilde{Q}_{ij}^{mm'} \tag{34}$$

The elements $\tilde{Q}_{ij}^{mm'}$ are defined rather than $q_{ij}^{mm'}$, since the elements $\tilde{Q}_{ij}^{mm'}$ will also be used in the calculation of the thermal diffusion coefficient. The elements are

$$\tilde{Q}_{ii}^{00} = 0 \tag{35a}$$

$$\tilde{Q}_{ij}^{00} = \frac{-8n_j m_j (n_i m_i + n_j m_j)}{\sqrt{m_i m_j}(m_i + m_j)} \Omega_{ij}^{(1,1)} - \frac{8n_k n_j m_k m_j}{\sqrt{m_i m_j}(m_i + m_k)} \Omega_{ik}^{(1,1)} \tag{35b}$$

where $k \neq i \neq j$.

$$\tilde{Q}_{ii}^{01} = -8 \sum_{j \neq i} \frac{n_i n_j m_j^2}{(m_i + m_j)^2} \left[\Omega_{ij}^{(1,2)} - \frac{5}{2} \Omega_{ij}^{(1,1)} \right] \tag{36a}$$

$$\tilde{Q}_{ij}^{01} = 8 \left(\frac{m_i}{m_j} \right)^{3/2} \frac{n_i n_j m_j^2}{(m_i + m_j)^2} \left[\Omega_{ij}^{(1,2)} - \frac{5}{2} \Omega_{ij}^{(1,1)} \right] \tag{36b}$$

$$\tilde{Q}_{ii}^{10} = \tilde{Q}_{ii}^{01} \tag{37a}$$

$$\tilde{Q}_{ij}^{10} = \frac{m_j}{m_i} \tilde{Q}_{ij}^{01} \tag{37b}$$

$$\tilde{Q}_{ii}^{11} = 4n_i^2 \Omega_{ii}^{(2,2)} + 8 \sum_{j \neq i} \frac{n_i n_j m_j}{(m_i + m_j)^3} \left[\frac{5}{4} (6m_i^2 + 5m_j^2) \Omega_{ij}^{(1,1)} - 5m_j^2 \Omega_{ij}^{(1,2)} + m_j^2 \Omega_{ij}^{(1,3)} \right]$$

$$+ 16 \sum_{j \neq i} \frac{n_i n_j m_i m_j^2}{(m_i + m_j)^3} \Omega_{ij}^{(2,2)} \tag{38a}$$

$$\tilde{Q}_{ij}^{11} = 8 \left(\frac{m_i}{m_j} \right)^{3/2} \frac{n_i n_j m_j}{(m_i + m_j)^3} \left[2m_j^2 \Omega_{ij}^{(2,2)} - \frac{55}{4} m_j^2 \Omega_{ij}^{(1,1)} + 5m_j^2 \Omega_{ij}^{(1,2)} - m_j^2 \Omega_{ij}^{(1,3)} \right] \tag{38b}$$

For these elements $\Omega_{ij} = \Omega_{ji}$, but $\tilde{Q}_{ij} \neq \tilde{Q}_{ji}$. The values for $\lambda_t(2)$ for partially ionized argon are shown in figure 3.

The last component of the thermal conductivity in equation (16) contains the thermal diffusion coefficient, D_i^T. The second-order expression is defined as

$$D_i^T = n_i\sqrt{\frac{m_i kT}{2}}\;\frac{\begin{vmatrix} \text{00 SUBDETERMINANT} & & & \text{01 SUBDETERMINANT} & & & \\ \tilde{Q}_{11}^{00} & \tilde{Q}_{12}^{00} & \tilde{Q}_{13}^{00} & \tilde{Q}_{11}^{01} & \tilde{Q}_{12}^{01} & \tilde{Q}_{13}^{01} & 0 \\ \tilde{Q}_{21}^{00} & \tilde{Q}_{22}^{00} & \tilde{Q}_{23}^{00} & \tilde{Q}_{21}^{01} & \tilde{Q}_{22}^{01} & \tilde{Q}_{23}^{01} & 0 \\ \tilde{Q}_{31}^{00} & \tilde{Q}_{32}^{00} & \tilde{Q}_{33}^{00} & \tilde{Q}_{31}^{01} & \tilde{Q}_{32}^{01} & \tilde{Q}_{33}^{01} & 0 \\ \text{10 SUBDETERMINANT} & & & \text{11 SUBDETERMINANT} & & & \\ \tilde{Q}_{11}^{10} & \tilde{Q}_{12}^{10} & \tilde{Q}_{13}^{10} & \tilde{Q}_{11}^{11} & \tilde{Q}_{12}^{11} & \tilde{Q}_{13}^{11} & \frac{15}{4}n_1\sqrt{\frac{2kT}{m_1}} \\ \tilde{Q}_{21}^{10} & \tilde{Q}_{22}^{10} & \tilde{Q}_{23}^{10} & \tilde{Q}_{21}^{11} & \tilde{Q}_{22}^{11} & \tilde{Q}_{23}^{11} & \frac{15}{4}n_2\sqrt{\frac{2kT}{m_2}} \\ \tilde{Q}_{31}^{10} & \tilde{Q}_{32}^{10} & \tilde{Q}_{33}^{10} & \tilde{Q}_{31}^{11} & \tilde{Q}_{32}^{11} & \tilde{Q}_{33}^{11} & \frac{15}{4}n_3\sqrt{\frac{2kT}{m_3}} \\ \delta_{i1} & \delta_{i2} & \delta_{i3} & 0 & 0 & 0 & 0 \end{vmatrix}}{\begin{vmatrix} \text{00 SUBDETERMINANT} & & & \text{01 SUBDETERMINANT} & & \\ \tilde{Q}_{11}^{00} & \tilde{Q}_{12}^{00} & \tilde{Q}_{13}^{00} & \tilde{Q}_{11}^{01} & \tilde{Q}_{12}^{01} & \tilde{Q}_{13}^{01} \\ \tilde{Q}_{21}^{00} & \tilde{Q}_{22}^{00} & \tilde{Q}_{23}^{00} & \tilde{Q}_{21}^{01} & \tilde{Q}_{22}^{01} & \tilde{Q}_{23}^{01} \\ \tilde{Q}_{31}^{00} & \tilde{Q}_{32}^{00} & \tilde{Q}_{33}^{00} & \tilde{Q}_{31}^{01} & \tilde{Q}_{32}^{01} & \tilde{Q}_{33}^{01} \\ \text{10 SUBDETERMINANT} & & & \text{11 SUBDETERMINANT} & & \\ \tilde{Q}_{11}^{10} & \tilde{Q}_{12}^{10} & \tilde{Q}_{13}^{10} & \tilde{Q}_{11}^{11} & \tilde{Q}_{12}^{11} & \tilde{Q}_{13}^{11} \\ \tilde{Q}_{21}^{10} & \tilde{Q}_{22}^{10} & \tilde{Q}_{23}^{10} & \tilde{Q}_{21}^{11} & \tilde{Q}_{22}^{11} & \tilde{Q}_{23}^{11} \\ \tilde{Q}_{31}^{10} & \tilde{Q}_{32}^{10} & \tilde{Q}_{33}^{10} & \tilde{Q}_{31}^{11} & \tilde{Q}_{32}^{11} & \tilde{Q}_{33}^{11} \end{vmatrix}} \tag{39}$$

The second-order expression for the viscosity is

$$\eta(2) = \frac{1}{2}\,kT\sum_j n_j b_{j0}(2) \tag{40}$$

where $b_{j0}(2)$ is a Sonine expansion coefficient of the second order. The second subscript in $b_{j0}(2)$ denotes the first Sonine polynomial ($m = 0$). However, this does not mean that the effect of the second Sonine polynomial ($m = 1$) has been dropped out, for the values of $b_{j0}(2)$ are derived from a set of linear equations containing the first and second Sonine polynomials.

The derivation of the Sonine expansion coefficients, $b_{j_o}(2)$, are included in appendix C, since they were not derived in reference 8. These coefficients are

$$b_{j_o}(2) = \frac{\begin{vmatrix} \text{00 SUBDETERMINANT} & & & \text{01 SUBDETERMINANT} & & & \\ \tilde{H}^{00}_{11} & \tilde{H}^{00}_{12} & \tilde{H}^{00}_{13} & \tilde{Q}^{01}_{11} & \tilde{Q}^{01}_{12} & \tilde{Q}^{01}_{13} & -5n_1 \\ \tilde{H}^{00}_{21} & \tilde{H}^{00}_{22} & \tilde{H}^{00}_{23} & \tilde{Q}^{01}_{21} & \tilde{Q}^{01}_{22} & \tilde{Q}^{01}_{23} & -5n_2 \\ \tilde{H}^{00}_{31} & \tilde{H}^{00}_{32} & \tilde{H}^{00}_{33} & \tilde{Q}^{01}_{31} & \tilde{Q}^{01}_{32} & \tilde{Q}^{01}_{33} & -5n_3 \\ \text{10 SUBDETERMINANT} & & & \text{11 SUBDETERMINANT} & & & \\ \tilde{Q}^{10}_{11} & \tilde{Q}^{10}_{12} & \tilde{Q}^{10}_{13} & \tilde{Q}^{11}_{11} & \tilde{Q}^{11}_{12} & \tilde{Q}^{11}_{13} & 0 \\ \tilde{Q}^{10}_{21} & \tilde{Q}^{10}_{22} & \tilde{Q}^{10}_{23} & \tilde{Q}^{11}_{21} & \tilde{Q}^{11}_{22} & \tilde{Q}^{11}_{23} & 0 \\ \tilde{Q}^{10}_{31} & \tilde{Q}^{10}_{32} & \tilde{Q}^{10}_{33} & \tilde{Q}^{11}_{31} & \tilde{Q}^{11}_{32} & \tilde{Q}^{11}_{33} & 0 \\ \delta_{j1} & \delta_{j2} & \delta_{j3} & 0 & 0 & 0 & 0 \end{vmatrix}}{\begin{vmatrix} \text{00 SUBDETERMINANT} & & & \text{01 SUBDETERMINANT} & & & \\ \tilde{H}^{00}_{11} & \tilde{H}^{00}_{12} & \tilde{H}^{00}_{13} & \tilde{Q}^{01}_{11} & \tilde{Q}^{01}_{12} & \tilde{Q}^{01}_{13} & \\ \tilde{H}^{00}_{21} & \tilde{H}^{00}_{22} & \tilde{H}^{00}_{23} & \tilde{Q}^{01}_{21} & \tilde{Q}^{01}_{22} & \tilde{Q}^{01}_{23} & \\ \tilde{H}^{00}_{31} & \tilde{H}^{00}_{32} & \tilde{H}^{00}_{33} & \tilde{Q}^{01}_{31} & \tilde{Q}^{01}_{32} & \tilde{Q}^{01}_{33} & \\ \text{10 SUBDETERMINANT} & & & \text{11 SUBDETERMINANT} & & & \\ \tilde{Q}^{10}_{11} & \tilde{Q}^{10}_{12} & \tilde{Q}^{10}_{13} & \tilde{Q}^{11}_{11} & \tilde{Q}^{11}_{12} & \tilde{Q}^{11}_{13} & \\ \tilde{Q}^{10}_{21} & \tilde{Q}^{10}_{22} & \tilde{Q}^{10}_{23} & \tilde{Q}^{11}_{21} & \tilde{Q}^{11}_{22} & \tilde{Q}^{11}_{23} & \\ \tilde{Q}^{10}_{31} & \tilde{Q}^{10}_{32} & \tilde{Q}^{10}_{33} & \tilde{Q}^{11}_{31} & \tilde{Q}^{11}_{32} & \tilde{Q}^{11}_{33} & \end{vmatrix}} \tag{41}$$

The elements in the 01, 10, and 11 subdeterminants are identical with those in equations (36), (37), and (38). The elements in the 00 subdeterminant are

$$\tilde{H}_{ii} = 4n_i^2\Omega_{ii}^{(2,2)} + \frac{16}{3}\sum_{j\neq i}\frac{n_i n_j m_j}{(m_i + m_j)^2}\left[5m_i\Omega_{ij}^{(1,1)} + \frac{3}{2}m_j\Omega_{ij}^{(2,2)}\right] \tag{42a}$$

$$\tilde{H}_{ij} = \frac{16}{3}\frac{n_i n_j m_j}{(m_i + m_j)^2}\left[\frac{3}{2}m_j\Omega_{ij}^{(2,2)} - 5m_j\Omega_{ij}^{(1,1)}\right] \tag{42b}$$

The values of $\eta(2)$ for partially ionized argon are shown in figure 4.

The second component of the thermal conductivity in equation (16) contains the multicomponent diffusion coefficients, D_{ij}. The second-order expression is defined as

$$D_{ij}(2) = \frac{\rho n_i}{2nm_j}\sqrt{\frac{2kT}{m_i}}\,c_{io}^{(j,i)}(2) \tag{43}$$

where $c_{io}^{(j,i)}(2)$ is a Sonine expansion coefficient of the second order. The derivation of $c_{io}^{(j,i)}(2)$ is shown in appendix C. These coefficients are

$$c_{io}^{(j,i)}(2) = \frac{\begin{array}{|ccc:ccc:c|}
\multicolumn{3}{|c:}{00\ \text{SUBDETERMINANT}} & \multicolumn{3}{c:}{01\ \text{SUBDETERMINANT}} & \\
\tilde{Q}_{11}^{00} & \tilde{Q}_{12}^{00} & \tilde{Q}_{13}^{00} & \tilde{Q}_{11}^{01} & \tilde{Q}_{12}^{01} & \tilde{Q}_{13}^{01} & 3\sqrt{\frac{kT}{2m_1}}(\delta_{j1}-\delta_{i1}) \\
\tilde{Q}_{21}^{00} & \tilde{Q}_{22}^{00} & \tilde{Q}_{23}^{00} & \tilde{Q}_{21}^{01} & \tilde{Q}_{22}^{01} & \tilde{Q}_{23}^{01} & 3\sqrt{\frac{kT}{2m_2}}(\delta_{j2}-\delta_{i2}) \\
\tilde{Q}_{31}^{00} & \tilde{Q}_{32}^{00} & \tilde{Q}_{33}^{00} & \tilde{Q}_{31}^{01} & \tilde{Q}_{32}^{01} & \tilde{Q}_{33}^{01} & 3\sqrt{\frac{kT}{2m_3}}(\delta_{j3}-\delta_{i3}) \\
\hdashline
\multicolumn{3}{|c:}{10\ \text{SUBDETERMINANT}} & \multicolumn{3}{c:}{11\ \text{SUBDETERMINANT}} & \\
\tilde{Q}_{11}^{10} & \tilde{Q}_{12}^{10} & \tilde{Q}_{13}^{10} & \tilde{Q}_{11}^{11} & \tilde{Q}_{12}^{11} & \tilde{Q}_{13}^{11} & 0 \\
\tilde{Q}_{21}^{10} & \tilde{Q}_{22}^{10} & \tilde{Q}_{23}^{10} & \tilde{Q}_{21}^{11} & \tilde{Q}_{22}^{11} & \tilde{Q}_{23}^{11} & 0 \\
\tilde{Q}_{31}^{10} & \tilde{Q}_{32}^{10} & \tilde{Q}_{33}^{10} & \tilde{Q}_{31}^{11} & \tilde{Q}_{32}^{11} & \tilde{Q}_{33}^{11} & 0 \\
\hdashline
\delta_{i1} & \delta_{i2} & \delta_{i3} & 0 & 0 & 0 & 0
\end{array}}{\begin{array}{|ccc:ccc|}
\multicolumn{3}{|c:}{00\ \text{SUBDETERMINANT}} & \multicolumn{3}{c:}{01\ \text{SUBDETERMINANT}} \\
\tilde{Q}_{11}^{00} & \tilde{Q}_{12}^{00} & \tilde{Q}_{13}^{00} & \tilde{Q}_{11}^{01} & \tilde{Q}_{12}^{01} & \tilde{Q}_{13}^{01} \\
\tilde{Q}_{21}^{00} & \tilde{Q}_{22}^{00} & \tilde{Q}_{23}^{00} & \tilde{Q}_{21}^{01} & \tilde{Q}_{22}^{01} & \tilde{Q}_{23}^{01} \\
\tilde{Q}_{31}^{00} & \tilde{Q}_{32}^{00} & \tilde{Q}_{33}^{00} & \tilde{Q}_{31}^{01} & \tilde{Q}_{32}^{01} & \tilde{Q}_{33}^{01} \\
\hdashline
\multicolumn{3}{|c:}{10\ \text{SUBDETERMINANT}} & \multicolumn{3}{c:}{11\ \text{SUBDETERMINANT}} \\
\tilde{Q}_{11}^{10} & \tilde{Q}_{12}^{10} & \tilde{Q}_{13}^{10} & \tilde{Q}_{11}^{11} & \tilde{Q}_{12}^{11} & \tilde{Q}_{13}^{11} \\
\tilde{Q}_{21}^{10} & \tilde{Q}_{22}^{10} & \tilde{Q}_{23}^{10} & \tilde{Q}_{21}^{11} & \tilde{Q}_{22}^{11} & \tilde{Q}_{23}^{11} \\
\tilde{Q}_{31}^{10} & \tilde{Q}_{32}^{10} & \tilde{Q}_{33}^{10} & \tilde{Q}_{31}^{11} & \tilde{Q}_{32}^{11} & \tilde{Q}_{33}^{11}
\end{array}} \qquad (44)$$

The elements in the four subdeterminants are identical with those in equations (35) to (38). The values of the various second-order multicomponent diffusion coefficients are shown in figure 5 for a pressure of 1 atmosphere.

The coefficient of electrical conductivity, σ, can be derived from the expression for the current density, $\underline{j}$, which is defined as

$$\underline{j} = n_I e \overline{V}_I - n_e e \overline{V}_e = \sigma \underline{E} \qquad (45)$$

where $\underline{E}$ is an externally applied electric field. Substituting equation (14) into (45) and retaining only those terms containing the electric field, we have

$$\sigma = \frac{e^2 n^2}{\rho p} (m_e n_e D_{Ie} + m_I n_I D_{eI}) \tag{46}$$

The calculated values of the electrical conductivity based on the second-order values of the multicomponent diffusion coefficients (eq. (43)) are shown in figure 6.

DISCUSSION OF RESULTS AND COMPARISONS

Basic Transport Coefficients for Partially Ionized Gases

In existing calculations of the basic transport coefficients for high-temperature reactive gases, where the number of species is much greater than for argon (refs. 1 to 6), the second-order expressions have not been used because of computational difficulties. For example, an equilibrium mixture of CO_2 and N_2 may have as many as eight species simultaneously. In this case the calculations for $\eta(2)$, $D_{ij}(2)$, $\lambda_t(2)$, and $D_i^T(2)$ would necessitate the use of the 16th order determinant. As a result, approximate methods were substituted and have been proven experimentally (refs. 4, 10, and 12) to be fairly good up to temperatures where dissociation occurs. However, the validity of these approximations at temperatures where ionization occurs, is questionable. In this section the second-order basic transport coefficients of argon will be compared with those calculated by these approximate methods. Any disparities which may appear for argon should be indicative of the disparities which would appear for other partially ionized gases.

The existing approximations assume that the first-order expressions for the components of viscosity and the multicomponent diffusion coefficients are sufficiently accurate. In other words, the approximation is equivalent to dropping the 01, 10, and 11 subdeterminants in equations (41) and (44). This assumption was justified by comparisons of calculated first-order values with experimental data (ref. 8), where the intermolecular forces were small, the masses of the different species were comparable, and the temperatures were relatively low (a few hundred degrees Kelvin above room temperature).

Viscosity.- First-order values of the viscosity of partially ionized argon were calculated, then compared with the second-order values of equation (40). The first-order approximation is quite good. The greatest difference between the first- and second-order values is only 1 percent and occurs at conditions of complete ionization. An examination of the magnitudes of the Sonine expansion coefficients, b_{io}, shows the reason why no large changes should be expected. The first-order values of the electron expansion coefficient, $b_{eo}(1)$, are larger than the second-order values by 12 to 15 percent, whereas the first-order values for the atom and ion, $b_{Ao}(1)$ and $b_{A^+o}(1)$, are lower than the corresponding second-order values by only 1 percent. This

comparison indicates that second-order effects are important only for electrons. However, b_{Ao} and b_{A^+o} are roughly three orders of magnitude larger than b_{eo} because of the minute electron mass. Consequently, for viscosity (i.e., transport of momentum), the second-order effects are negligible.

Multicomponent diffusion coefficients.- First-order values of the multicomponent diffusion coefficients were calculated, then compared with the second-order values of equation (43) in figure 5. For the coefficients $D_{A\text{-}A^+}$, $D_{A^+\text{-}A}$, and $D_{A\text{-}e}$, there is only a few percent difference between the first- and second-order values. However, the second-order coefficients $D_{A^+\text{-}e}(2)$, $D_{e\text{-}A}(2)$, and $D_{e\text{-}A^+}(2)$ are larger than the corresponding first-order coefficients by 25 percent at 50-percent ionization and by 45 percent at complete ionization. Several factors are responsible for the discrepancy between $D_{ij}(1)$ and $D_{ij}(2)$. According to Hirschfelder et al. in reference 8 "the use of one term alone does not describe the dependence of the diffusion coefficient on concentration; the slight concentration-dependence is brought out when the first two terms in the Sonine polynomial are used." More important may be the neglect of the 11 subdeterminant which completely drops out the electron-electron interactions.[4] The elements in the determinants for $D_{A^+\text{-}e}(2)$, $D_{e\text{-}A}(2)$, and $D_{e\text{-}A^+}(2)$ show that the electron-electron interaction becomes important because of the combined effects of large intermolecular force and small mass.

These discrepancies have important implications in the calculation of the last two components of the thermal conductivity (eq. (16)). If the assumption is made that the first-order multicomponent diffusion coefficients are sufficiently accurate, then they can be expressed in terms of the binary coefficients

$$\mathscr{D}_{ij}(1) = \frac{3(m_i + m_j)}{16 n m_i m_j} \frac{kT}{\Omega_{ij}^{(1,1)}} = \mathscr{D}_{ji}(1) \tag{47}$$

This expression of $D_{ij}(1)$ in terms of $\mathscr{D}_{ij}(1)$ can result in considerable simplifications in the expressions for the concentration gradients and diffusion velocities. However, a 25 to 45 percent error in certain of the first order diffusion coefficients could mean a much greater error in some of the concentration gradients and diffusion velocities. For example, the first component of the velocity in equation (14) can be a difference as well as a sum of the quantities $m_j D_{ij} \underline{d}_j$ because

$$\Sigma \underline{d}_j = 0 \tag{48}$$

Consequently, for partially or fully ionized gases, the second-order diffusion coefficients should be used for accurate predictions of λ_r and λ_d.

---

[4]Unlike the elements in the viscosity determinants (eqs. (38a) and (42a)) which contain like interactions in both the 00 and 11 subdeterminants, the elements in the multicomponent diffusion determinants (eqs. (35a) and (38a)) contain like interactions in the 11 subdeterminant only.

The significance of the quantity D_{ij} is not given for a mixture with more than two components. An examination of the first component of the diffusion velocity (eq. (14)) indicates that D_{ij} may be defined as a measure of the diffusion of species i because of the interaction of species i with species j. However, an examination of the terms for the Sonine expansion coefficients $c_{io}^{(j,i)}$ (eq. (44)) shows that interactions between all species affect the value of D_{ij}. Consequently, D_{ij} may be described more aptly as a measure of the diffusion of species i with respect to species j for all interactions, including interactions between like particles (e.g., electron-electron). It may be instructive to compare the various $D_{ij}(2)$ in figure 5 with this description in mind. The values of $D_{A-A^+}(2)$ and $D_{A^+-A}(2)$ are identical within five decimal places for conditions ranging from less than 1 percent ionization to almost full ionization. Even the values of the binary diffusion coefficient, $\mathscr{D}_{ij}$, are within 1 percent of these values. The values of $D_{e-A}(2)$ and $D_{e-A^+}(2)$ differ by only 1 percent at most for all conditions. These characteristics indicate that the atom and the ion diffuse with respect to each other, independent of any electron effects. This is possible despite the large Coulomb forces between ions and electrons, because of the much greater mass of the atom and ion. Figure 5 also shows that $D_{A-e}(2)$ is at least an order of magnitude larger than $D_{A^+-e}(2)$ at ionization levels greater than 25 percent. This indicates that although the electron does not affect ion or atom diffusion, its own diffusion is affected more by the ion than the atom because of the large Coulombic forces.

Translational thermal conductivity.- In the Chapman-Enskog formulation, the first-order approximations (i.e., neglect of the 01, 10, and 11 subdeterminants) for the translational thermal conductivity, λ_t, and the thermal diffusion coefficients, D_i^T, are both identically zero. Muckenfuss and Curtiss (ref. 30) searched for a simplification of the second-order λ_t. As a first step they assumed that first-order multicomponent diffusion coefficients were sufficiently accurate for nonreactive monatomic gases, and could be expressed in terms of binary diffusion coefficients. As a result, the heat flux vector of equation (16) could be expressed as

$$\underline{q} = -\lambda_\infty \frac{\partial T}{\partial \underline{r}} + \sum_i n_i h_i \underline{V}_i + \frac{kT}{n} \sum_i \sum_j \frac{n_j D_i^T}{m \mathscr{D}_{ij}(1)} (\underline{V}_i - \underline{V}_j) \tag{49}$$

where

$$\lambda_\infty = \lambda_t - \frac{k}{2n} \sum_i \sum_j \frac{n_i n_j}{\mathscr{D}_{ij}(1)} \left(\frac{D_i^T}{n_i m_i} - \frac{D_j^T}{n_j m_j} \right) \tag{50}$$

In other words, the thermal diffusive component, λ_d, was split into two parts, one part proportional to the temperature gradient and the other proportional to the differences in diffusion velocities. The first part of λ_d was then

added to the translational thermal conductivity, λ_t, and the sum[5] defined as λ_∞. Muckenfuss and Curtiss reasoned that since thermal diffusive effects are small for nonreactive gases near room temperature, then λ_∞ could be replaced by a modification of the determinant form of equation (33) for λ_t. This modification consisted in discarding the 00, 01, and 10 subdeterminants. Numerical calculations were made for two ternary mixtures, He-A-Xe and Ne-A-Kr at 311° K. Muckenfuss and Curtiss concluded that thermal diffusion effects were proportional to the mass disparity between the interacting species. For example, the difference between λ_t and λ_∞ (eq. (50)) was 2 percent for the He-A-Xe mixture ($M_{Xe}/M_{He} \sim 33$) but only 0.5 percent for the Ne-A-Kr mixture ($M_{Kr}/M_{Ne} \sim 4$). The calculations also showed that if the elements in the 00, 01, and 10 subdeterminants in equation (33) were discarded a difference of only 2 percent would be incurred for the He-A-Xe mixture and an 0.5-percent error for the Ne-A-Kr mixtures. Consequently, Muckenfuss and Curtiss stated that equation (50) "is found to be identical with an 'approximate' formula for the thermal conductivity derived on the assumption that the thermal diffusion coefficients are negligibly small." As a result, existing approximations (refs. 1 to 6) have made use of the following simplifications: (1) The quantities D_i^T for all species are assumed to be zero, and (2) the approximation for the translational thermal conductivity is assumed to be equal to the approximations for λ_∞. That is, they both can be derived from the second-order expression $\lambda_t(2)$ (eq. (33)), if the 00, 01, and 10 subdeterminants are discarded. These simplifications have been used for a partially ionized gas where the mass disparity is extremely large ($M_{atom}/M_{electron} \sim 10^4$).

The validity of the λ_t approximation for a partially ionized gas can be determined from figure 7. This figure compares the second-order λ_t and the approximate λ_t at pressures of 10^{-4}, 10^{-1}, and 10^{2} atmospheres. The second-order values are larger by 30 percent at 50-percent ionization and larger by 50 percent at complete ionization at the lower pressures. The smaller disparity at 100 atmospheres can be attributed to an increase in the Debye shielding effect (i.e., a greater departure from the Coulomb potential). A similar calculation shows that the second-order values are higher by almost 100 percent for a mixture of doubly ionized atoms and electrons. The source of the discrepancies can be seen by an inspection of the magnitudes of the elements in the $\lambda_t(2)$ determinants. The determinant shown below is the denominator of equation (33) for a temperature of 15,000° K and a pressure of 10^{-4} atmosphere (99-percent ionization).

00 SUBDETERMINANT			01 SUBDETERMINANT		
0	1	10^{-1}	10^{-1}	10^{-5}	10^{-8}
10^{-4}	0	10^{-5}	10^{-5}	10^{-9}	10^{-8}
1	1	0	10^{-13}	10^{-10}	10^{-5}
10 SUBDETERMINANT			**11 SUBDETERMINANT**		
10^{-1}	10^{-5}	10^{-13}	1	10^{-4}	10^{-11}
10^{-5}	10^{-9}	10^{-10}	10^{-4}	10^{-2}	10^{-9}
10^{-8}	10^{-5}	10^{-5}	10^{-11}	10^{-9}	10^{-4}

[5]This separation of the thermal diffusive component, λ_d, into two parts is not a valid operation for a partially ionized gas because of the discrepancy between the first- and second-order values of the multicomponent coefficients.

The values of the elements have been rounded off to the nearest power of 10, then divided through to give a value of unity to the largest values. When these values were substituted into the expanded terms of equation (33), the elements in the 01 and 10 subdeterminants were found to contribute very little to the final value of λ_t, whereas the elements in the 00 subdeterminant were contained in the dominant terms. This comparison shows that the complete second-order expression for λ_t (eq. (33)) must be used.

Another approximation for the translational thermal conductivity of a partially ionized gas has been proposed by Fay (ref. 31). His expression for λ_t is

$$\lambda_t = \lambda_{t_1} + \lambda_p \tag{51}$$

where λ_{t_1} is the translational thermal conductivity of pure atomic argon, calculated from equations (22) and (23), and λ_p is the thermal conductivity of a singly ionized argon plasma as specified by Spitzer in reference 26. The λ_t values calculated by equation (51) are compared with those from the second-order theory (eq. (33)) in figure 8. Comparisons were made at the lower pressures (10^{-4} and 10^{-1} atm). It can be seen that equation (51) is a poor approximation at 10^{-4} atmosphere, and a fair approximation at 10^{-1} atmosphere. The large discrepancy at 10^{-4} atmosphere can be attributed to the fact that λ_{t_1} is not dependent upon density, whereas λ_p increases rapidly with density. A more reasonable expression for λ_t

$$\lambda_t = (1 - \epsilon)\lambda_{t_1} + \epsilon\lambda_p \tag{52}$$

can be used for degrees of ionization, ϵ, greater than 0.5. Neither equation (51) nor (52) is a good approximation in the region of moderate degrees of ionization ($0.2 < \epsilon < 0.5$).

Thermal diffusion coefficients.- The expressions for the last two components of the thermal conductivity, λ_r and λ_d, in equations (14) and (16) contain the thermal diffusion coefficients, D_i^T. Existing approximations have assumed that D_i^T is identically zero. Typical values of the second-order thermal diffusion coefficients for the argon atom, ion, and electrons are shown in figure 9. In the expressions for the diffusive velocity (eq. (14)) and the heat flux vector (eq. (16)), D_i^T always occur in combination with the number density n_i, and the mass, m_i, in the denominator. Although the electron thermal diffusion coefficient, D_e^T, is at most two orders of magnitude smaller than those for the atom and ion, the electron mass is four orders of magnitude smaller. Consequently, thermal diffusive effects can be attributed almost entirely to the electron term. This does not mean, however, that only the electron interactions are important. The role of heavy particle diffusion will be discussed later. In its present form, the second-order theory cannot predict accurately the concentration gradients of electrons. However, an order of magnitude calculation using a range of expected values for $\partial X_e/\partial \underline{r}$ shows that the contribution of electron thermal diffusion to λ_r and λ_d can be of the same order of magnitude as λ_t.

The question arises as to whether D_e^T for partially ionized argon can be used for other partially ionized gases. Inspection of the magnitudes of the determinant elements in equation (39) shows that the value of D_e^T is mainly determined by the values of the collision integrals for the electron-electron, electron-ion, ion-ion, and electron-atom interactions. Also, D_e^T is not sensitive to changes in the remaining interactions. All partially ionized gases have essentially the same value of $\Omega_{A^+-e}^{(l,s)}$ for a given electron density and temperature for the following reasons: (1) All electron-ion interactions are described by the shielded Coulomb potential (eq. (31)), and (2) mass effects are determined by the reduced masses of binary systems which are essentially the same for all ion-electron systems.

The electron-atom collision integrals for all gases do not have the same values, as evidenced by the comparison of $\bar{\Omega}_{A-e}^{(1,1)}$ for hydrogen, nitrogen, and oxygen in reference 6. It would be exceedingly difficult to assess the relative effects of electron-ion and electron-atom interaction by inspection of the elements in the determinant expression for D_e^T. However, this can be done simply by changing the constants in the electron-argon atom potential (eq. (30)), then comparing the resulting values of D_e^T. Two sets of changes in φ_{A-e} were made to include extreme values of Ω_{A-e} which are found for other atoms of interest (e.g., ref. 6). The first resulted in an increase in the Ω_{A-e} integrals by a factor of two, and the second in a decrease by a factor of six at 5,000° K. As to be expected, dissimilarities showed up for conditions of low degrees of ionization. For example, the differences in D_e^T were as high as 50 percent at 1-percent ionization. However, it is believed that the thermal diffusive effects are relatively small in this region because of the rapid drop in the magnitude of D_e^T with decreasing temperature (fig. 9). At 25-percent ionization the maximum difference drops to approximately 2 percent, and at 50-percent ionization the difference is less than 1 percent. These considerations show that the thermal diffusion of electrons is dictated by the ion-electron interaction rather than the atom-electron interaction. These considerations also show that the D_e^T values for partially ionized argon can be used as a good approximation for other partially ionized gases. These D_e^T values are presented in figure 10 as a function of electron density and temperature.

Another interesting conclusion can be reached by an inspection of the various D_i^T in figure 9. It can be seen that the atom and ion thermal diffusion coefficients are within 1 percent of each other in magnitude from a few percent ionization up to extremely high degrees of ionization. As the number of atoms approaches zero, $D_{A^+}^T$ decreases in value, changes sign, then approaches the value of D_e^T near 100-percent ionization. These variations imply that the diffusion motion of both the atom and ion are essentially independent of that for the electron, up to large degrees of ionization (approximately 95 percent). The diffusive motion of the electrons, in turn, is dictated by the ion rather than the atom because of the much greater magnitude of the Coulombic forces. The same conclusion was reached from an examination of the multicomponent diffusion coefficients, $D_{ij}(2)$. These variations point out that for a partially ionized gas, we can use some of the concepts of plasma physics directly, but other concepts must be modified to account for

the strong atom-ion momentum coupling. The electrical conductivity is an example in point. The variations have extremely important implications for other situations. Heavy particle diffusion also would dominate where the heavier particles were ions of a single type diffusing with respect to each other due to temperature and/or concentration gradients, or ions of a given charge diffusing with respect to ions of a different charge. This point should be kept in mind for the subsequent discussion of the electrical conductivity of a partially ionized gas and the basic transport coefficients of a fully ionized gas.

Electrical conductivity.- The existing approximations for calculating the electrical conductivity of a partially ionized gas (refs. 6, 32, and 33) are based on simple kinetic theory which uses the concepts of an electron mean free path. In references 6 and 32, the Coulombic cross sections are empirically modified so that the resulting values of the electrical conductivity, σ, agree with Spitzer's values (ref. 26) at the limit of complete ionization. The approximation by Lin, Resler, and Kantrowitz (ref. 33) is a typical example. They used an unrealistic model which adds the resistivity of an electron gas (ref. 26) and the resistivity of a Lorentzian gas.[6] In other words, the atom-atom, atom-ion, and ion-ion interactions were completely ignored. Their values are shown in figure 11. Also shown are the experimental values of the electrical conductivity of argon obtained by Lin, Resler, and Kantrowitz (ref. 33) in a series of shock-tube experiments. The experimental values are divided into two groups, those where equilibrium was reached during the available time interval ($T > 10{,}000^\circ$ K) and those where the conductivity was still rising, at the end of the available time interval ($6{,}000^\circ < T < 10{,}000^\circ$ K). For the latter group the experimental points represent the maximum conductivity attained. Experimental points below $6{,}000^\circ$ K were not considered to be accurate because of the relatively large amount of electrons originating from impurity atoms.

The experimental values were lower than those predicted in reference 33 by a factor of 25 at $6{,}500^\circ$ K and by a factor of 7 at $8{,}000^\circ$ K. At temperatures above $10{,}000^\circ$ K, the agreement is fairly good. Lin et al. attributed the disparity at the lower degrees of ionization to insufficient testing time to reach equilibrium, and inaccurate values of the electron-atom cross section. It is a matter of conjecture, however, as to whether these two effects could explain such large disparities.

In contrast, the electrical conductivity values calculated by the second-order Chapman-Enskog formulation (eq. (46)) are also shown in figure 11. The agreement is much better in the region of low ionization where the predicted values were higher than Lin's experimental values by approximately 50 percent. At temperatures above $10{,}000^\circ$ K, the agreeement is good, indicating the validity of the rigorous Chapman-Enskog formulation for calculating the electrical conductivity of partially ionized gases at high degrees of ionization.

---

[6]A Lorentzian gas is defined as a binary gas where the mass of one type of particle is very small compared with the mass of the other, and where the interaction between the light particles is negligible compared with the interaction between unlike particles.

Indirectly, the agreement is also an indication of this validity for calculating the translational thermal conductivity of partially ionized gases because the determinant elements for both these conductivities are identical except for a multiplicative constant.

Cross sections.- In addition to the approximations described in the preceding paragraphs, Hansen made several other simplifications in reference 1, which affected the values of the viscosity and translational thermal conductivity. The simplification which produced the greatest changes consisted of relating the interparticle potential directly to the collision cross section[7] $\bar{\Omega}_{ij}^{(1,1)}$ and $\bar{\Omega}_{ij}^{(2,2)}$. The purpose of the simplification was to bypass the extremely complex steps which lead from the interparticle potential to the collision variables χ, γ_{ij}, and b, and finally to the collision integral (eq. (17)). Hansen's simplification consisted of taking the effective collision diameter, σ_{ij}, as the interparticle distance where the potential is equal to an empirically determined value. The effective collision cross section is then defined as

$$\bar{\Omega}_{ij} = \pi\sigma_{ij}^2(r) \tag{53}$$

For the viscosity cross section $\bar{\Omega}_{ij}^{(2,2)}$ (i.e., the transfer of momentum and energy), the value of the potential is taken as $\pm kT$, and for the diffusion cross section $\bar{\Omega}_{ij}^{(1,1)}$, the value is taken as $\pm 2kT$.

Figure 12 shows comparisons between the cross sections obtained by the empirical method and the Chapman-Enskog cross sections. The results are presented in the form of a ratio of the empirical cross section to the Chapman-Enskog cross section. The value of the inverse power, n, used in the various interparticle potentials is shown in the upper margin. The rigorous and empirical cross sections are within a few percent of each other for atom-atom ($r^{-8.33}$) and atom-ion (approximately $r^{-14.4}$) interactions. For atom-electron interactions ($r^{-3.65}$), the viscosity cross sections $\bar{\Omega}_{A\text{-}e}^{(2,2)}$ agree within a few percent, but the diffusion cross section $\bar{\Omega}_{A\text{-}e}^{(1,1)}$ for the empirical method is 13 percent lower. The empirical method is completely inadequate for obtaining Coulombic type cross sections (eq. (31)). For this case the effective inverse power is much smaller (equal to or more than 1 because of the shielding

---

[7]The collision cross sections, $\bar{\Omega}_{ij}$, are related to the collision integrals, Ω_{ij}, by

$$\bar{\Omega}_{ij}^{(1,1)} = \left(\frac{2\pi\mu_{ij}}{kT}\right)^{1/2} \Omega_{ij}^{(1,1)}$$

$$\bar{\Omega}_{ij}^{(2,2)} = \left(\frac{\pi\mu_{ij}}{2kT}\right)^{1/2} \Omega_{ij}^{(1,1)}$$

correction), and the strength of the potential is much greater. The result is that the empirical viscosity cross section is 20 percent lower at a pressure of 10^2 atmosphere, and 80 percent lower at a pressure of 10^{-4} atmosphere. The disparity for the diffusion cross sections is even greater. For example, the empirical diffusion cross section is 95 percent lower at a pressure of 10^{-4} atmosphere.

To determine whether the discrepancies for the Coulombic cross sections stem from the increased magnitude of the potential or its range (i.e., n), the rigorous and empirical cross sections were calculated for a hypothetical series of inverse-power potentials,

$$\varphi_{ij}(r) = Kr^{-n} \tag{54}$$

The constant of proportionality, K, was adjusted to give all the potentials the same magnitude at a given intermolecular distance. The results are shown as the solid lines in figure 12. A comparison of the cross sections for this hypothetical series with those for the argon cross sections indicates that the shortcomings of the empirical method are independent of the strength of the potential (i.e., the constant of proportionality), but are strongly dependent upon the "hardness" of the assumed model. In other words, the empirical method fails for low inverse power (i.e., "squishy" models). As a result, the empirical method for calculating viscosity cross sections should not be used for inverse powers less than 2, and that for calculating diffusion cross sections should not be used for inverse powers less than 5.

These discrepancies in the empirical cross sections are reflected in large errors in the viscosity and translational thermal conductivity. The magnitude of these errors can be seen by substituting the empirical cross sections into the 00 subdeterminant for η and the 11 subdeterminant for λ_t, then comparing corresponding values η and λ_t based on the Chapman-Enskog cross sections (figs. 7 and 13). The η values based on the empirical cross sections are 5 percent smaller for neutral argon, but larger by varying amounts at appreciable degrees of ionization. For complete ionization, where the values of η are relatively small, the discrepancies range from 250 percent at the lowest pressure to 40 percent at the highest pressure. The λ_t values for both sets of cross sections are approximately the same at zero ionization. As the degree of ionization increases, the λ_t values based on the empirical cross sections are greater. For example, the discrepancy at a pressure of 10^{-4} atmosphere for completely ionized argon is 140 percent. Comparing the discrepancies in the basic transport coefficients (figs. 7 and 13) with the discrepancies in the cross sections (fig. 12) points out two facts. First, the diffusive cross sections do not have an appreciable effect on η and λ_t. Second, the relatively good agreement at the highest pressure can be attributed to the fact that the increased Debye shielding effect has made the colliding particles "harder."

For a fully ionized gas (i.e., a mixture of equal numbers of electrons and singly ionized atoms) all binary interactions are described by the shielded Coulomb potential (eq. (31)). Using equation (31) is equivalent to assuming a finite upper limit on the impact parameter in the collision integral (eq. (17)). In other words, a limit on the range of the Coulomb force between two particles is established. It was shown in reference 27 that this upper limit corresponds approximately to the Debye shielding length, h, defined in equation (32). However, a comparison of h with the average particle distance, $n^{-1/3}$, in the following table shows that h is larger than $n^{-1/3}$ for the range of temperatures and pressures in this paper.

P, atm	T, °K	$h/n^{-1/3}$
10^{-4}	15,000	4.42
10^{-2}	18,000	2.32
1	30,000	1.51
10^{2}	50,000	.99

This physical situation is not in accord with the basic assumption of binary collisions and, at first appearance, indicates that the Boltzmann equation is not valid for gases with an appreciable degree of ionization. This situation prompted Spitzer and his coworkers (refs. 34 and 35) to derive a theory which describes transport phenomena (specifically electrical and translational thermal conductivity) due to many long-range simultaneous Coulombic interactions with a given particle. The time rate of change of the electron and ion distribution functions caused by particle interactions for the Boltzmann equation (i.e., the right side of eq. (3)) is replaced by the Fokker-Planck expression. Equation (3) then becomes

$$\frac{\partial f_i}{\partial t} + \underline{v}_i \cdot \frac{\partial f_i}{\partial \underline{r}} + \frac{1}{m}\left(\underline{X}_i \cdot \frac{\partial f_i}{\partial \underline{v}_i}\right) = \sum_j \int_0^\infty \int_0^{2\pi} \int_0^{b_o} (f_i' f_j' - f_i f_j) g_{ij} b \, db \, d\epsilon \, d\underline{v}_j$$

$$+ \frac{1}{2} \sum_{X=1}^{3} \sum_{X'=1}^{3} \frac{\partial^2}{\partial v_X \partial v_{X'}} \left(f_j \langle \Delta v_{X,i} \Delta v_{X,j} \rangle \right)$$

$$- \sum_{X=1}^{3} \frac{\partial}{\partial v_X} \left(f_j \langle \Delta v_{X,i} \rangle \right) \qquad (55)$$

The first term on the right side of equation (55) differs from the right side of equation (4) only in that the upper limit of integration is taken as b_o, the distance where the deflection angle is $\pi/2$, rather than ∞. This initial term accounts for close encounters. Spitzer assumed that the cumulative effects of the first term (large angle deflections) are small compared to the second term (small angle deflections). Consequently, the first term on the right side of equation (55) was neglected. The second term accounts for distant encounters which are defined as those with impact parameters between b_o and h. The quantity $\langle \Delta v_{x,j} \rangle$ represents the mean value of the velocity change in particle i, in the x, y, or z direction, in unit time, resulting from distant encounters with particles of type j. Distant encounters are defined as those with impact parameters between b_o and h. Spitzer derived expressions for the various $\langle \Delta v \rangle$ retaining only those terms proportional to $\ln \Lambda$, where

$$\Lambda = \frac{h}{b_o} = \frac{3}{2Z_i Z_j e^3} \left(\frac{k^3 T^3}{\pi n_e} \right)^{1/2} \tag{56}$$

Neglecting nondominant terms introduces an error of the order of $1/\ln \Lambda$.

As a result of Spitzer's analysis, the Boltzmann equation was considered inappropriate for calculating transport properties of a fully ionized gas for a long period of time. Recently Gross (ref. 36), Grad (ref. 37), Koga (ref. 38), and others re-examined the mathematical implications of the Boltzmann and Fokker-Planck equations. They concluded that the Boltzmann equation was valid after all. Grad stated that

> ". . . The critical point here is that, although the two physical pictures are entirely different, their mathematical descriptions are identical! The net effect of many successive independent small impulses is the same as many simultaneous independent small impulses, provided only that the means and variances of the two impulse distributions are the same (actually, the entire probability distributions were taken to be the same). Thus we conclude, without setting pencil to paper, that the Fokker-Planck equation, which is an immediate consequence of the simultaneous grazing impulse model, must yield results identical with those obtained from the Boltzmann equation, provided that an appropriate grazing collision approximation is made and the same cut-off is used in the latter computation.
>
> "For example, the Fokker-Planck equation itself can be obtained by a simple formal manipulation of the Boltzmann collision term; all the collision analysis is classical and need not be repeated. Furthermore, all the transport coefficients which emerge from the Fokker-Planck equation (including heat conductivity, thermal diffusivity, the perpendicular as well as parallel electrical resistivity, all evaluated for an arbitrary magnetic field) are given by well known collision integrals evaluated for the Boltzmann equation with coulomb potential and need not be recomputed . . .

"To improve this result to next order . . . requires inclusion of large angle deflections (which is a triviality if we use the Boltzmann rather than the Fokker-Planck equation) . . ."

In the following sections the second-order Chapman-Enskog values of the electrical and translational thermal conductivity will be compared with Spitzer's values.

The values of λ_t calculated by the Chapman-Enskog approach should be compared with Spitzer's value of the thermal conductivity before any charge separation effects are applied. The equivalence of these two quantities can be shown by a comparison of the heat flux and current density expressions for the two approaches. The current density is defined as

$$\underline{j} = n_I e \overline{\underline{V}}_I - n_e e \overline{\underline{V}}_e \tag{57}$$

Substituting equation (14) into (57) and neglecting the term containing D_I^T/m_I^T, we have the Chapman-Enskog expression for the current density

$$\underline{j} = K_1(m_e D_{Ie} + m_I D_{eI})\underline{E} + \left[K_2\left(m_e D_{Ie} \frac{\partial x_e}{\partial T} - m_I D_{eI} \frac{\partial x_I}{\partial T}\right) + \frac{D_e^T}{m_e^T}\right] \frac{\partial T}{\partial \underline{r}} \tag{58}$$

where the K's are products of thermodynamic quantities, such as number densities, pressure, etc. The corresponding Spitzer expression from reference 26 is

$$\underline{j} = \frac{1}{\eta} \underline{E} + \alpha \frac{\partial T}{\partial \underline{r}} \tag{59}$$

The functional dependence of the heat flux vector[8] of equation (16) can be expressed as

$$\underline{q} = -\lambda_{total} \frac{\partial T}{\partial \underline{r}} = -\lambda_t \frac{\partial T}{\partial \underline{r}} - \lambda_d \frac{\partial T}{\partial \underline{r}} \tag{60}$$

where

$$\lambda_d = \lambda_d(D_{Ie}, D_{eI}, D_e^T, \partial x_I/\partial T, \partial x_e/\partial T, \underline{E}) \tag{61}$$

While the functional dependence of λ_d on $\partial x_I/\partial T$, $\partial x_e/\partial T$, D_e^T, and $\underline{E}$ is explicit (eqs. (15) and (16)), the D_{Ie} and D_{eI} dependence is implicit in the calculation of $\partial x_I/\partial T$ and $\partial x_e/\partial T$. The corresponding Spitzer expression from reference 26 is

---

[8]The reactive thermal conductivity is zero for a binary mixture of electrons and ions of a single type, because of the absence of any chemical reactions.

$$\underline{q} = -\lambda_t \frac{\partial T}{\partial \underline{r}} - \beta \underline{E} \tag{62}$$

where the coefficients in equations (59) and (62) are related to the charge separation correction, ϵ, by

$$\epsilon = 1 - \frac{\beta\alpha\eta}{\lambda_t} \tag{63}$$

Spitzer's final expression for the total thermal conductivity is then

$$\lambda_{total} = \lambda_t - \beta\alpha\eta \tag{64}$$

Comparing equation (58) with (59), equation (60) with (64), and noting the functional dependence of equation (61) shows that the charge separation effects in the Chapman-Enskog formulation are contained in the thermal diffusive component of the thermal conductivity.

In principle, the Chapman-Enskog values of λ_t, η, and σ should be the same as the Spitzer values because of the equivalence of the Boltzmann, and Fokker-Planck equations. However, some basic differences arise in going from the basic equations to the expressions for the transport coefficients. These differences are summarized in table I. It can be seen that the Chapman-Enskog formulation is more complete in two respects. First, close encounters (i.e., large-angle deflections) are accounted for. This is reflected in the modes of velocity description. For example, Spitzer uses the concept of the diffusion coefficient, $\langle v_{x,i} \rangle$, which is valid only for small angle deflections, whereas Chapman and Enskog express the velocity in terms of Sonine polynomials, which is valid for both large and small angle deflections. It is also reflected in the lower limit of integration for the impact parameter. Chapman and Enskog use zero, whereas both Spitzer and Braginskii (ref. 39) use the quantity b_0, the impact parameter corresponding to a deflection angle of $\pi/2$. The second advantage of the Chapman-Enskog formulation is that the ion-ion interaction,[9] as well as the effect of this interaction on ion-electron and electron-electron interactions are also accounted for. The discussion in the preceding section on partially ionized gases pointed out that the effect of heavy particle diffusion could become quite important.

The values of the translational thermal conductivity, λ_t, electrical conductivity, and viscosity, η, for the various approaches are given in table I. The Chapman-Enskog values of the viscosity are almost identical with the Braginskii values at conditions of high Λ. As the large-angle encounters become more important (i.e., lower values of Λ) the Chapman-Enskog values become slightly larger than the Braginskii values. This agreement is not unexpected, since the Sonine polynomial expansion was used in both approaches. The relatively large difference (16 percent) at the smallest Λ may be attributed to the greater importance of large-angle deflections (impact parameters between 0 and b_0). Koga presented a detailed discussion of this point in reference 38. The Chapman-Enskog values of the electrical conductivity agree

[9]Spitzer did not derive an expression for the viscosity as the predominate interaction for this coefficient, the ion-ion interaction, was neglected.

quite well with the Spitzer values, especially at large Λ. At the condition of smallest Λ, the Chapman-Enskog value is 7 percent larger. Again, this small disparity may be attributed to large-angle deflections.

This excellent agreement between the Chapman-Enskog and Spitzer values of the electrical conductivity brings up an apparent paradox. The comparison for the translational thermal conductivity shows that the Chapman-Enskog values are lower by a factor of 3. A comparison of the elements in the Chapman-Enskog determinant for the electrical conductivity (eq. (44)) with those for the translational thermal conductivity (eq. (33)) shows the source of the disparity. The relation between the two sets of elements is given in equation (34). It is seen that the elements for the translational thermal conductivity are proportional to those for the electrical conductivity, where the constant of proportionality contains the factor $\sqrt{m_i m_j}$. Consequently, if it is assumed that the electron-electron interactions are of equal importance for the two conductivities, then the electron-ion interaction is 100 times as important in the translational conductivity, and the ion-ion interaction is 10,000 times as important. Yet, this last interaction is precisely the one Spitzer ignored and the second is one he incompletely described.

It should be pointed out that both the Chapman-Enskog and Spitzer approaches are accurate to within a factor $1/\ln \Lambda$ (ref. 37). The uncertainty is attributed to the neglect of nondominant terms. Although there have been several theories which account for these nondominant terms (refs. 40 to 42), the development of these theories has not progressed to the point where they will yield numerical values for the various transport coefficients.

Reactive and Thermal Diffusive Components of Thermal Conductivity

The calculation of the last two components of thermal conductivity, λ_r and λ_d, requires two sets of variables. The first set can be described as microscopic in viewpoint and the second as macroscopic. The first set consists of the basic transport coefficients described in the preceding sections. These coefficients are defined as the ones prescribed only by collision processes. Although the expressions for calculating these coefficients are relatively complex, at least their solution is presented in closed form.

The second set of variables are the concentration gradients for the various species. Because of their macroscopic nature, the concentration gradients are affected if any forces, $\underline{X}(\underline{r})$, external or internal, enter the general Boltzmann equation (eq. (3)). For a partially or fully ionized gas, the existence of a difference in the ion and electron concentration gradients induces a charge separation field, $\underline{E}_s$, given by Poisson's equation

$$\nabla \cdot \underline{E}_s = [n_I(1) - n_e(1)]e \tag{65}$$

where $n_i(1)$[10] are the nonequilibrium number densities. The force dependence means that the gradients can no longer be presented in closed form, as was the case for dissociating gases (ref. 9) where no force term existed. If the coupling between the concentration gradients and the charge separation field were properly accounted for in the solution of the Boltzmann equation, the complexity of the calculation of λ_r and λ_d would be significantly increased.[11] The existing calculation of the gradients and the extent to which charge separation is accounted for are discussed in this section.

An expression for the reactive thermal conductivity of a dissociating gas was derived by Butler and Brokaw (ref. 9). They made no claims that it could be used for a partially ionized gas. Nevertheless, this expression is being used for a partially ionized gas (refs. 1 to 6), and in some cases for a doubly ionized gas (refs. 4 and 6). Butler and Brokaw solved for the concentration gradients by using two expressions. The first expression is obtained by taking the gradient of both sides of the expression for the equilibrium constant, K_p

$$K_p = \prod_{i=1}^{\nu} (p_i)^{a_i} = \prod_{i=1}^{\nu} (x_i p)^{a_i} \tag{66}$$

where the a_i's are the stoichiometric coefficients for the reaction. The result of the differentiation is a relation between the concentration gradients and known thermodynamic quantities

$$\frac{\partial \ln K_p}{\partial T} \frac{\partial T}{\partial \underline{r}} = \sum \frac{a_i}{x_i} \frac{\partial x_i}{\partial \underline{r}} \tag{67}$$

Equation (67) is very general and is valid for partially or fully ionized gases, provided the reaction rates are sufficiently rapid (i.e., local chemical equilibrium).

The second expression states that the net flux of atoms of each kind, either as free atoms or combined in molecules, is zero for steady-state conditions. This condition can be expressed as

$$\sum_i x_i \underline{V}_i \alpha_{ij} = 0 \qquad j = 1,2, \ldots, \nu \tag{68}$$

---

[10]The nonequilibrium number densities, $n_i(1)$, in equation (65) differ fundamentally from the equilibrium values used throughout the preceding portions of this paper. The values of the equilibrium, or zero order, number densities differ from the nonequilibrium values by a very small amount and consequently could be used where the difference of n_I and n_e is not a factor. However, the equilibrium values cannot be used in equation (65); otherwise a zero value of $\underline{E}_s$ would result.

[11]Meador in a private communication points out that a rigorous development of the Chapman-Enskog formulation would necessitate a dependence of the Sonine polynomial expansion on the charge separation field.

where α_{ij} is the integer denoting the number of atoms of type j contained in the ith molecule. For the water gas reaction $H_2O + CO \rightleftarrows CO_2 + H_2$, the diffusion velocities are related as follows:

$$x_{H_2O}\underline{\bar{V}}_{H_2O} + x_{H_2}\underline{\bar{V}}_{H_2} = 0 \text{ (H atoms)} \tag{69a}$$

$$x_{CO}\underline{\bar{V}}_{CO} + x_{CO_2}\underline{\bar{V}}_{CO_2} = 0 \text{ (C atoms)} \tag{69b}$$

$$x_{H_2O}\underline{\bar{V}}_{H_2O} + x_{CO}\underline{\bar{V}}_{CO} + 2x_{CO_2}\underline{\bar{V}}_{CO_2} = 0 \text{ (O atoms)} \tag{69c}$$

At this point Butler and Brokaw simplified the expression for the diffusive velocities (eqs. (14) and (15)) as follows: (1) The first-order expressions for the multicomponent diffusion coefficients were used as they were considered sufficiently accurate; (2) thermal diffusion effects were assumed to be negligible; and (3) macroscopic force fields were assumed to be absent. These three assumptions are valid for a dissociating gas. The final expression for λ_r results from these simplifications and the combining of equations (67) and (68). The expression is given as

$$\lambda_r = \frac{RT^2 \left(\frac{\partial \ln K_p}{\partial T}\right)^2}{\sum_i \sum_j \frac{RT}{p\mathscr{D}_{ij}(1)} \frac{a_i}{x_i} (a_i x_j - a_j x_i)} \tag{70}$$

This expression should be re-examined for a partially or fully ionized gas. For partially ionized gases, there are defects in equation (70) which should be obvious in light of the discussion in previous sections. These defects lie in the three simplifying assumptions which were made for a dissociating gas. Second-order multicomponent diffusion coefficients should have been used and thermal diffusion effects should have been included in the expression for the diffusion velocities. Since the coefficients $D_{ij}(2)$ and $D_i^T(2)$ can be calculated, they can be incorporated into the calculation of λ_r and λ_d without undue difficulty. However, the solution would not be in the form of a single equation, but rather a set of simultaneous equations.

The greatest defect of equation (70) is its complete neglect of the charge separation field. To determine whether the effect of the charge separation field can be included in the framework of the Chapman-Enskog formulation, the functional dependence of the field will be examined in this and subsequent paragraphs. Ambipolar diffusion of charged particles due to inhomogeneities (i.e., temperature or concentration gradients) results in a charge separation field. This phenomenon has been discussed quite thoroughly by Allis in reference 43 for the case of a fully ionized gas. For the case where the over-all dimensions of the plasma are greater than either the Debye length or the mean free path, Allis makes the assumption of proportionality,

$$\frac{1}{x_I}\frac{\partial x_I}{\partial \underline{r}} = \frac{1}{x_e}\frac{\partial x_e}{\partial \underline{r}} \tag{71}$$

which results in the expression for the charge separation field

$$\underline{E}_s = (D_s - D_e) \frac{m_e \nu_{c_e}}{e} \cdot \frac{1}{x_e} \frac{\partial x_e}{\partial \underline{r}} \tag{72}$$

The quantity D_e is the field free ambipolar diffusion coefficient for the electron. For a particle of species i, D_i is defined as

$$D_i = \frac{v_i^2}{3\nu_{c_i}(v_i)} \tag{73}$$

where the collision frequency, ν_{c_i}, depends upon the particle velocity, v_i. The quantity D_s is the effective ambipolar diffusion coefficient for the electron and is an explicit function of the electrical conductivity, σ, the collision frequencies ν_{c_1} and ν_{c_e}, and, more important, a function of the space charge density, $(n_I(1) - n_e(1))e$.

Once the functional dependence of the charge separation field for a fully ionized gas is known, two questions arise: First, what modifications must be made for partially ionized gases. Second, are the expressions in equations (72) and (73) compatible with the Chapman-Enskog formulation. The answer to the first question is that the effects of neutral particles are automatically accounted for if one uses the electrical conductivity (eq. (46)) and collision frequencies for partially ionized gases. The answer to the second question is that equations (72) and (73) are not compatible because the ambipolar diffusion coefficients and the collision frequencies are both velocity dependent. As a result, the expression for $\underline{E}_s$ is also velocity dependent. If $\underline{E}_s$ is to be included in the total force, $\underline{X}_i$, in the Boltzmann equation (eq. (3)), then an extensive modification of the entire Chapman-Enskog formulation would be required. Specifically, this would necessitate a dependence of the Sonine polynomial expansion on the charge separation field. However, if the gross assumption is made that the ambipolar diffusion coefficients and collision frequencies are averaged over all velocities (i.e., the particle velocity can be approximated by the mean kinetic velocity, $\bar{v}$), then the ambipolar diffusion coefficient can be expressed as

$$D_i = \frac{kT}{m_i \nu_{c_i}(T)} \tag{74}$$

As a result, the charge separation force would satisfy the requirement in the Chapman-Enskog formulation that any component of the force term is independent of position and time but not of velocity.

The system of linear equations, which, in principle, should yield solutions for the concentration gradients in the form $\partial x_A/\partial T$, $\partial x_I/\partial T$, and $\partial x_e/\partial T$, and the charge separation field, $\underline{E}_s$, may now be written (eqs. (75), (76), (77), and (78)). These equations stem from equations (67), (68), and (72). Equation (78) indicates that $\underline{E}_s$ is a function of the difference in the first-order number densities, $n_I(1)$ and $n_e(1)$, as are the last two components of the thermal conductivity, λ_r and λ_d. Consequently, for a specified temperature the value of the total thermal conductivity would not be a constant, as is the case for the translational thermal conductivity, but would vary in the

direction of the temperature (i.e., concentration) gradient. This would mean that the total thermal conductivity would be a function of the temperature (i.e., concentration) gradient as well as the temperature,[12] and would greatly increase the complexity of the solution of λ_r and λ_d. Until this difficulty is resolved, accurate predictions of the last two components of the thermal conductivity for a partially ionized gas will not be possible.

$$-\frac{1}{x_A}\frac{\partial x_A}{\partial T}+\frac{1}{x_I}\frac{\partial x_I}{\partial T}+\frac{1}{x_e}\frac{\partial x_e}{\partial T}=\frac{1}{T}\left(T\,\frac{d\ \ln K_p}{dT}\right) \tag{75}$$

$$\frac{n^2}{\rho}\left[m_I D_{AI}\left(\frac{\partial x_I}{\partial T}-\frac{n_I}{p}\,\frac{E_s e}{\partial T/\partial r}\right)+m_e D_{Ae}\left(\frac{\partial x_e}{\partial T}+\frac{n_e}{p}\,\frac{E_s e}{\partial T/\partial r}\right)\right]-\frac{D_A^T}{m_A T}$$

$$=-\frac{n^2}{\rho}\left[m_A D_{IA}\,\frac{\partial x_A}{\partial T}+m_e D_{Ie}\left(\frac{\partial x_e}{\partial T}+\frac{n_e}{p}\,\frac{E_s e}{\partial T/\partial r}\right)\right]+\frac{D_I^T}{m_I T} \tag{76}$$

$$\frac{n^2}{\rho}\left[m_I D_{AI}\left(\frac{\partial x_I}{\partial T}-\frac{n_I}{p}\,\frac{E_s e}{\partial T/\partial r}\right)+m_e D_{Ae}\left(\frac{\partial x_e}{\partial T}+\frac{n_e}{p}\,\frac{E_s e}{\partial T/\partial r}\right)\right]-\frac{D_A^T}{m_A T}$$

$$=-\frac{n^2}{\rho}\left[m_A D_{eA}\,\frac{\partial x_A}{\partial T}+m_I D_{eI}\left(\frac{\partial x_I}{\partial T}-\frac{n_I}{p}\,\frac{E_s e}{\partial T/\partial r}\right)\right]+\frac{D_e^T}{m_e T} \tag{77}$$

$$\frac{E_s e}{\partial T/\partial r}=kTm_e\nu_{c_e}\left\{\left(\frac{2}{m_I\nu_{c_I}+m_e\nu_{c_e}}\right)\left[1+\frac{e^2}{m_e\nu_{c_e}\sigma}\,(n_I-n_e)\right]-\frac{1}{m_e\nu_{c_e}}\right\}\frac{1}{x_e}\,\frac{\partial x_e}{\partial T} \tag{78}$$

---

[12] It was pointed out in the introduction that in Maecker's experiment (ref. 10) there may be either an experimentally induced error or an unpredicted phenomenon, because the experimental values of the total thermal conductivity at the given temperature increase as the arc current is increased. A possible cause is the change in the temperature gradient due to the change in arc current.

CONCLUDING REMARKS

Existing methods for calculating transport coefficients of a partially ionized gas are based on the Chapman-Enskog expansion of the Boltzmann equation. However, significant simplifications in the theory were made for the case of a nonreactive mixture of monatomic gases near room temperature. These simplifications were carried over to the case of dissociating and ionizing gases without justification. Comparison of the values of the basic transport coefficients calculated by the existing methods with those calculated by the rigorous second-order Chapman-Enskog formulation shows relatively large disparities for partially ionized gases. For example, the existing methods underestimated the translational thermal conductivity and certain multicomponent diffusion coefficients by 25 to 60 percent at high degrees of ionization, and overestimated the electrical conductivity by an order of magnitude at low degrees of ionization. In addition, the existing methods completely overlooked thermal diffusive effects. A comparison of the electrical conductivity values, calculated by the rigorous second-order Chapman-Enskog formulation with experimental values, indicates the validity of the approach for calculating the translational thermal conductivity, as well as the electrical conductivity, at high degrees of ionization.

The thermal diffusion coefficients for the atom, ion, and electron were calculated in this paper. A comparison of these coefficients shows that the thermal diffusion effects can be attributed almost entirely to the electron term, and that the values of D_e^T calculated for partially ionized argon can be used for other partially ionized gases to a good degree of accuracy. Also, a comparison of these coefficients and the multicomponent diffusion coefficients shows that the diffusive motions of the ion and atom are strongly coupled and are almost independent of the diffusive motion of the electron up to high degrees of ionization. This behavior can be attributed to the extremely small mass of the electron. It should be pointed out that this dominance of heavy particle diffusion also would exist if the heavier particles were ions of a single type diffusing with respect to each other due to temperature and/or concentration gradients, or ions of a given charge diffusing with respect to ions of a different charge.

The calculations in this paper were carried out to the point of complete ionization (i.e., a mixture of equal numbers of singly ionized argon atoms and electrons). The values of translational thermal conductivity and electrical conductivity calculated by the second-order Chapman-Enskog formulation (binary collisions) were compared with those calculated by Spitzer approach (simultaneous collisions). The two sets of electrical conductivity values compare favorably (discrepancies of less than 4 percent for most cases). However, the Chapman-Enskog values of the translational thermal conductivity are lower by a factor of three. This large disparity can be attributed to Spitzer's neglect of ion-ion interactions and their effect on electron-ion interactions, which are more important by orders of magnitude in the translational thermal conductivity as compared to the electrical conductivity.

In addition to accurate values of the basic transport coefficients (microscopic viewpoint), accurate values of the atom, ion, and electron concentration gradients (macroscopic viewpoint) are needed for the calculation of the last two components of the thermal conductivity, λ_r and λ_d. Existing calculations of the concentration gradients utilize approximate basic transport coefficients which are in considerable error. The existing methods also neglect the charge-separation field, $\underline{E}_s$, which may profoundly affect the concentration gradients of ions and electrons. The functional dependence of the charge-separation field has been examined. The examination indicates that $\underline{E}_s$ is a function of the difference in the first-order number densities of ions and electrons. Consequently, for a specified temperature, the value of the total thermal conductivity would not be a constant, but would vary in the direction of the temperature gradient. This would greatly increase the complexity of the solution of λ_r and λ_d. Until the difficulty is resolved, accurate predictions of the last two components of the thermal conductivity for a partially ionized gas will not be possible.

Ames Research Center
National Aeronautics and Space Administration
Moffett Field, Calif., Sept. 17, 1964

APPENDIX A

THERMODYNAMIC PROPERTIES OF PARTIALLY IONIZED ARGON

The calculation of the thermodynamic properties of an equilibrium gas is well established. The particular approach used in this paper is admittedly an approximate one. Refinements such as the lowering of the ionization potential and virial corrections to the equation of state have been omitted because of the added complexity.

Only the pertinent equations for the thermodynamic quantities will be given in the following section. The development of the equations and the assumptions used can be found in references 1 and 4. All thermodynamic functions can be expressed in terms of the partition function. This function for a given mode of energy is defined as

$$Q = \sum_i g_i \exp(-\epsilon_i/kT) \tag{A1}$$

where ϵ_i is the ith quantum level, and g_i is the degeneracy or the total number of states which have different internal configurations but have the same energy level. The partition function of equation (2) reduces to

$$Q_t = \left(\frac{2\pi mk}{h^2}\right)^{3/2} \frac{R}{p} (T)^{5/2} \tag{A2}$$

for the translational mode (ref. 44). The functions for the various particles are

$$\ln Q_p(A) = \frac{5}{2}\ln T + 1.8662 + \ln[\sum_i g_i \exp(-\epsilon_i/kT)] \tag{A3a}$$

$$\ln Q_p(A^+) = \frac{5}{2}\ln T + 1.8662 + \ln[\sum_j g_j \exp(-\epsilon_j/kT)] \tag{A3b}$$

$$\ln Q_p(e^-) = \frac{5}{2}\ln T + 14.234 \tag{A3c}$$

The atomic energy levels and the first ionization potential, as derived from spectroscopic analyses, are taken from reference 45. The cutoff terms are arbitrarily taken where the outer electron energy initially reaches the excited state corresponding to the fifth principle quantum number (ref. 46).

The equilibrium constant is the basis for the determination of the equilibrium mol fractions $x(A)$, $x(A^+)$, and $x(e^-)$. The pressure equilibrium constant for single ionization expressed in terms of the partition functions is

$$\ln K_p = - \frac{E_I}{kT} + \ln Q_p(A^+) + \ln Q_p(e^-) - \ln Q_p(A) \qquad (A4)$$

where the ionization potential, E_I/k, has the value 182,850° K (ref. 45).

Thermodynamic functions determined separately for each of the species A, A^+, and e^- are combined with the equilibrium mol fractions and their corresponding derivatives to yield the thermodynamic properties of the equilibrium mixture. Generally, in engineering calculations the energy per fixed mass of gas is needed rather than the energy per mol. This quantity can be obtained by multiplying E/RT, the energy per mol, by Z, the total number of mols per mol of initially neutral argon (i.e., a fixed mass of 39.944 grams). The expression for the dimensionless energy is given as

$$\frac{ZE}{RT} = Z \sum_i x_i \frac{E_i}{RT} \qquad (A5)$$

where E_i is the energy per mol for component i. The dimensionless enthalpy per initial mol of argon becomes

$$\frac{ZH}{RT} = \frac{ZE}{RT} + Z \qquad (A6)$$

The compressibility, Z, dimensionless energy, ZE/RT, and dimensionless enthalpy, ZH/RT, which have been calculated from the preceding equations, are shown in figures 14, 15, and 16. The entropy per initial mol of argon is obtained from the separate entropies of the various species by the summation

$$\frac{ZS}{R} = Z\left(\sum_i x_i \frac{S_{i_o}}{R} \sum_i x_i \ln x_i - \ln \frac{p}{p_o}\right) \qquad (A7)$$

where p_o is the reference pressure of the standard state, in this case 1 atmosphere, and S_{i_o}/R is the entropy of component i at 1 atmosphere. The entropy values are shown in figure 17.

The specific heat at constant density per initial mol of undissociated nitrogen is given by

$$\frac{Zc_v}{R} = Z \sum_i x_i \frac{c_i}{R} + T \sum_i \frac{E_i}{RT} \left(\frac{\partial Z x_i}{\partial T}\right)_\rho \qquad (A8)$$

where c_i is the derivative of energy for component i, that is, $\partial E_i/\partial T$. The corresponding equation for the specific heat at constant pressure is

$$\frac{Zc_p}{R} = Z\sum_i x_i\left(\frac{c_i}{R} + 1\right) + T\sum_i\left(\frac{E_i}{RT} + 1\right)\left(\frac{\partial Zx_i}{\partial T}\right)_p \qquad (A9)$$

The specific heats calculated from equations (A8) and (A9) are presented in figures 18 and 19.

The speed of sound can be calculated from the specific heat values determined above. The dimensionless speed-of-sound parameter, $a^2\rho/p$, was derived in reference 1 in terms of variables already calculated

$$\frac{a^2\rho}{p} = \gamma\,\frac{1 + (T/Z)(\partial Z/\partial T)_\rho}{1 + (T/Z)(\partial Z/\partial T)_p} \qquad (A10)$$

This dimensionless speed-of-sound parameter is shown in figure 20 as a function of temperature.

The calculation of these thermodynamic properties is based on the use of the ideal gas law to describe the partial pressure for each component (i.e., atoms, ions, and electrons). Strictly speaking, the use of this law implies that particles are vanishingly small, and that intermolecular forces are nonexistent. The actual existence of intermolecular forces means some deviation from the ideal gas law. It can be seen in reference 47 that the ideal gas approximation is accurate to within 1 percent for the range where argon exists in the atomic form ($T < 5{,}000^\circ$ K), except for small regions of pressures ($p > 10^2$ atm).

At temperatures greater than $5{,}000^\circ$ K the amount of ionized species becomes appreciable, and the use of the ideal gas law must be examined in the light of the screened Coulomb potential of equation (31). Duclos used this potential in reference 48 to calculate the contribution of electrostatic energy to the thermodynamic properties of a fully ionized gas. The Debye pressure correction to the ideal gas equation of state was found to be

$$\Delta p_d = -\frac{e^2 n_3}{3h} \qquad (A11)$$

For the case of a fully ionized gas (i.e., a mixture of singly ionized argon atoms and electrons) the quantity h is the Debye shielding distance as defined in equation (32). The fractional pressure correction is then

$$\frac{\Delta p_d}{p_{ideal}} = -\frac{\sqrt{2\pi n_3}\, e^3}{3(kT)^{3/2}} \qquad (A12)$$

For a given temperature the pressure correction varies as the square root of the electron density, n_3. The correction for a partially ionized gas can be approximated by multiplying the right side of equation (A12) by the percentage

ionization. This approximation is based on the fact that the range and magnitude of the Coulomb force is an order of magnitude greater than those for interaction between A-A, $A-A^+$, and $A-e^-$.

The variation of electron density with temperature and pressure is shown in figure 21, along with lines of constant percentage ionization. A line representing conditions where the quantity $\Delta p_d/p_{ideal}$ is equal to 1 percent for a fully ionized gas is also superimposed upon figure 21. Above this line the correction is greater than 1 percent. It can be seen that the shielded Coulomb potential results in less than 1 percent departure over the largest part of the range covered in this report. At the point of highest electron concentration ($T = 30{,}000^{\circ}$ K, $p = 10^3$ atm) where the ionization is approximately 50 percent, the equation of state correction is of the order of 4 percent.

APPENDIX B

SHOCK-WAVE VARIABLES FOR PARTIALLY IONIZED ARGON

For a range of temperatures and pressures where ideal gas behavior is no longer valid, the shock-wave relations cannot be given analytically in terms of initial conditions, but must be obtained by iteration. These iterative solutions must satisfy certain conservation relations (ref. 49) which are expressed in terms of state variables in front of and behind shock waves. The specific approach taken in this paper is outlined in the following paragraphs.

The solution for the incident shock-wave quantities begins with the specifications of an initial temperature, T_1, pressure, p_1, and pressure ratio across the incident shock, p_{21}. The temperature behind the incident shock, T_2, is determined by a single iteration.

The iteration proceeds as follows. Assumption of a T_2 for a given p_{21} allows the compressibility Z_2 and enthalpy Z_2H_2/RT_2 to be calculated by the methods described earlier. These quantities are then used to express the enthalpy ratio and density ratio across the incident shock

$$h_{21} = \frac{(Z_2H_2/RT_2)T_2}{(Z_1H_1/RT_1)T_1} \tag{B1}$$

$$\rho_{21} = p_{21}\frac{T_1Z_1}{T_2Z_2} \tag{B2}$$

Iteration on T_2 will lead to the proper choice of T_2 such that the resulting state variables and enthalpy will satisfy the basic shock relation

$$\frac{2h_1\rho_1}{p_1}(h_{21} - 1) = (p_{21} - 1)(\rho_{12} + 1) \tag{B3}$$

where the quantity

$$\frac{h_1\rho_1}{p_1} = \frac{(Z_1H_1/RT_1)}{Z_1} \tag{B4}$$

The derivation of the basic shock relation can be found on page 21 of reference 49.

The basic shock relation also will be used for the solution of the reflected shock wave in the form

$$\frac{2h_2\rho_2}{p_2}(h_{32} - 1) = (p_{32} - 1)(\rho_{23} + 1) \tag{B5}$$

The solution of the reflected shock wave will require an additional relation for a double iteration, as neither p_3 nor T_3 can be specified initially. This relation can be derived from an expression on page 22 of reference 49, as follows

$$v_2^2 = (u_1 - u_2)^2 = \frac{p_1}{\rho_1}(p_{21} - 1)(1 - \rho_{12}) \tag{B6}$$

where v_2 is the velocity of the gas behind the shock wave relative to a stationary reference system (e.g., shock-tube wall), and the u's are the velocities with reference to the incident shock wave. The form of the equation is also valid for the reflected shock.

$$(w_2 - w_3)^2 = \frac{p_2}{\rho_2}(p_{32} - 1)(1 - \rho_{23}) \tag{B7}$$

where the w's are the velocities relative to the reflected shock wave. The boundary conditions require that

$$w_2 = v_2 + w_3 \tag{B8}$$

$$(w_2 - w_3)^2 = (u_1 - u_2)^2 \tag{B9}$$

and the state variables behind incident and reflected shocks may be related by combining equations (B6) and (B7)

$$\frac{p_1}{\rho_1}(p_{21} - 1)(1 - \rho_{12}) = \frac{p_2}{\rho_2}(p_{32} - 1)(1 - \rho_{23}) \tag{B10}$$

This relation plus the basic shock relation (eq. (B5)) must be simultaneously satisfied by the state variables and enthalpies.

The initial step in the double iteration is to assume a value of p_3 and iterate on T_3, until the basic shock-wave equation (eq. (B5)) is satisfied. The quantities h_{32}, ρ_{32}, and $h_2\rho_2/p_2$, required for this first iteration, can be determined from equations (B1), (B2), and (B4) by replacing the subscript 1 by 2, and the subscript 2 by 3. The resulting T_3 is not necessarily the correct T_3 for the problem, but just the T_3 which should correspond to the assumed p_3. The next step is to take the state variables previously calculated for T_2 and p_2, and the state variables for the T_3 and p_3 which satisfy equation (B5), and apply them to calculate both sides of equation (B10). If equation (B10) is not satisfied, then a new value of p_3 must be assumed and the above process repeated in its entirety.

The iterative solutions for the pressure, density, temperature, and enthalpy are presented in figure 22 for the incident shock and figure 23 for the reflected shock. The solutions are given for an initial temperature of 293° K and five initial pressures varying from 1 to 10^{-4} atmosphere. The

degree of ionization, in the form of the compressibility, Z, is also presented in figures 22 and 23. Rather than using p_{21} as the independent variable, it is more convenient to use the shock-wave Mach number M_s, which is more easily determined in a shock tube experiment. This quantity is defined as the speed of the incident shock wave divided by the speed of sound in undisturbed argon, and is related to the pressure ratio p_{21} by

$$M_s = \frac{p_{21} - 1}{\gamma_1(1 - \rho_{12})^{1/2}} \tag{B11}$$

where γ is the ratio of specific heats, and is equal to 5/3 for the initial conditions assumed in this paper. The state variables are presented as the ratio of the calculated real-gas variable to that for the ideal gas (superscript*). This dimensionless form was chosen to maintain the same degree of accuracy on the graphs throughout the range of shock-wave Mach numbers. Note that the displacements of the curves are about proportional to the logarithm of the initial pressure p_1, so it is possible to interpolate between the curves with reasonable accuracy. The expressions for the ideal gas variables behind incident and reflected shocks are

Incident Shock

$$p^*_{21} = \frac{2\gamma M^2 - (\gamma - 1)}{\gamma + 1} \tag{B12a}$$

$$\rho^*_{21} = \frac{(\gamma + 1)M^2}{(\gamma - 1)M^2 + 2} \tag{B12b}$$

$$T^*_{21} = h^*_{21} = \frac{p^*_{21}}{\rho^*_{21}} \tag{B12c}$$

Reflected Shock

$$p^*_{32} = \frac{(\alpha + 2)p^*_{21} - 1}{\alpha + p^*_{21}} \tag{B13a}$$

$$\rho^*_{32} = \frac{(1 + \alpha p^*_{32})}{(\alpha + p^*_{32})} \tag{B13b}$$

$$T^*_{32} = h^*_{32} = \frac{p^*_{32}}{\rho^*_{32}} \tag{B13c}$$

where

$$\alpha = \frac{\gamma + 1}{\gamma - 1} \tag{B13d}$$

APPENDIX C

SECOND-ORDER EXPRESSIONS FOR VISCOSITY AND MULTICOMPONENT DIFFUSION COEFFICIENTS

The mathematical formalism required for the second-order viscosity and multicomponent diffusion coefficients is described in detail in reference 8. Unfortunately, no explicit expressions for the second-order values of η and D_{ij} are given since the first-order values were considered sufficiently accurate for a neutral gas. Consequently, a brief outline of the derivation of $\eta(2)$ and $D_{ij}(2)$ is given in this appendix. The physical connotations of the variables will not be discussed, as they can be found in reference 8.

The second-order viscosity coefficient is expressed in terms of the Sonine expansion coefficients, b_{jo}, as

$$\eta(2) = \frac{1}{2} kT\Sigma n_j b_{jo}(2) \tag{C1}$$

The Sonine expansion coefficients, in turn, are the solutions of a set of linear equations, with the $\tilde{Q}_{ij}^{mm'}$ and $\tilde{H}_{ij}^{oo}$ (as defined in eqs. (35) to (38) and (42)) as constant coefficients. These equations are

$$\sum_{j}\sum_{m'=o}^{1} \tilde{Q}_{ij}^{mm'} b_{jm'}(2) = -R_{im}^{(h,k)} \qquad (m = 0,1) \tag{C2}$$

where $\tilde{Q}_{ij}^{oo}$ is replaced by $\tilde{H}_{ij}^{oo}$ when $m = 0$ and $m' = 0$. The variable $R_{im}^{(h,k)}$ for both the viscosity and multicomponent diffusion coefficients is defined as

$$R_{im}^{(h,k)} = \int \left(\underline{\underline{R}}_i^{(h,k)} : \underline{\underline{W}}_i \right) S_n^{(m)}(W_i^2)\, d\underline{V}_i \tag{C3}$$

where the term inside the parenthesis denotes the trace of the tensor product of $\underline{\underline{R}}_i^{(h,k)}$ and $\underline{\underline{W}}_i$ for the viscosity coefficient. The tensor $\underline{\underline{R}}_i^{(h,k)}$ is defined as

$$\left(\underline{\underline{R}}_i^{(h,k)} \right)_{\text{viscosity}} = -2f_{o_i} \left(\underline{W}_i \underline{W}_i - \frac{1}{3} W_i^2 \underline{\underline{U}} \right) \tag{C4}$$

and the tensor $\underline{\underline{W}}_i$ is defined as

$$\left(\underline{\underline{W}}_i \right)_{\text{viscosity}} = \underline{W}_i \underline{W}_i - \frac{1}{3} W_i^2 \underline{\underline{U}} \tag{C5}$$

The Maxwellian distribution, f_{o_i}, is given in equation (2). The reduced velocity $\underline{W}_i$ is defined as

$$\underline{W}_i = \sqrt{\frac{m_i}{2kT}}\,\underline{V}_i \tag{C6}$$

The quantity $\underline{W}_i\underline{W}_i$ is the dyadic and $\underline{\underline{U}}$ is the unit tensor. The Sonine polynomial of order $n = 5/2$ is required for the viscosity coefficient. This particular polynomial satisfies the orthogonality relation

$$\int f_{o_i} S_{5/2}^{(m)}(W_i^2) V_i^4 \, d\underline{V}_i = 15 n_i \left(\frac{kT}{m_i}\right)^2 \delta_{mo} \tag{C7}$$

Combining equations (C3), (C4), and (C5) we have

$$\left(R_{im}^{(h,k)}\right)_{\text{viscosity}} = -\frac{4}{3}\int W_i^4 f_{o_i} S_{5/2}^{(m)}(W_i^2)\, d\underline{V}_i \tag{C8}$$

The integration can be performed through the use of spherical coordinates

$$d\underline{V}_i = V^2 \sin\varphi \, d\theta \, d\varphi \, dV \tag{C9}$$

Combining equations (C7), (C8), and (C9) we have

$$\left(R_{io}^{(h,k)}\right)_{\text{viscosity}} = -\frac{4}{3}\int W_i^4 f_{o_i} \, d\underline{V}_i = -5n_i \qquad (m = 0) \tag{C10}$$

$$\left(R_{i1}^{(h,k)}\right)_{\text{viscosity}} = -\frac{4}{3}\int W_i^4 f_{o_i} S_{5/2}^{(1)}(W_i^2)\, d\underline{V}_i = 0 \qquad (m = 1) \tag{C11}$$

Combining equation (C2) with (C10) and (C11) we have a set of six simultaneous equations

$$\tilde{H}_{i1}^{00} b_{10}(2) + \tilde{H}_{i2}^{00} b_{20}(2) + \tilde{H}_{i3}^{00} b_{30}(2) + \tilde{Q}_{i1}^{01} b_{11}(2) + \tilde{Q}_{i2}^{01} b_{21}(2) + \tilde{Q}_{i3}^{01} b_{31}(2) = 5n_i$$

$$\text{for } (m = 0;\ i = 1,2,3) \tag{C12}$$

$$\tilde{Q}_{i1}^{10} b_{10}(2) + \tilde{Q}_{i2}^{10} b_{20}(2) + \tilde{Q}_{i3}^{10} b_{30}(2) + \tilde{Q}_{i1}^{11} b_{11}(2) + \tilde{Q}_{i2}^{11} b_{21}(2) + \tilde{Q}_{i3}^{11} b_{31}(2) = 0$$

$$\text{for } (m = 1;\ i = 1,2,3) \tag{C13}$$

where the quantities $\tilde{H}_{ij}^{00}$, $\tilde{Q}_{ij}^{01}$, $\tilde{Q}_{ij}^{10}$, and $\tilde{Q}_{ij}^{11}$ are defined in equations (42), (36), (37), and (38). The application of Cramer's rule to the six simultaneous equations (eqs. (C12) and (C13)) results in the determinant expression, equation (41).

The second-order multicomponent diffusion coefficients are derived in the same manner and are expressed in terms of the Sonine expansion coefficients as

$$D_{ij}(2) = \frac{\rho n_i}{2nm_j}\sqrt{\frac{2kT}{m_i}}\, c_{io}^{(j,i)}(2) \tag{C14}$$

In this case, the set of linear equations for $c_{io}^{(j,i)}$ are

$$\sum_{j}\sum_{m'=o}^{1} \tilde{Q}_{ij}^{mm'} c_{jm'}^{(h,k)}(2) = -\left[R_m^{(h,k)}\right]_{diffusion} \qquad (m = 0,1) \tag{C15}$$

For the multicomponent diffusion coefficients the tensor $\underline{\underline{R}}_i^{(h,k)}$ is defined as

$$\left[\underline{\underline{R}}_i^{(h,k)}\right]_{diffusion} = \frac{1}{n_i} f_{o_i}(\delta_{ih} - \delta_{ik})\underline{V}_i \tag{C16}$$

and the tensor $\underline{\underline{W}}_i$ is defined as

$$(\underline{\underline{W}}_i)_{diffusion} = \underline{W}_i = \sqrt{\frac{m_i}{2kT}}\,\underline{V}_i \tag{C17}$$

The Sonine polynomial of order $n = 3/2$ is required for the multicomponent diffusion coefficients. This particular polynomial satisfies the orthogonality relation

$$\int f_{o_i} S_{3/2}^{(m)}(W_i^2) V_i^2 \, d\underline{V}_i = \frac{3n_i kT}{m_i}\delta_{mo} \tag{C18}$$

Combining equations (C3), (C16), and (C17) we have

$$\left[R_{im}^{(h,k)}\right]_{diffusion} = \frac{1}{n_i}\sqrt{\frac{m_i}{2kT}}\int f_{o_i}\underline{V}_i^2 S_{3/2}^{(m)}(W_i^2)\, d\underline{V}_i(\delta_{ih} - \delta_{ik}) \tag{C19}$$

Combining equations (C9), (C18), and (C19), we have

$$\left[R_{io}^{(h,k)}\right]_{diffusion} = 3\sqrt{\frac{kT}{2m_i}}(\delta_{ih} - \delta_{ik}) \qquad (m = 0) \tag{C20}$$

$$\left[R_{i1}^{(h,k)}\right]_{\text{diffusion}} = 0 \qquad (m = 1) \qquad (C21)$$

Combining equation (C14) with (C20) and (C21) we have a set of six simultaneous equations

$$\tilde{Q}_{i1}^{oo}{}^{(h,k)}c_{1o}(2) + \tilde{Q}_{i2}^{oo}{}^{(h,k)}c_{2o}(2) + \tilde{Q}_{i3}^{oo}{}^{(h,k)}c_{3o}(2)$$

$$+ \tilde{Q}_{i1}^{o1}{}^{(h,k)}c_{11}(2) + \tilde{Q}_{i2}^{o1}{}^{(h,k)}c_{21}(2) + \tilde{Q}_{i3}^{o1}{}^{(h,k)}c_{31}(2) = -3\sqrt{\frac{kT}{2m_i}}\,(\delta_{ih} - \delta_{ik})$$

$$(m = 0;\ i = 1,2,3) \qquad (C22)$$

$$\tilde{Q}_{i1}^{1o}{}^{(h,k)}c_{1o}(2) + \tilde{Q}_{i2}^{1o}{}^{(h,k)}c_{2o}(2) + \tilde{Q}_{i3}^{1o}{}^{(h,k)}c_{3o}(2)$$

$$+ \tilde{Q}_{i1}^{11}{}^{(h,k)}c_{11}(2) + \tilde{Q}_{i2}^{11}{}^{(h,k)}c_{21}(2) + \tilde{Q}_{i3}^{11}{}^{(h,k)}c_{31}(2) = 0$$

$$(m = 1;\ i = 1,2,3) \qquad (C23)$$

where the quantities $\tilde{Q}_{ij}^{oo}$, $\tilde{Q}_{ij}^{o1}$, $\tilde{Q}_{ij}^{1o}$, and $\tilde{Q}_{ij}^{11}$ are defined in equations (35) to (38). The application of Cramer's rule to the six simultaneous equations (eqs. (C22) and (C23)) results in the determinant expression, equation (44).

REFERENCES

1. Hansen, C. Frederick: Approximations for the Thermodynamic and Transport Properties of High-Temperature Air. NASA TR R-50, 1959.

2. Thomas, M.: The High Temperature Transport Properties of Carbon Dioxide. Douglas Aircraft Co. SM 37790, 1960.

3. Vanderslice, J. T., Weissman, Stanley, Mason, E. A., and Fallon, R. J.: High-Temperature Transport Properties of Dissociating Hydrogen. Phys. of Fluids, vol. 5, no. 2, Feb. 1962, pp. 155-164.

4. Ahtye, Warren F., and Peng, Tzy-Cheng: Approximations for the Thermodynamic and Transport Properties of High-Temperature Nitrogen With Shock-Tube Applications. NASA TN D-1303, 1962.

5. Peng, Tzy-Cheng, and Pindroh, Albert L.: An Improved Calculation of Gas Properties at High Temperatures: Air. Boeing Co. D 2-11722, 1962.

6. Yos, Jerrold M.: Transport Properties of Nitrogen, Hydrogen, Oxygen, and Air to 30,000° K. Avco Rep. RAD TM-63-7, 1963.

7. Chapman, Sydney, and Cowling, T. G.: The Mathematical Theory of Non-Uniform Gases. Second ed., Cambridge Univ. Press, London, 1952.

8. Hirschfelder, Joseph O., Curtiss, Charles F., and Bird, R. Byron: Molecular Theory of Gases and Liquids. John Wiley and Sons, Inc., N. Y., 1954.

9. Butler, James N., and Brokaw, Richard S.: Thermal Conductivity of Gas Mixtures in Chemical Equilibrium. Jour. Chem. Phys., vol. 26, no. 6, June 1957, pp. 1636-1643.

10. Maecker, H.: The Properties of Nitrogen to 15,000° K. Presented at Meeting on Properties of Gases at High Temperature, AGARD, Aachen, Sept. 21-23, 1959. AGARD Rep. 324.

11. Knof, Hans, Mason, E. A., and Vanderslice, J. T.: Interaction Energies, Charge Exchange Cross Sections and Diffusion Cross Sections for N^+-N and O^+-O Collisions. Univ. of Maryland IMP NASA 35, 1963.

12. Peng, Tzy-Cheng, and Ahtye, Warren F.: Experimental and Theoretical Study of Heat Conduction for Air up to 5,000° K. NASA TN D-687, 1961.

13. John, R. R., et al.: Theoretical and Experimental Investigation of Arc Plasma Generation Technology. Part I. Applied Research on Direct and Alternating Current Electric Arc Plasma Generators. Avco Corp. ASD-TDR-62-729, 1963.

14. Rose, P. H., and Stankevics, J. O.: Stagnation Point Heat Transfer Measurements in Partially Ionized Air. Avco-Everett Research Lab. Res. Rep. 143, BSD-TDR-62-348, 1963.

15. Bosnjakovic, Fran: Thermodynamic and Transport Processes in Multicomponent Systems. Univ. of Minnesota ARL 62-359, 1962.

16. Amdur, I.: An Experimental Approach to the Determination of Gaseous Transport Properties at Very High Temperatures. Proc. Conference on Physical Chemistry in Aerodynamics and Space Flight, Pergamon Press, N. Y., 1961, pp. 228-235.

17. Amdur, I., and Mason, E. A.: Scattering of High-Velocity Neutral Particles: III, Argon-Argon. Jour. Chem. Phys., vol. 22, no. 4, 1954 (April), pp. 670-671.

18. Kihara, Taro, Taylor, Marion H., and Hirschfelder, Joseph O.: Transport Properties for Gases Assuming Inverse Power Intermolecular Potentials. Phys. of Fluids, vol. 3, no. 5, Sept. - Oct. 1960, pp. 715-720.

19. Mason, Edward A., Vanderslice, Joseph T., and Yos, Jerrold M.: Transport Properties of High-Temperature Multicomponent Gas Mixtures. Phys. of Fluids, vol. 2, no. 6, Nov. - Dec. 1959, pp. 688-694.

20. Cramer, W. H.: Elastic and Inelastic Scattering of Low-Velocity Ions: Ne^+ in A, A^+ in Ne, and A^+ in A. Jour. Chem. Phys., vol. 30, no. 3, March 1959, pp. 641-642.

21. Cloney, Robert D., Mason, Edward A., and Vanderslice, Joseph T.: Binding Energy of Ar_2^+ from Ion Scattering Data. Jour. Chem. Phys., vol. 36, no. 4, Feb. 15, 1962, pp. 1103-1104.

22. Monchick, Louis: Collision Integrals for the Exponential Repulsive Potential. Phys. of Fluids, vol. 2, no. 6, Nov. - Dec. 1959, pp. 695-700.

23. Hartree, D. R., and Hartree, W.: Self-Consistent Field with Exchange for Potassium and Argon. Proc. Roy. Soc., A, vol. 166, 1938, pp. 450-464.

24. Hammerling, P., Shine, W. W., and Kivel, B.: Low-Energy Elastic Scattering of Electrons by Oxygen and Nitrogen. Jour. Appl. Phys., vol. 28, no. 7, July 1957, pp. 760-764.

25. Kivel, B.: Elastic Scattering of Low Energy Electrons by Argon. Avco Research Note 129, 1959.

26. Spitzer, Lyman, Jr.: Physics of Fully Ionized Gases. Second ed., Interscience Publishers, N. Y., 1962.

27. Liboff, Richard L.: Transport Coefficients Determined Using the Shielded Coulomb Potential. Phys. of Fluids, vol. 2, no. 1, Jan. - Feb. 1959, pp. 40-46.

28. Landshoff, Rolf: Convergence of the Chapman-Enskog Method for a Completely Ionized Gas. Phys. Rev., vol. 82, no. 3, May 1, 1951, p. 442.

29. Landshoff, Rolf: Transport Phenomena in a Completely Ionized Gas in Presence of a Magnetic Field. Phys. Rev., vol. 76, no. 7, Oct. 1, 1949, pp. 904-909.

30. Muckenfuss, Charles, and Curtiss, C. F.: Thermal Conductivity of Multicomponent Gas Mixtures. Jour. Chem. Phys., vol. 29, no. 6, Dec. 1958, pp. 1273-1277.

31. Fay, James A.: Energy Transfer in a Dense Plasma. Massachusetts Institute of Technology, Fluid Mechanics Lab. Pub. 63-1, 1963.

32. Viegas, John R., and Peng, T. C.: Electrical Conductivity of Ionized Air in Thermodynamic Equilibrium. ARS Jour., vol. 31, no. 5, May 1961, pp. 654-657.

33. Lin, Shao - Chi, Resler, E. L., and Kantrowitz, Arthur: Electrical Conductivity of Highly Ionized Argon Produced by Shock Waves. J. Appl. Phys., vol. 26, no. 1, Jan. 1955, pp. 95-109.

34. Cohen, Robert S., Spitzer, Lyman, Jr., and Routly, Paul Mc R.: The Electrical Conductivity of an Ionized Gas. Phys. Rev., vol. 80, no. 2, Oct. 15, 1950, pp. 230-238.

35. Spitzer, Lyman, Jr., and Härm, Richard: Transport Phenomena in a Completely Ionized Gas. Phys. Rev., vol. 89, no. 5, March 1953, pp. 977-981.

36. Burgers, Johannes, ed.: Statistical Plasma Mechanics. Symposium of Plasma Dynamics, Addison-Wesley Publishing Co., Reading, Mass., 1960, pp. 164-169.

37. Grad, H.: Modern Kinetic Theory of Plasmas. Proc. Fifth Int. Conf. on Ionization Phenomena in Gases, Vol. II, North-Holland Publ. Co., Amsterdam, 1962, pp. 1630-1649.

38. Koga, Toyoki: The Generalized Validity of the Boltzmann Equation for Ionized Gases. Proc. Third Int. Symposium on Rarified Gas Dynamics, Vol. I, Academic Press, N. Y., 1963, pp. 75-93.

39. Braginskii, S. I.: Transport Phenomena in a Completely Ionized Two-Temperature Plasma. Soviet Physics JETP, 1958, vol. 6 (2), pp. 358-369.

40. Kaufman, Allan N.: Plasma Transport Theory. The Theory of Natural and Ionized Gases. De Witt, Cecile, and De Toeuf, Jean-Francois, eds. John Wiley and Sons, Inc., N. Y., 1960, pp. 295-353.

41. Rostoker, Norman, and Rosenbluth, M. N.: Test Particles in a Completely Ionized Plasma. Phys. Fluids, vol. 3, no. 1, Jan. - Feb. 1960, pp. 1-14.

42. Rudin, M.: Transport and Correlation in a Highly Ionized Gas. Vidya Rep. 101, Itek Corp., 1963.

43. Allis, W. P.: Motions of Ions and Electrons. Handbuch Der Physik, vol. 21, Springer, Berlin, 1956, pp. 383-444.

44. Glasstone, Samuel: Theoretical Chemistry. D. Van Nostrand Co., Inc. N. Y., 1944.

45. Moore, Charlotte E.: Atomic Energy Levels. Vol. 1, Nat. Bur. of Stds., Circular 467, 1949.

46. Gilmore, F. R.: Equilibrium Composition and Thermodynamic Properties of Air to 24,000° K. Rand Corp. RM 1543, 1955.

47. Hilsenrath, Joseph, et al.: Tables of Thermodynamic and Transport Properties of Air, Argon, Carbon Dioxide, Carbon Monoxide, Hydrogen, Nitrogen, Oxygen, and Steam. Pergamon Press, N. Y., 1960.

48. Duclos, Donald P.: The Equation of State of an Ionized Gas. Arnold Engineering Development Center TN 60-192, 1960.

49. Bradley, John N.: Shock Waves in Chemistry and Physics. John Wiley and Sons, Inc., N. Y., 1962.

TABLE I.- COMPARISON OF VARIOUS APPROACHES FOR CALCULATING THE TRANSPORT COEFFICIENTS OF A FULLY IONIZED GAS

Partial differential equation for f_i	Approach	Transport coefficient	b_{min}	b_{max}	Velocity description	Particle interactions considered
Boltzmann	Chapman-Enskog	λ_t, η, σ	0	h	$\overline{V}_i$ Sonine polynomial	I-I, I-e, e-e (ions mobile)
Fokker-Planck	Spitzer	λ_t, σ	b_o	h	$\langle v_{x,i} \rangle$	I-e, e-e (ions at rest)
Fokker-Planck	Braginskii (ref. 39)	η	b_o	h	$\overline{V}_i$ Sonine polynomial	I-I (ions mobile)

P, atm	T, ^{o}K	η, gram/cm-sec	η, gram/cm-sec	σ, stat mho/cm	σ, stat mho/cm	λ_t, erg/^{o}K cm-sec	λ_t, erg/^{o}K cm-sec	$\ln \Lambda$ (a)
Approach		Chapman-Enskog	[a]Braginskii	Chapman-Enskog	[a]Spitzer	Chapman-Enskog	[a]Spitzer	
10^{-4}	15,000	4.60×10^{-5}	4.70×10^{-5}	3.15×10^{13}	3.13×10^{13}	5.32×10^{4}	1.51×10^{5}	8.08
10^{-2}	18,000	9.97×10^{-5}	9.86×10^{-5}	5.52×10^{13}	5.41×10^{13}	1.12×10^{5}	3.11×10^{5}	6.15
1	30,000	4.71×10^{-4}	4.51×10^{-4}	1.53×10^{14}	1.47×10^{14}	5.20×10^{5}	1.42×10^{6}	4.87
10^{2}	50,000	2.51×10^{-3}	2.18×10^{-3}	4.62×10^{14}	4.29×10^{14}	2.66×10^{6}	6.88×10^{6}	3.59

[a]For consistency, equation (32) was used for h instead of the equation in footnote 2.

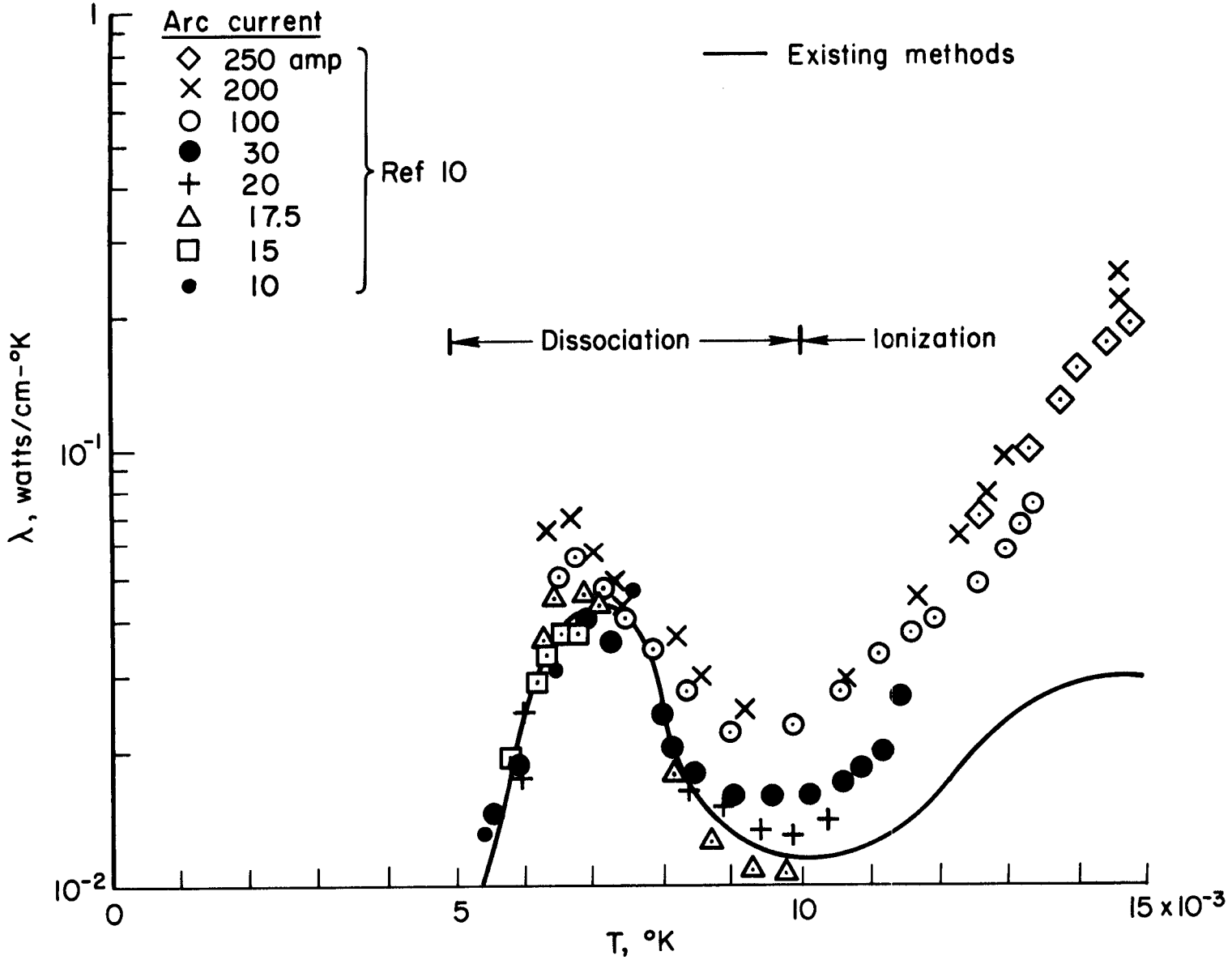

Figure 1.- Comparison of experimental and theoretical thermal conductivities for nitrogen (p = 1 atm).

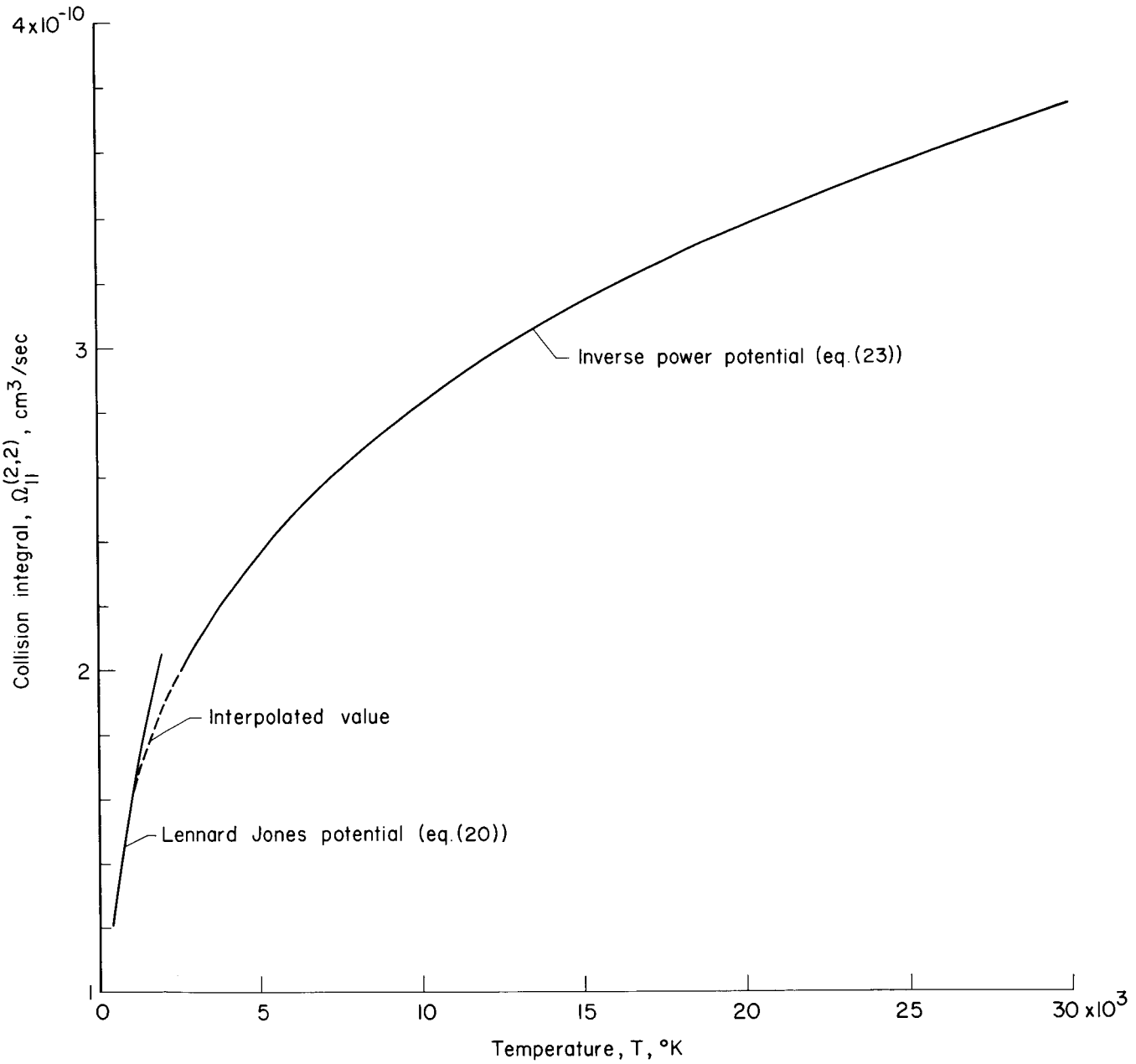

(a) Atom-atom.

Figure 2.- Collison integrals for argon as a function of temperature.

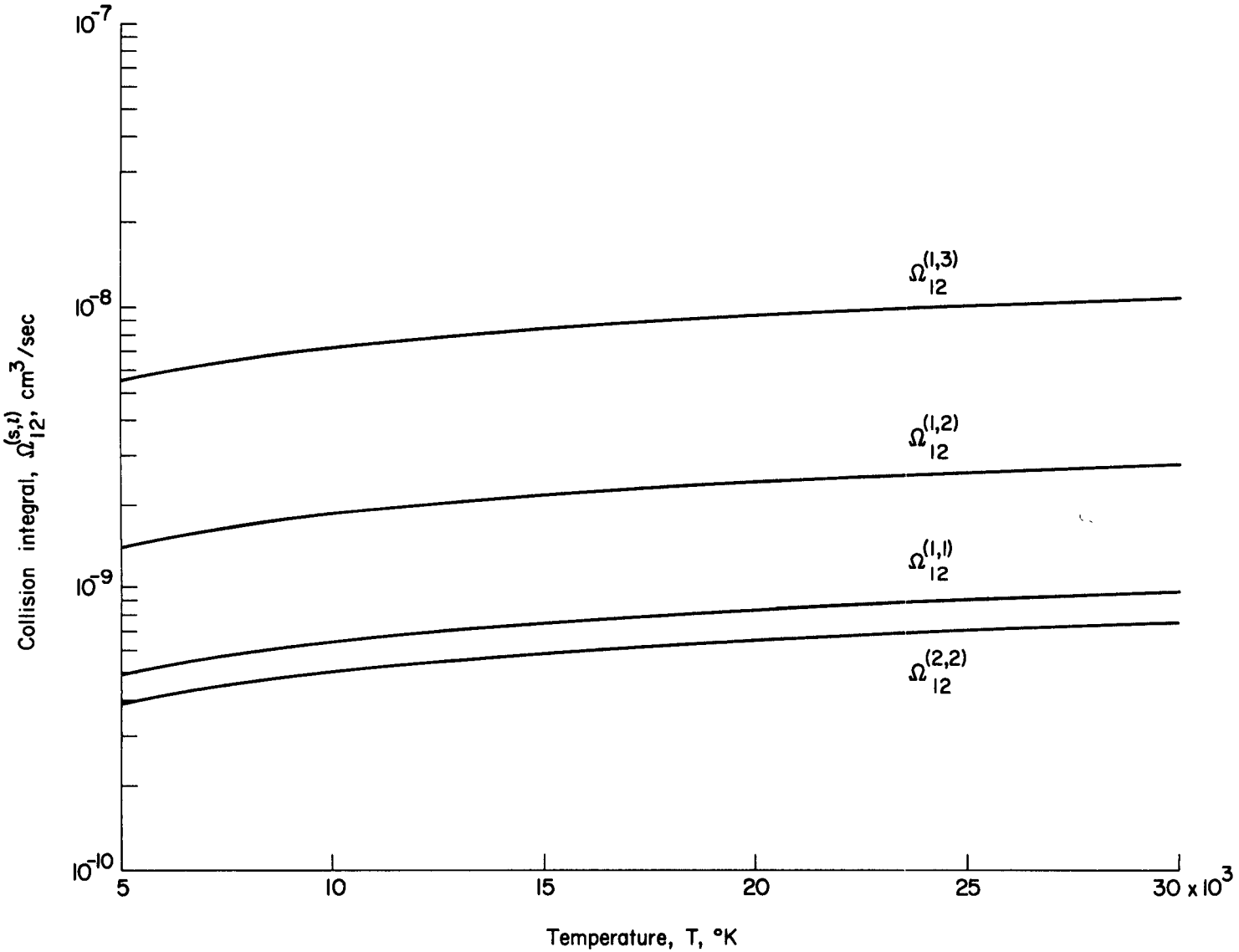

(b) Atom-ion.

Figure 2.- Continued.

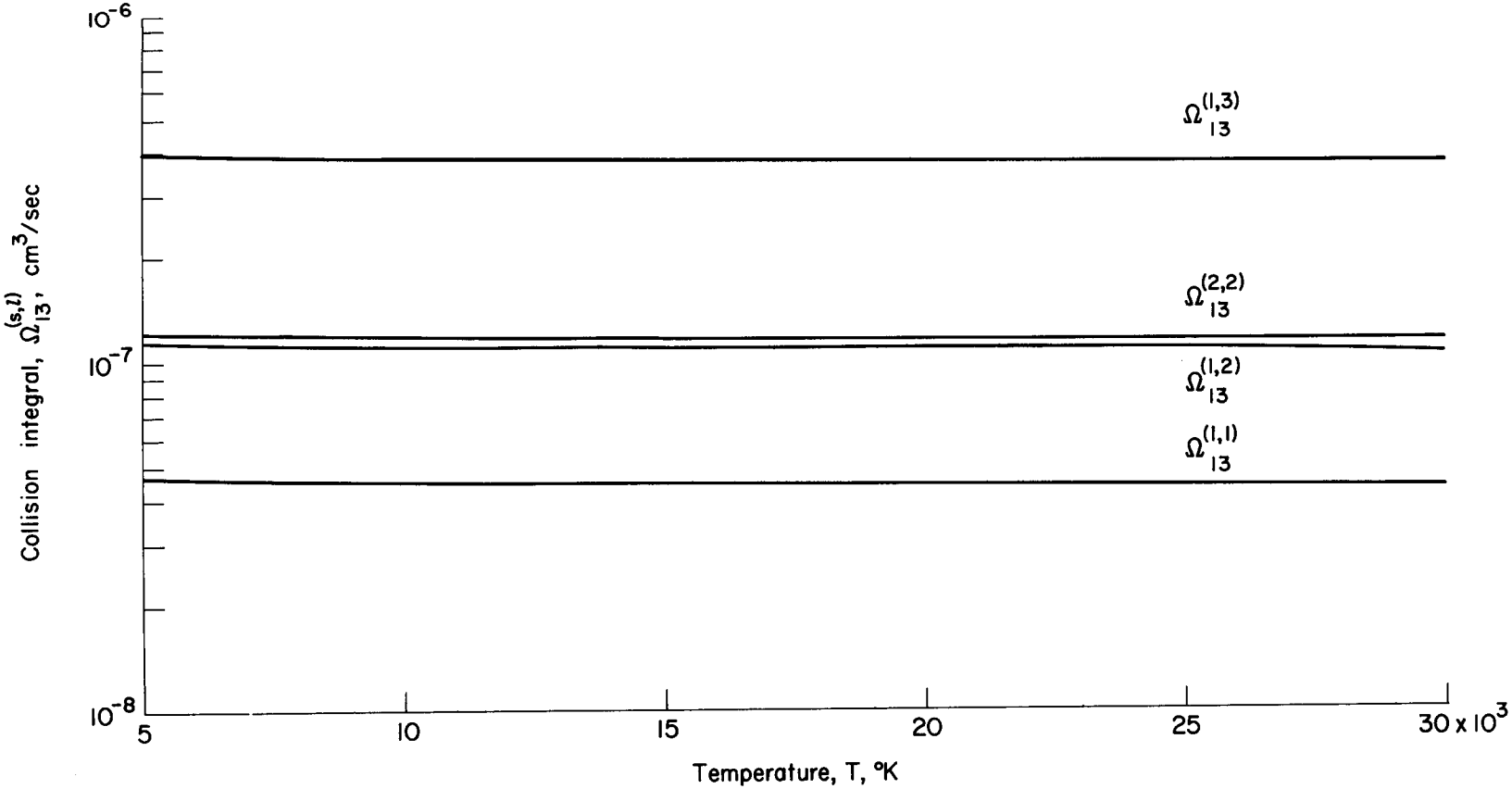

(c) Atom-electron.

Figure 2.- Continued.

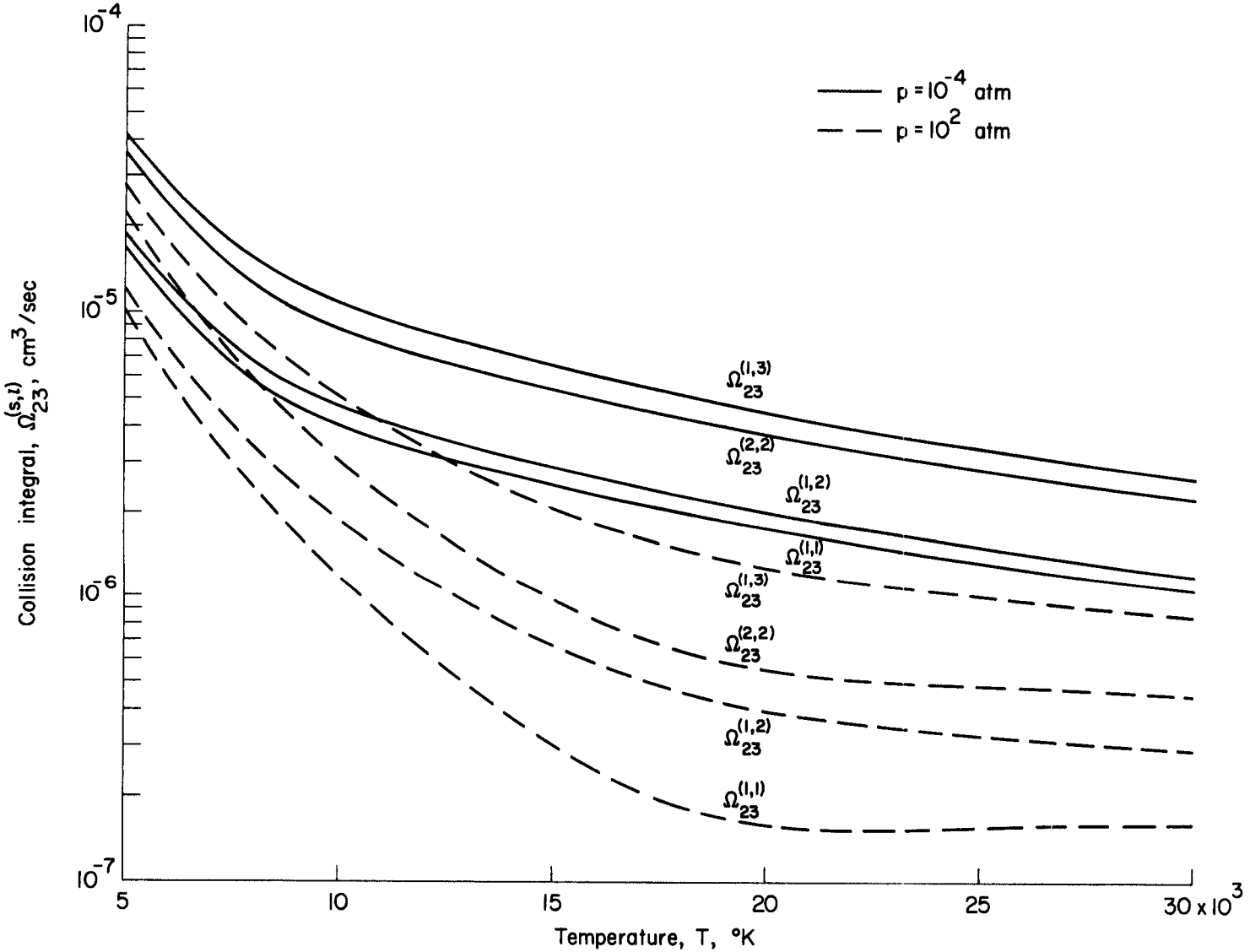

(d) Ion-electron.

Figure 2.- Continued.

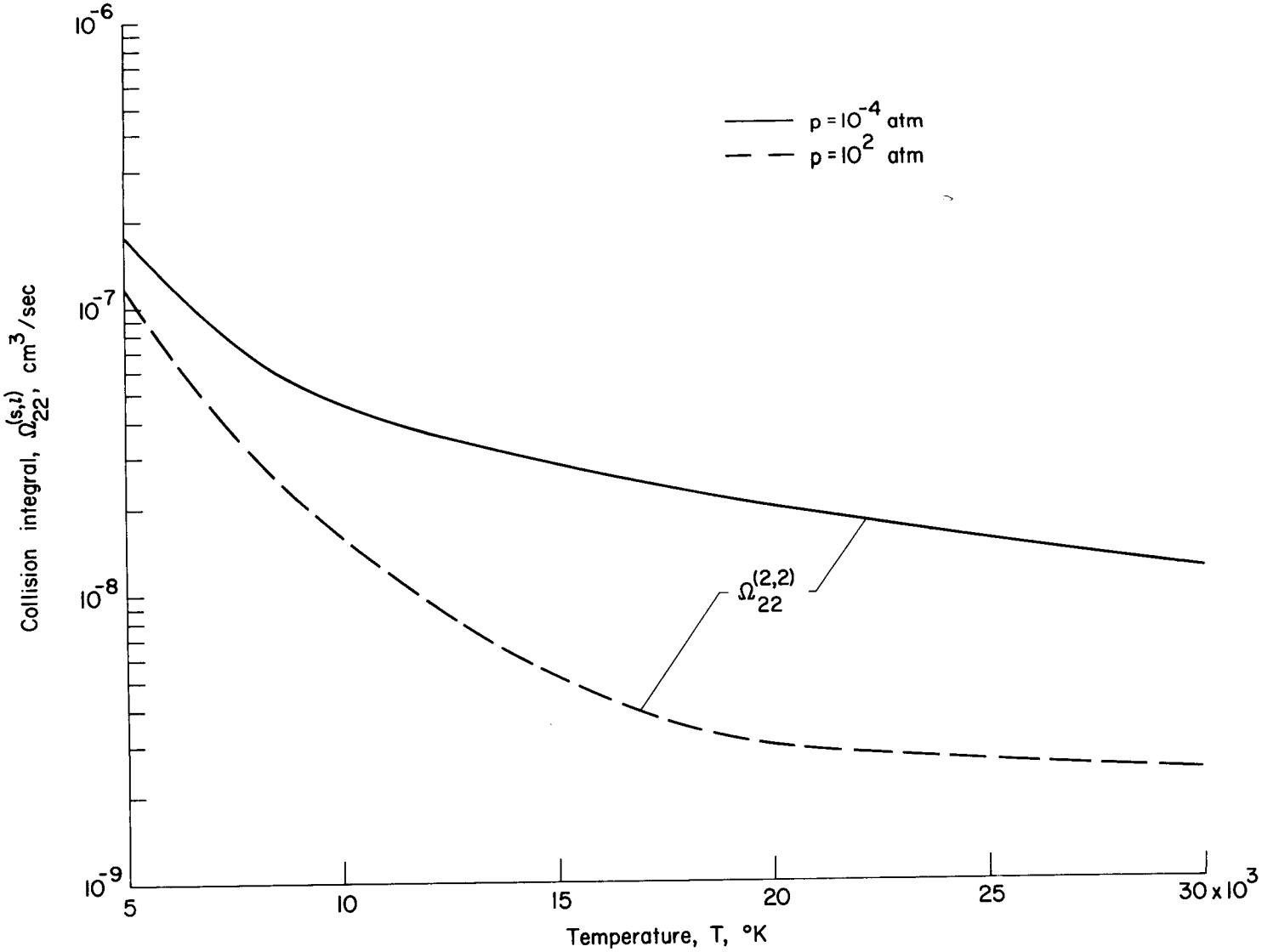

(e) Ion-ion.

Figure 2.- Continued.

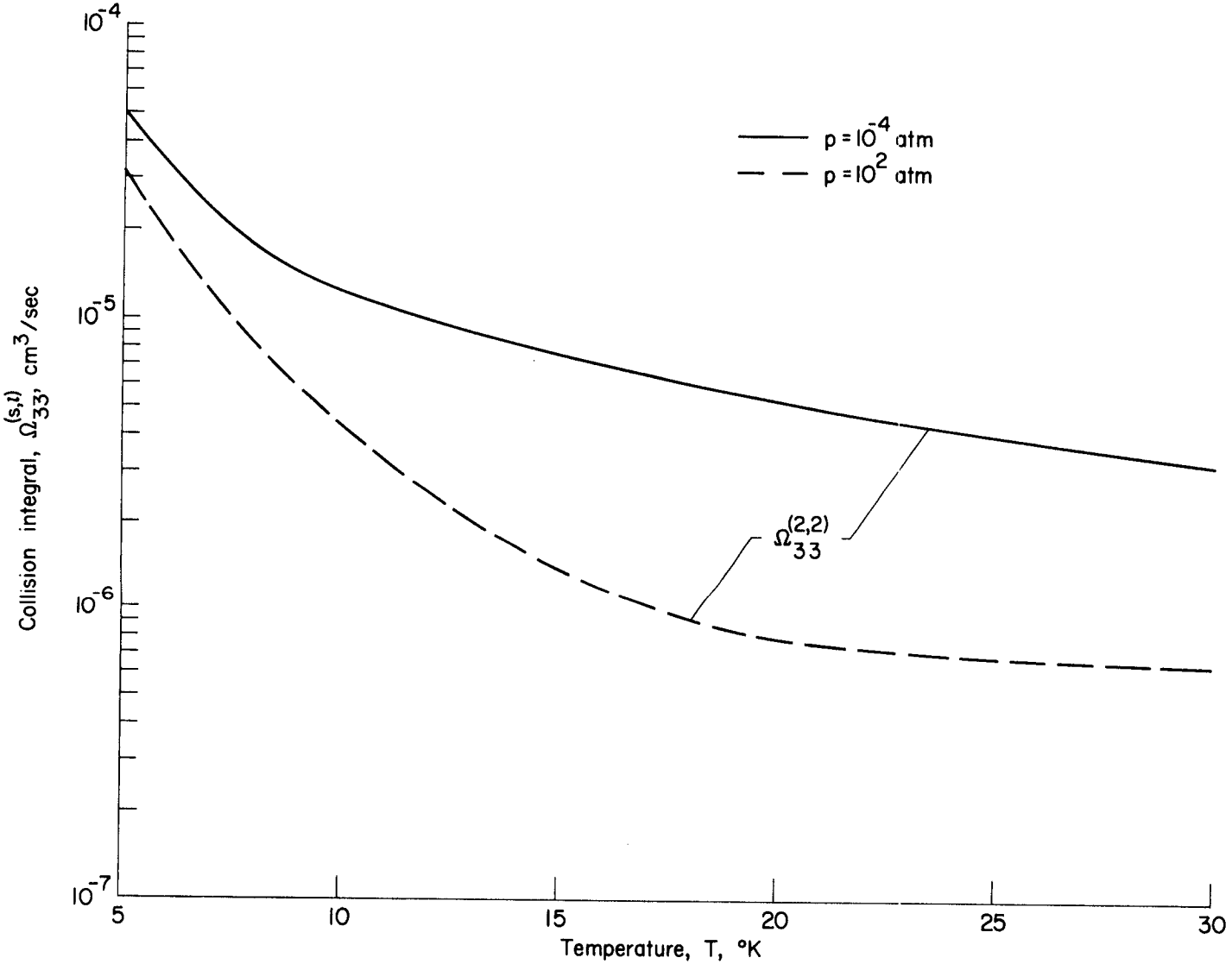

(f) Electron-electron.

Figure 2.- Concluded.

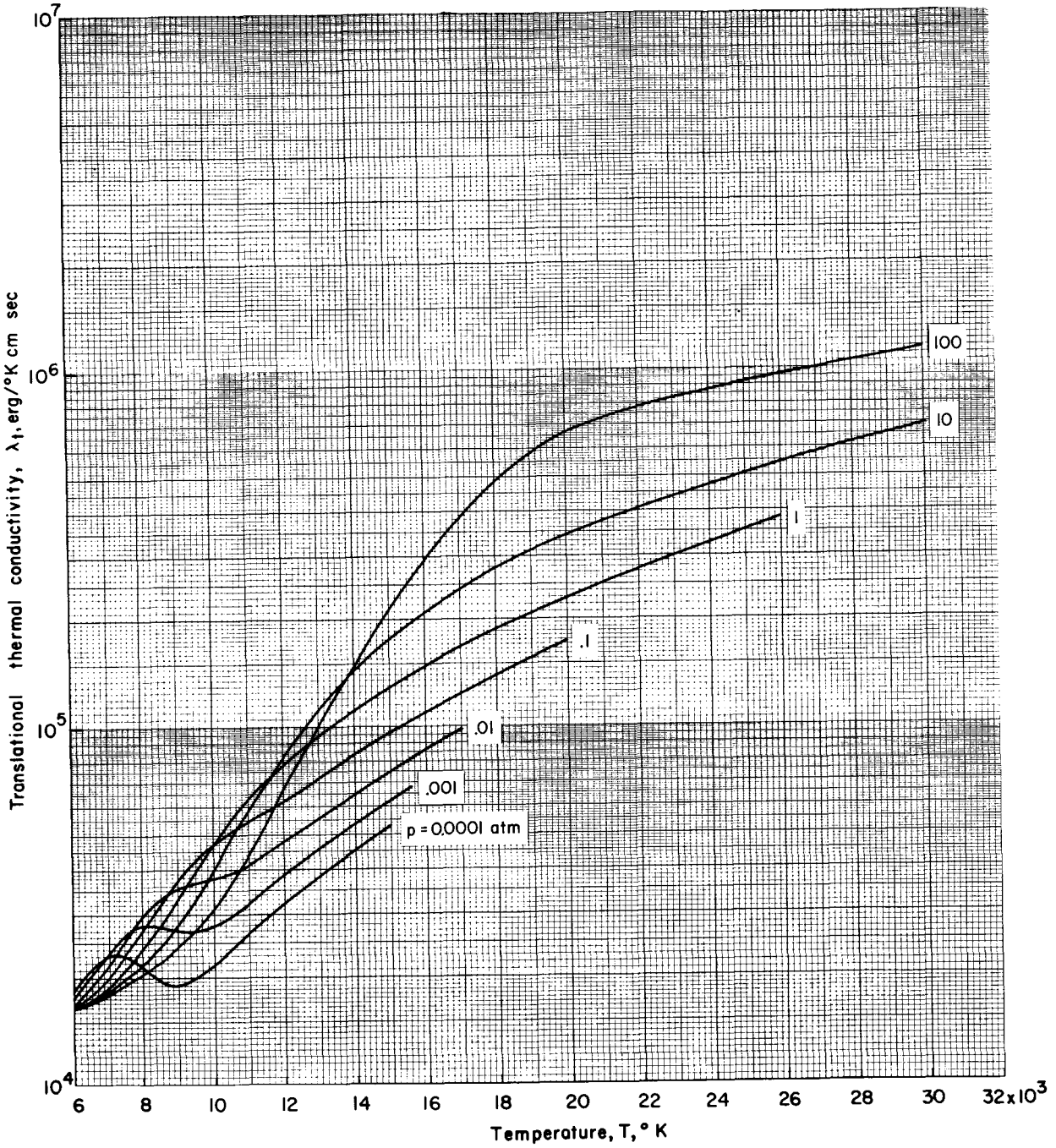

Figure 3.- Translational thermal conductivity of argon as a function of temperature.

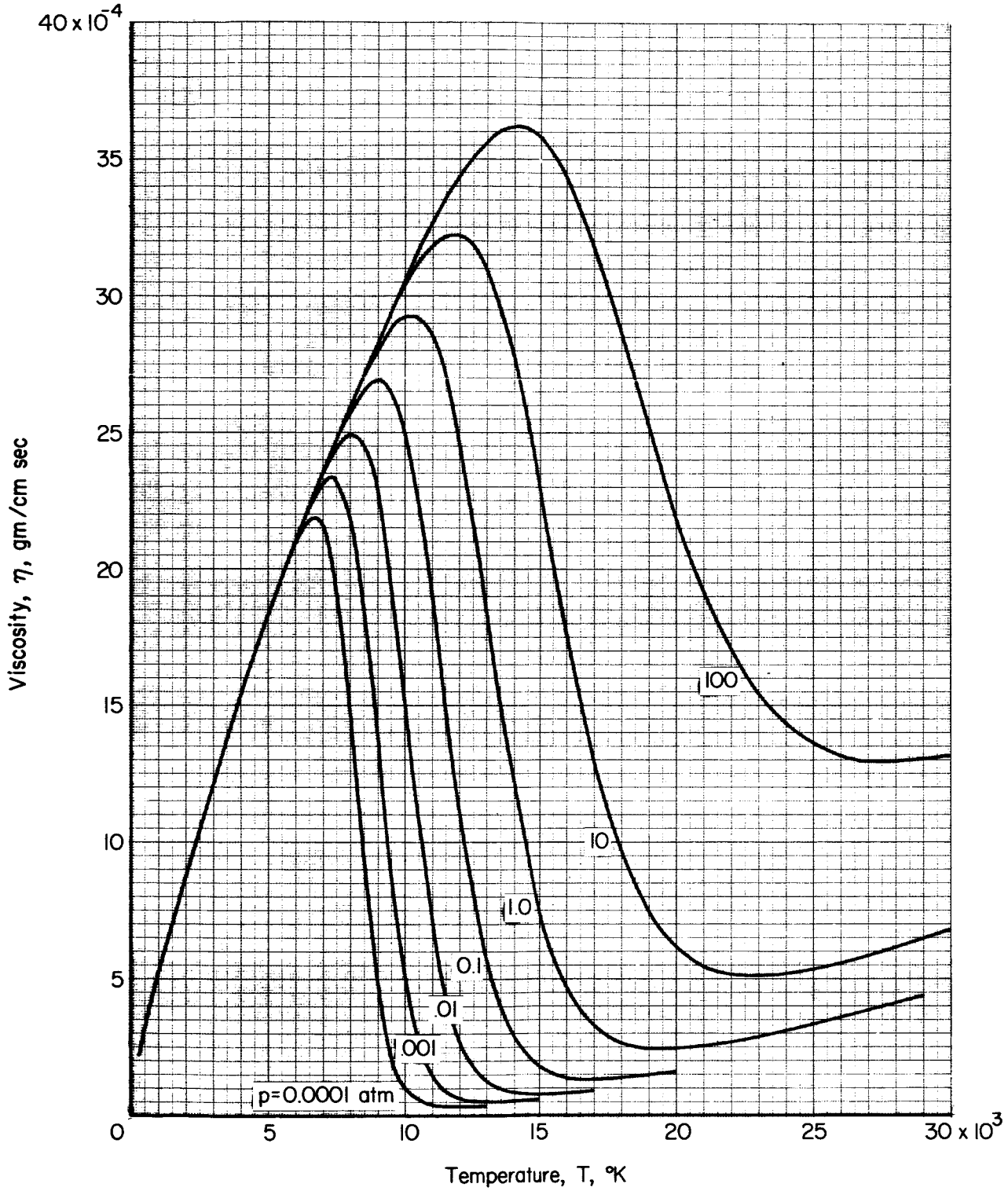

Figure 4.- Viscosity coefficient of argon as a function of temperature.

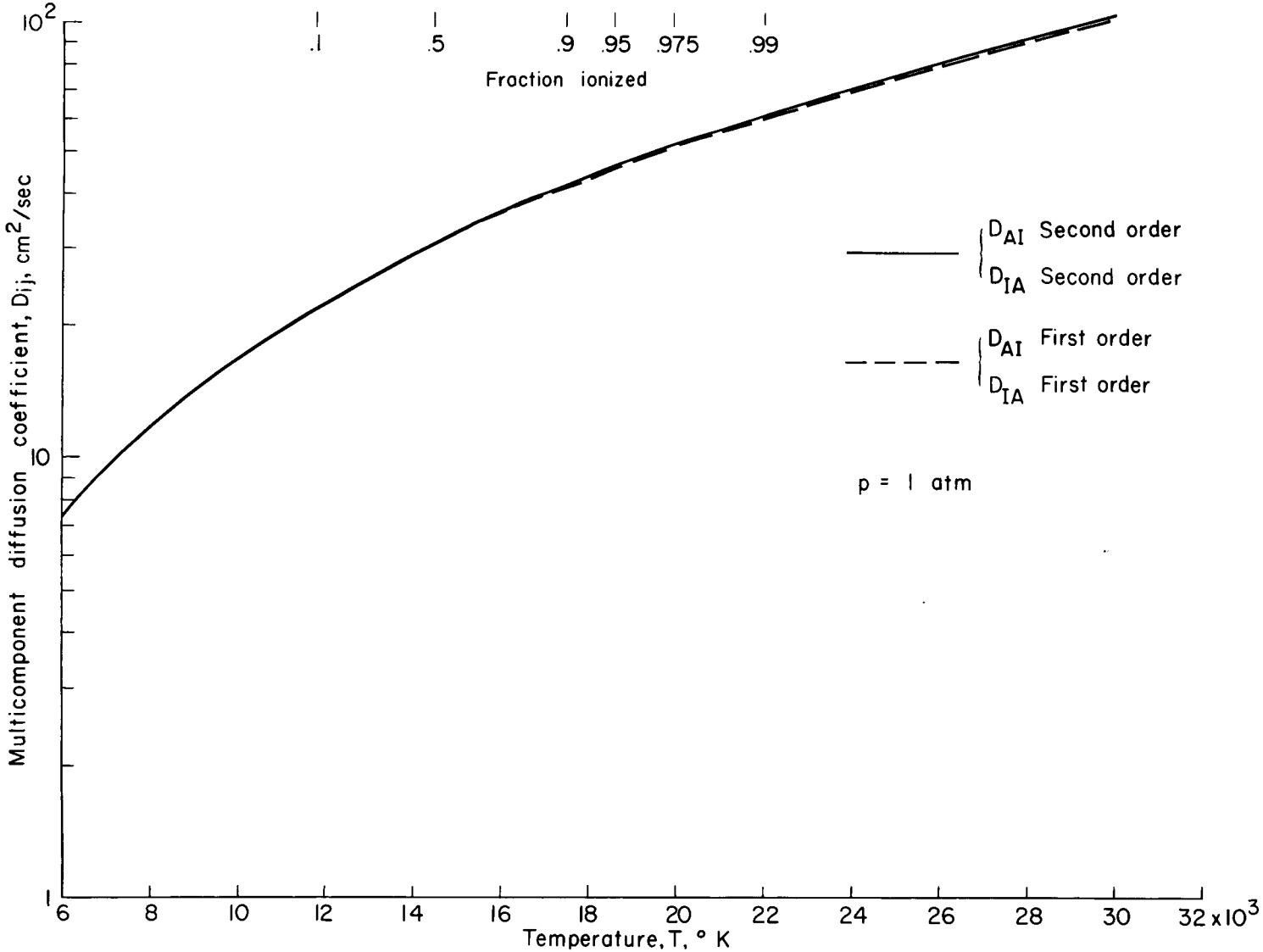

(a) Atom-ion and ion-atom.

Figure 5.- Multicomponent diffusion coefficients for argon as a function of temperature.

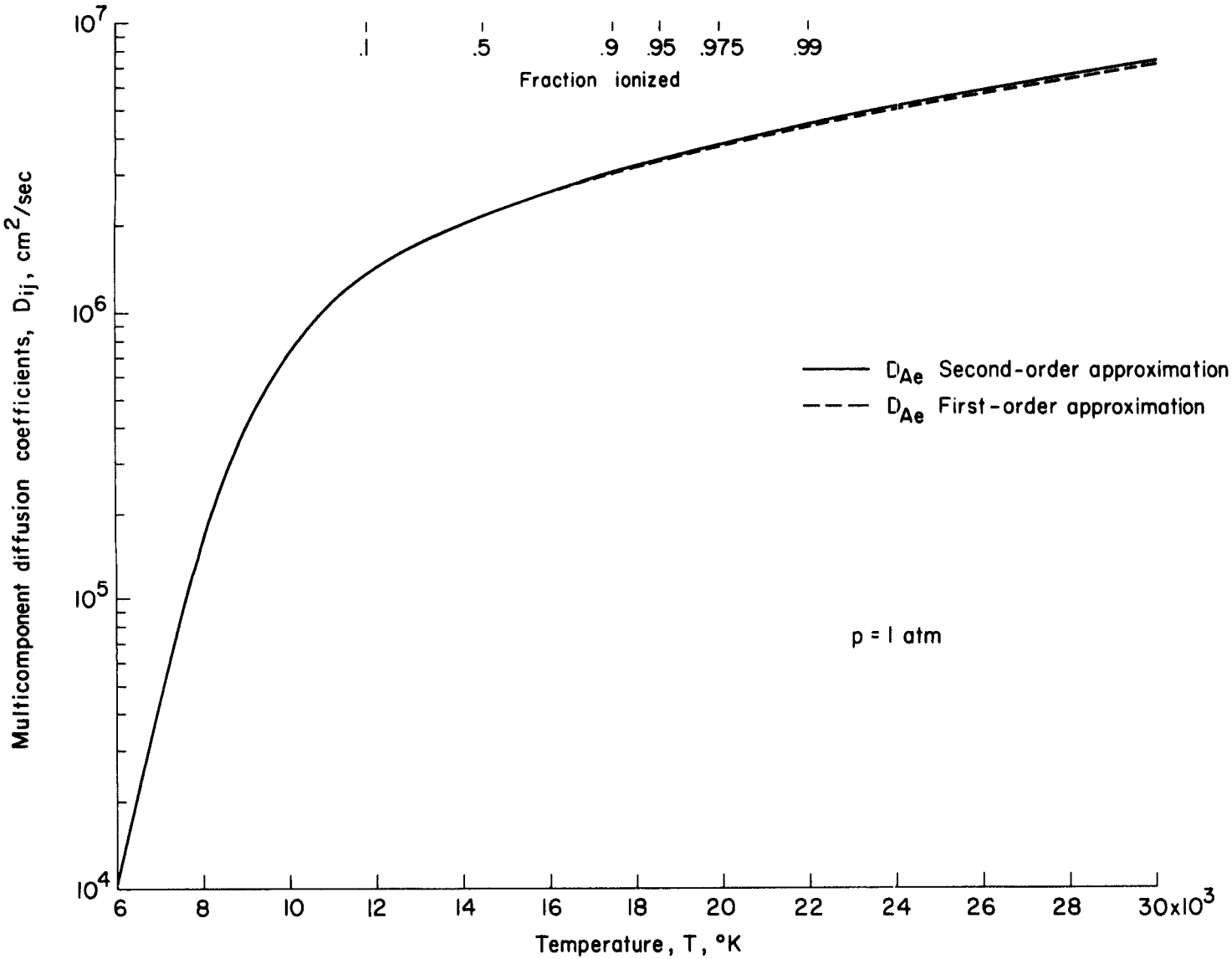

(b) Atom-electron.

Figure 5.- Continued.

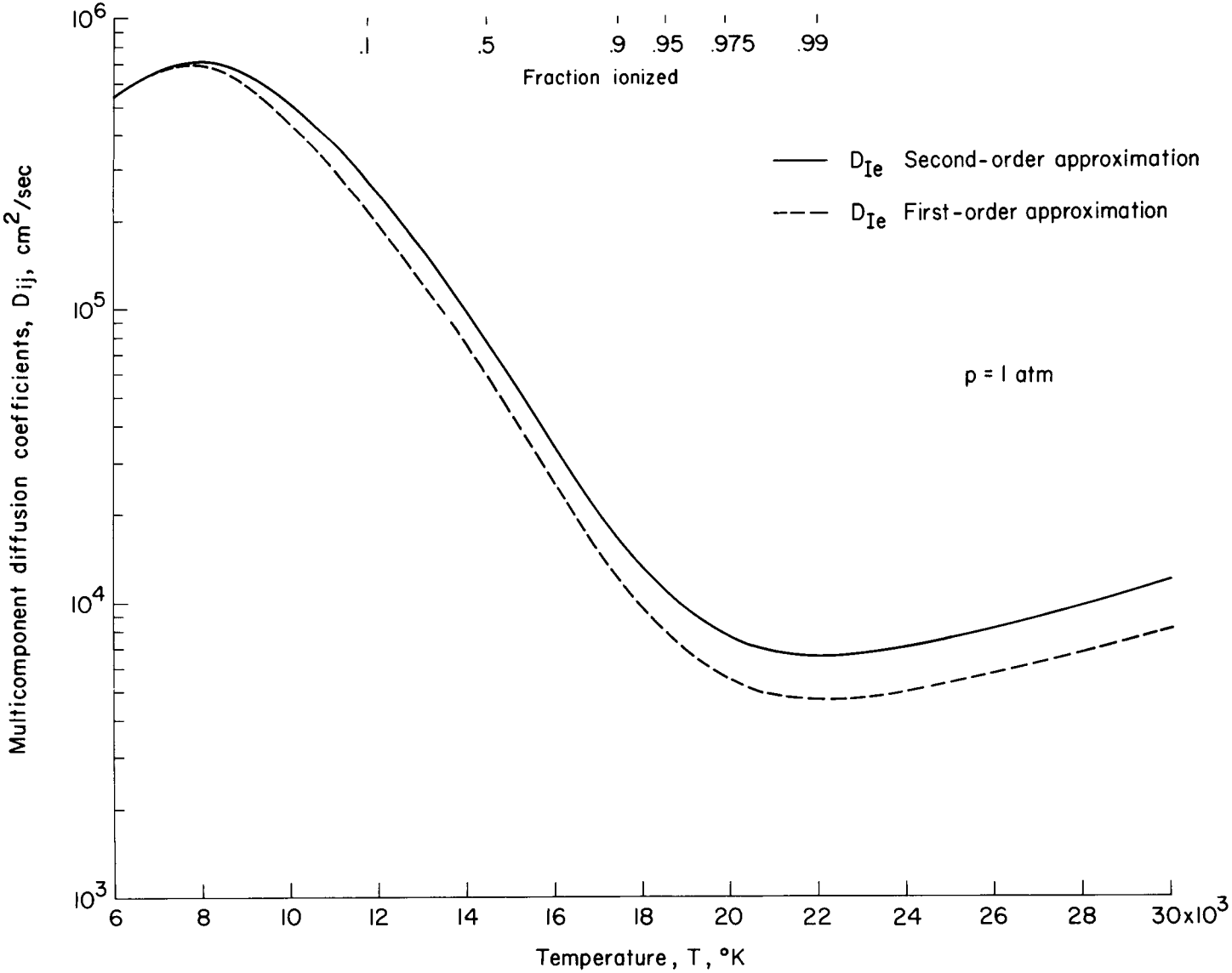

(c) Ion-electron.

Figure 5.- Continued.

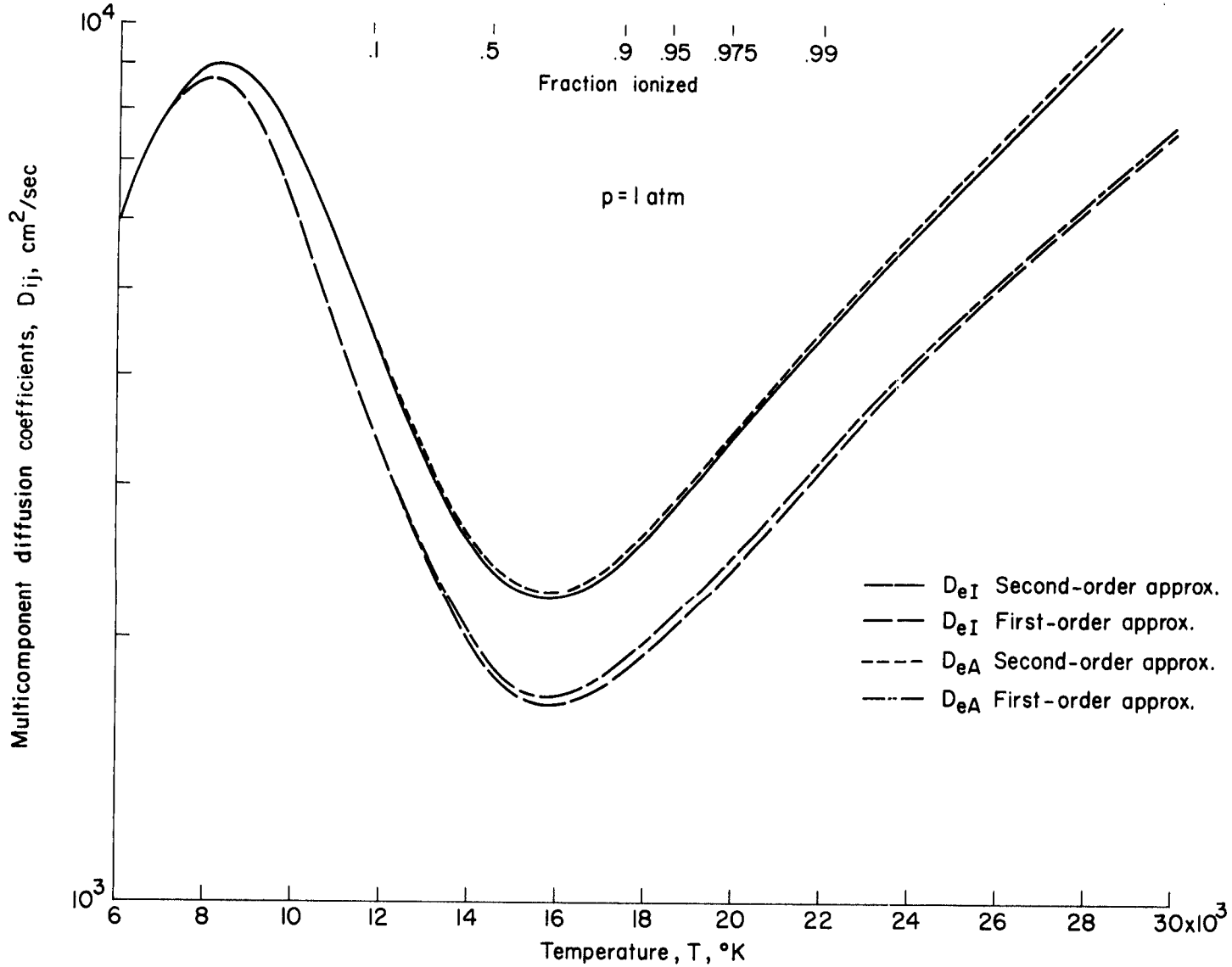

(d) Electron-atom and electron-ion.

Figure 5.- Concluded.

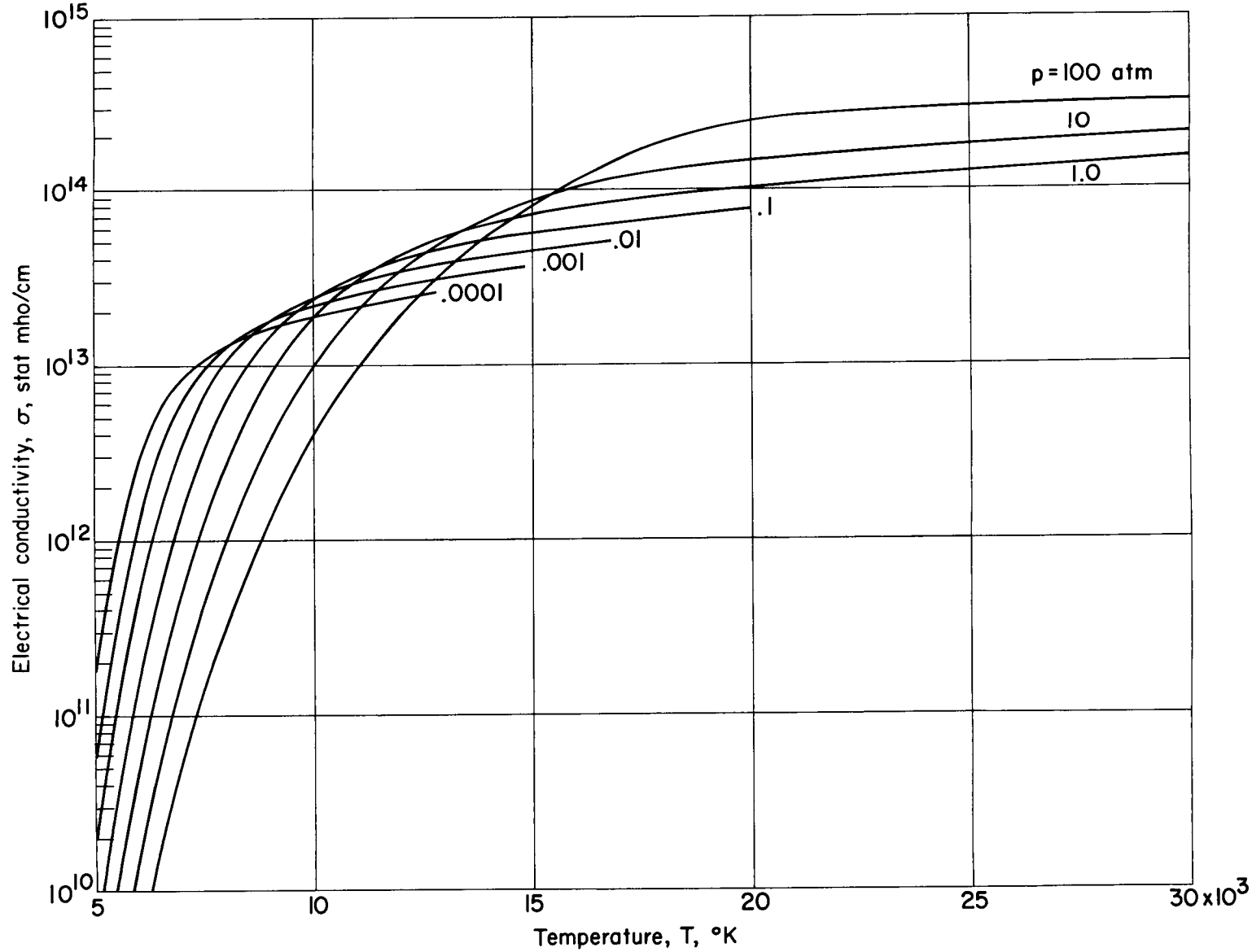

Figure 6.- Electrical conductivity of argon as a function of temperature.

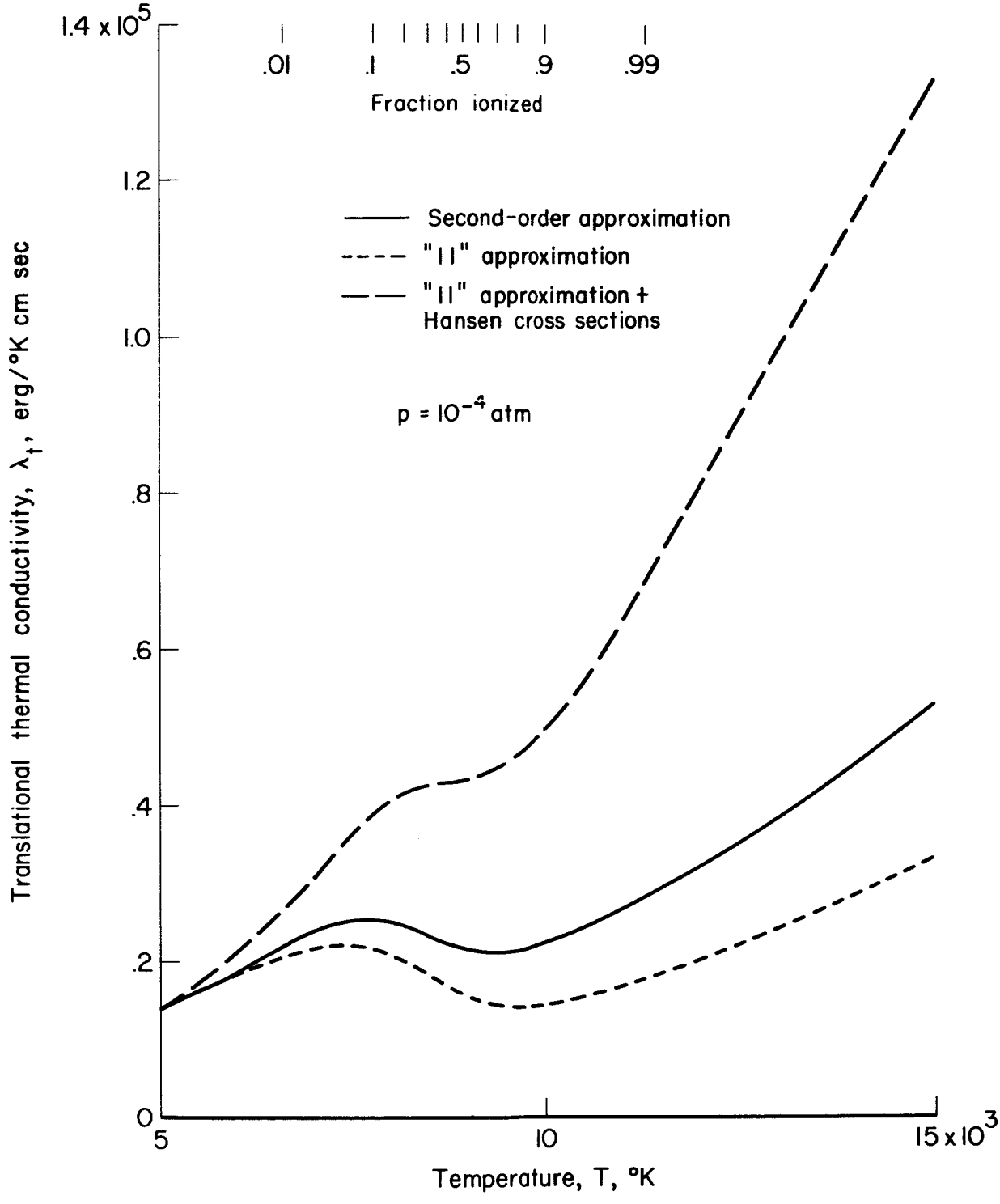

(a) $p = 10^{-4}$ atm

Figure 7.- Comparison of second-order method with "11" and Hansen approximations for calculating the translational thermal conductivity.

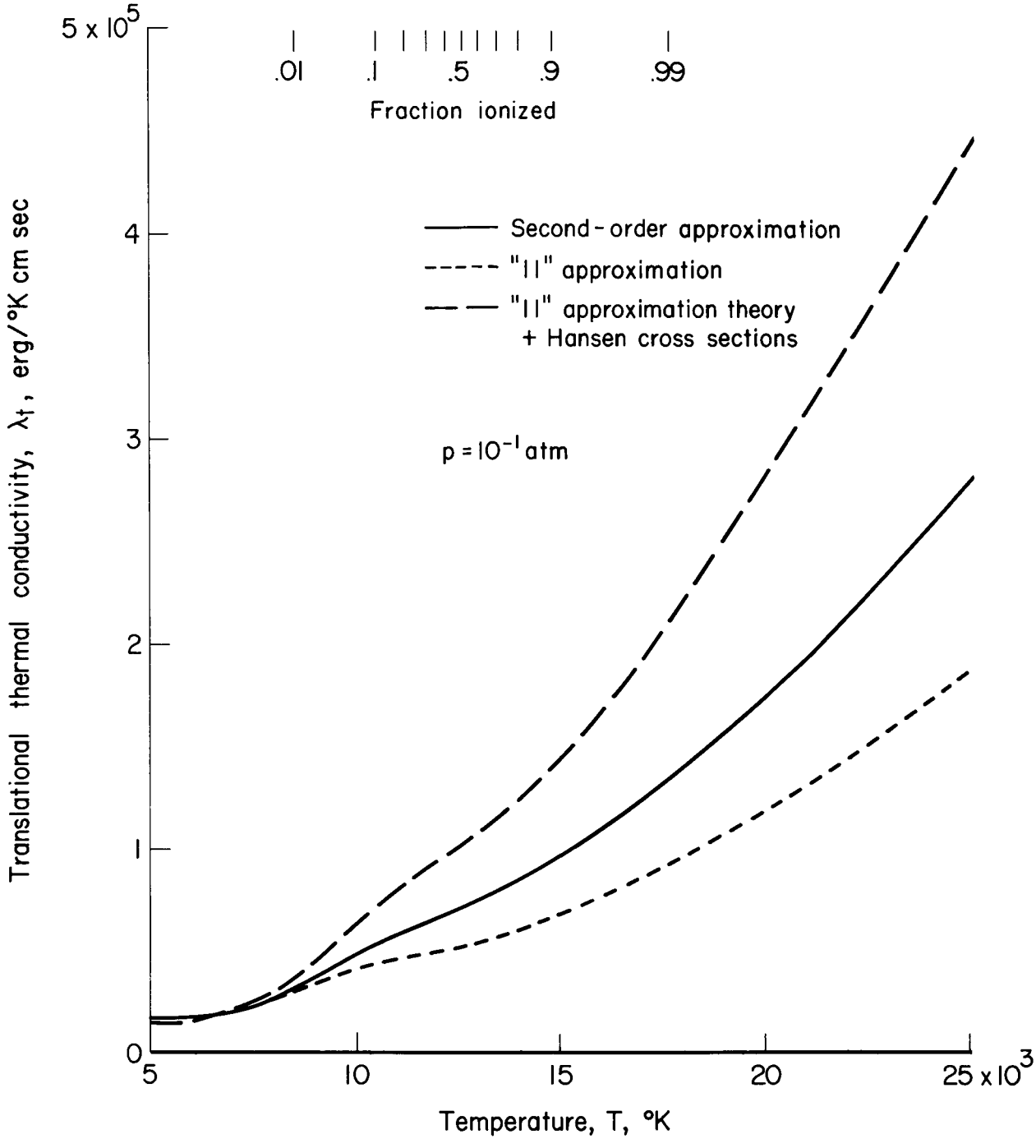

(b) $p = 10^{-1}$ atm

Figure 7.- Continued.

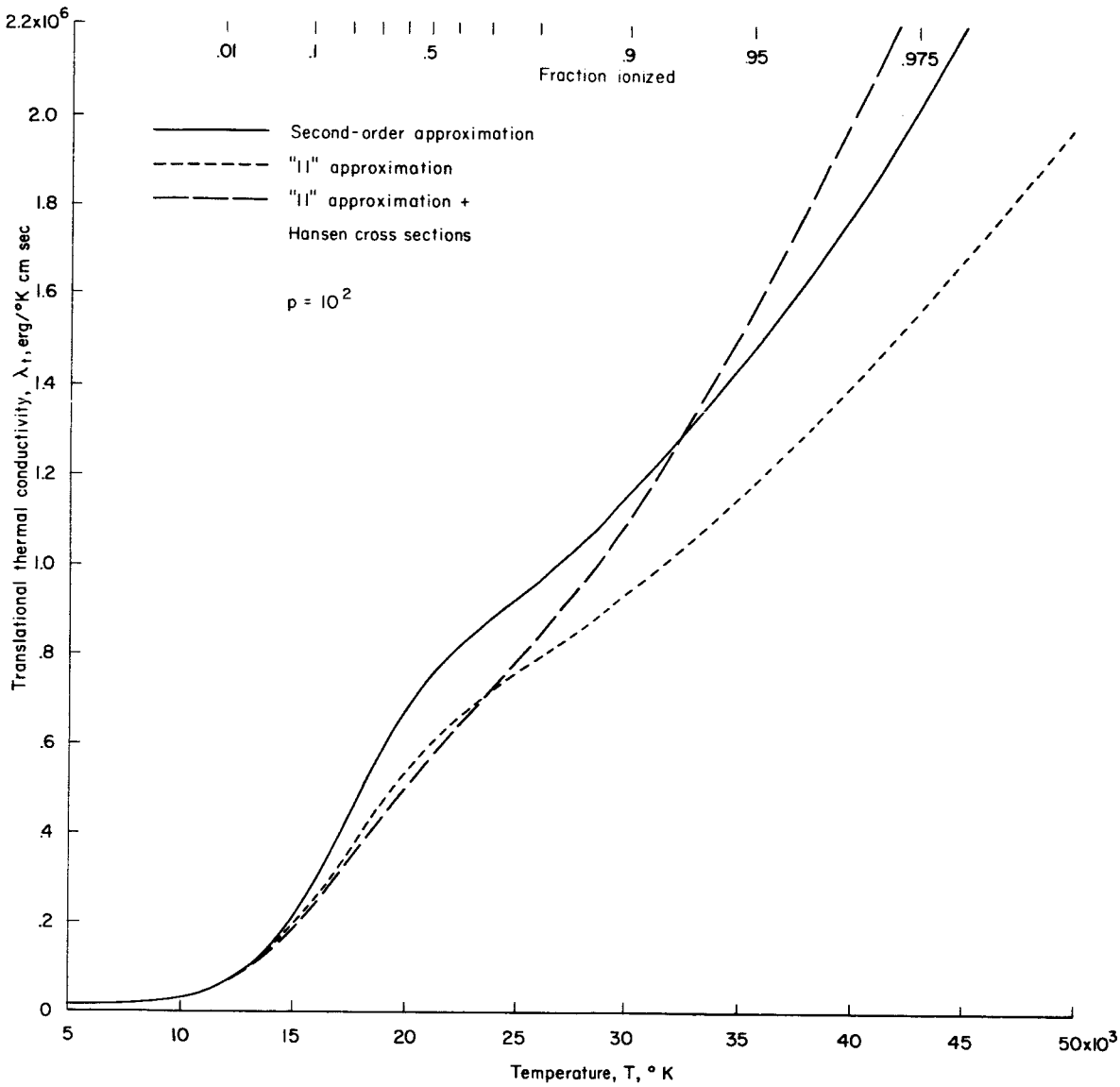

(c) $p = 10^2$ atm

Figure 7.- Concluded.

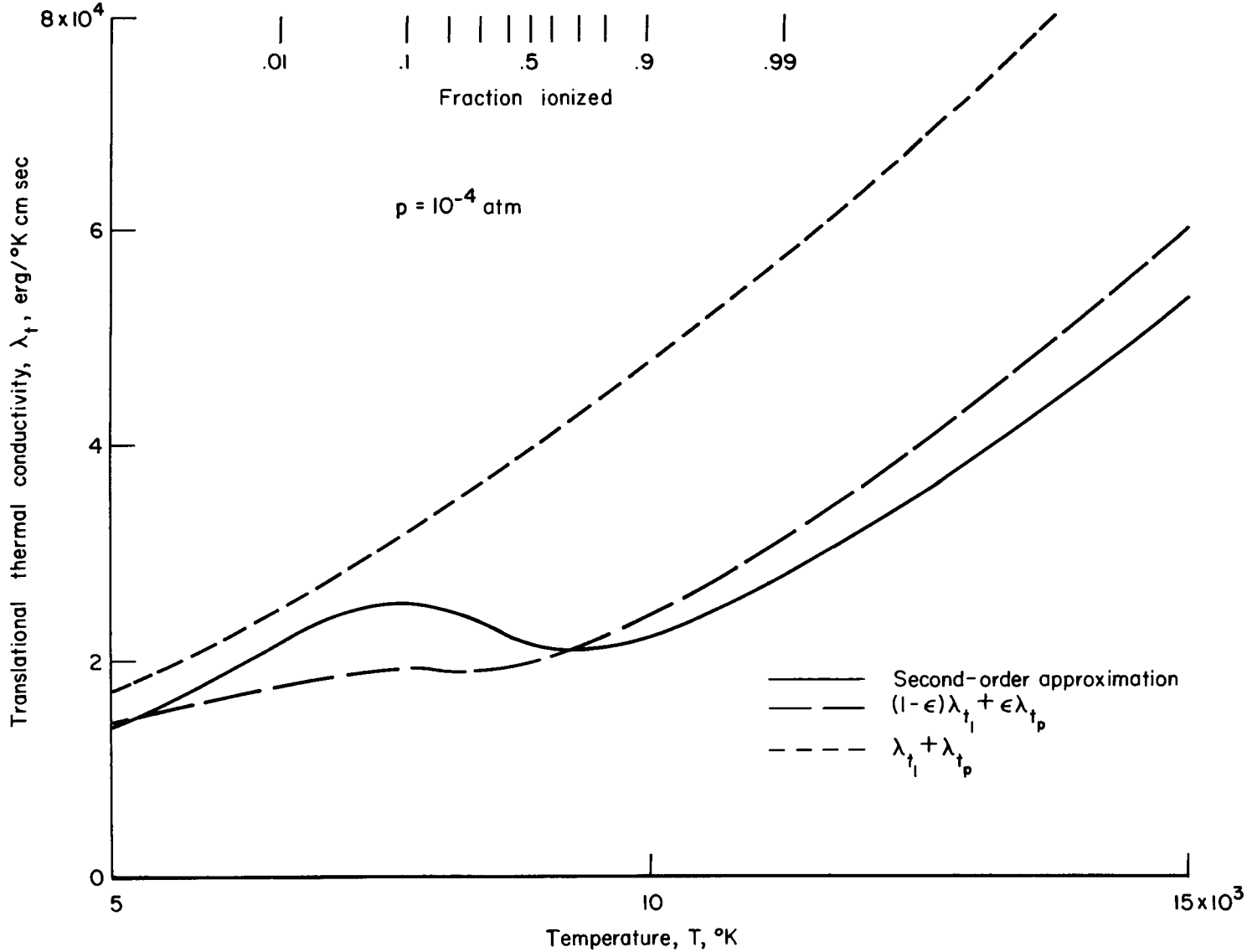

(a) $p = 10^{-4}$

Figure 8.- Comparison of second-order method with Fay approximation for calculating the translational thermal conductivity.

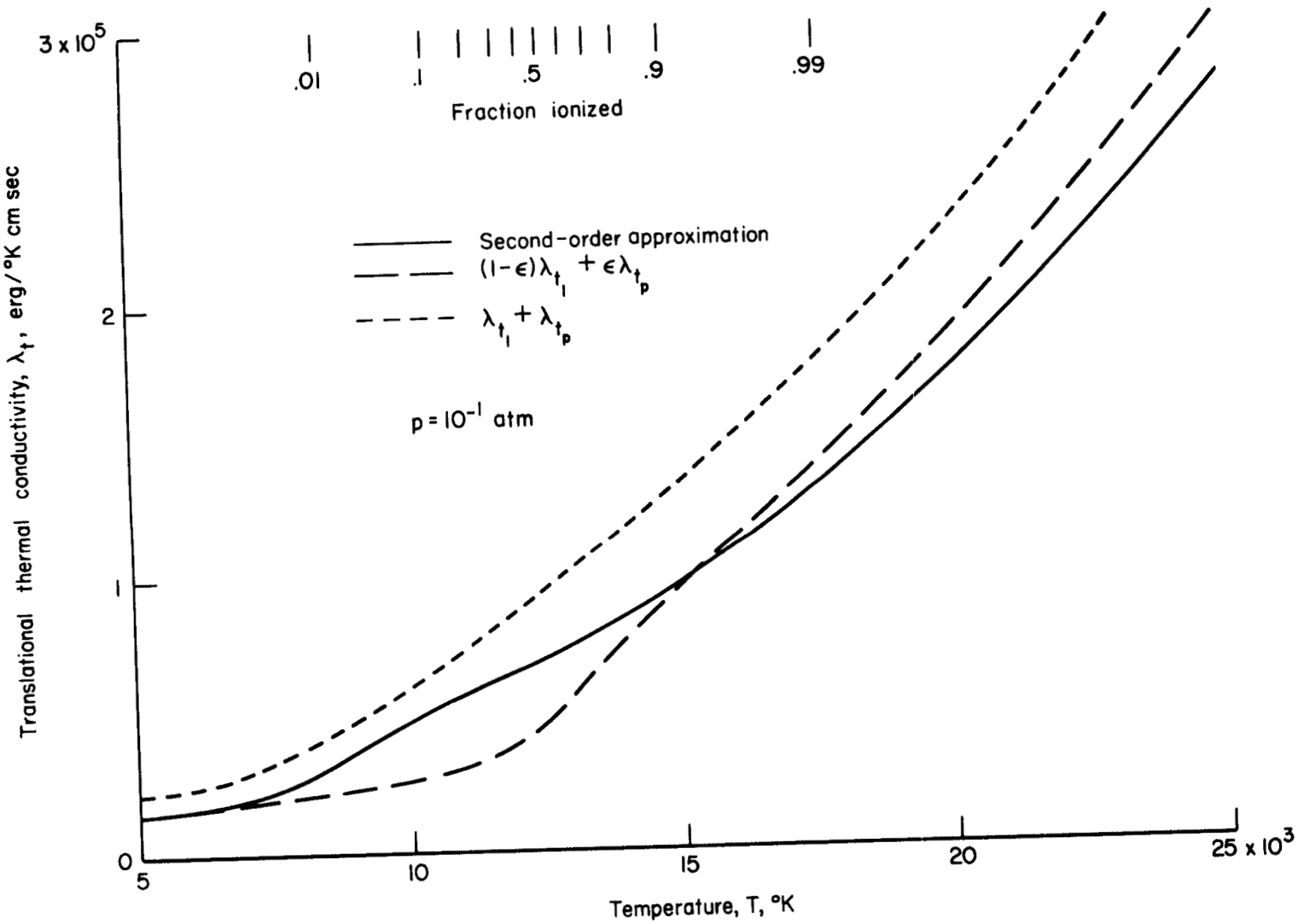

(b) $p = 10^{-1}$

Figure 8.- Concluded.

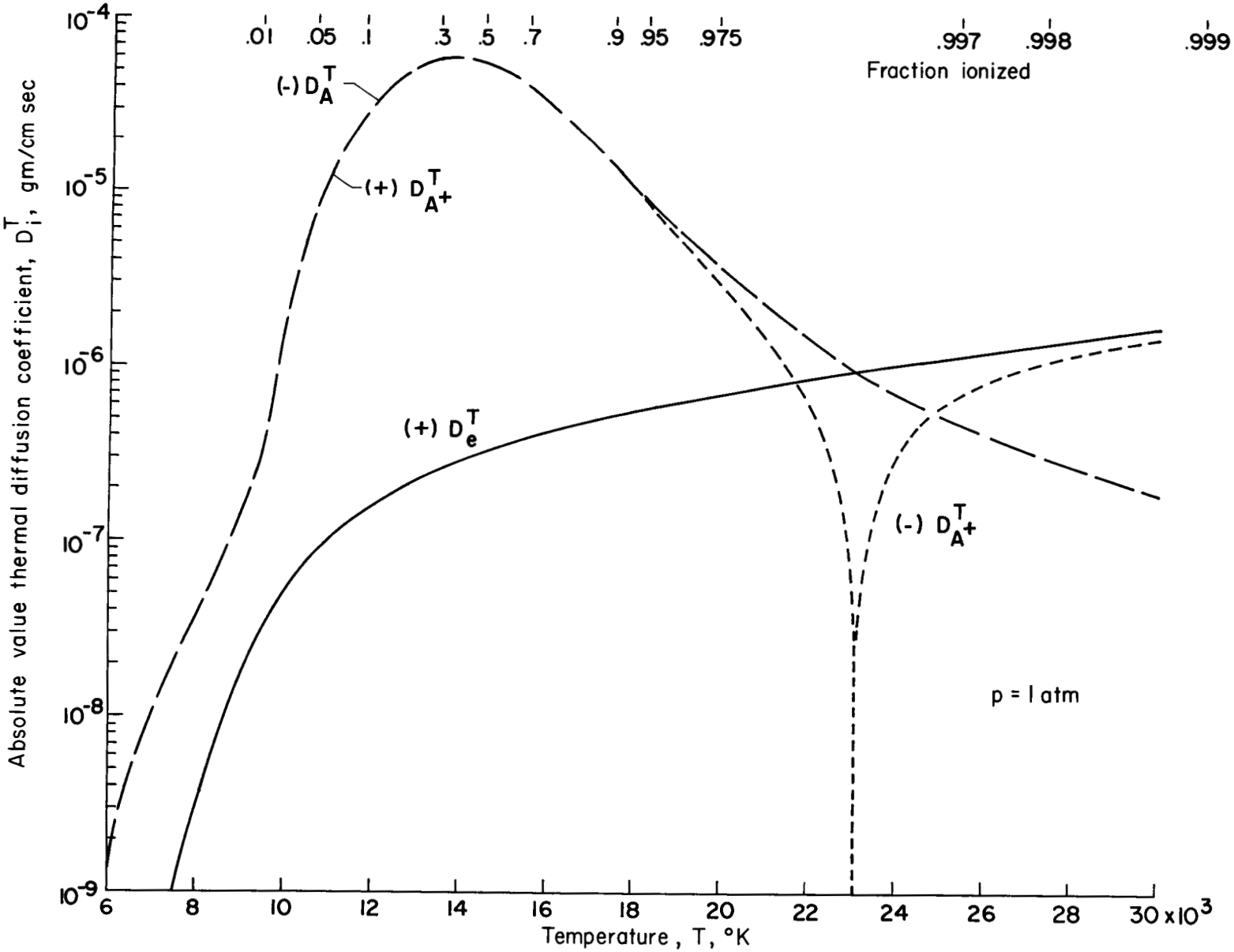

Figure 9.- Thermal diffusion coefficients for argon as a function of temperature.

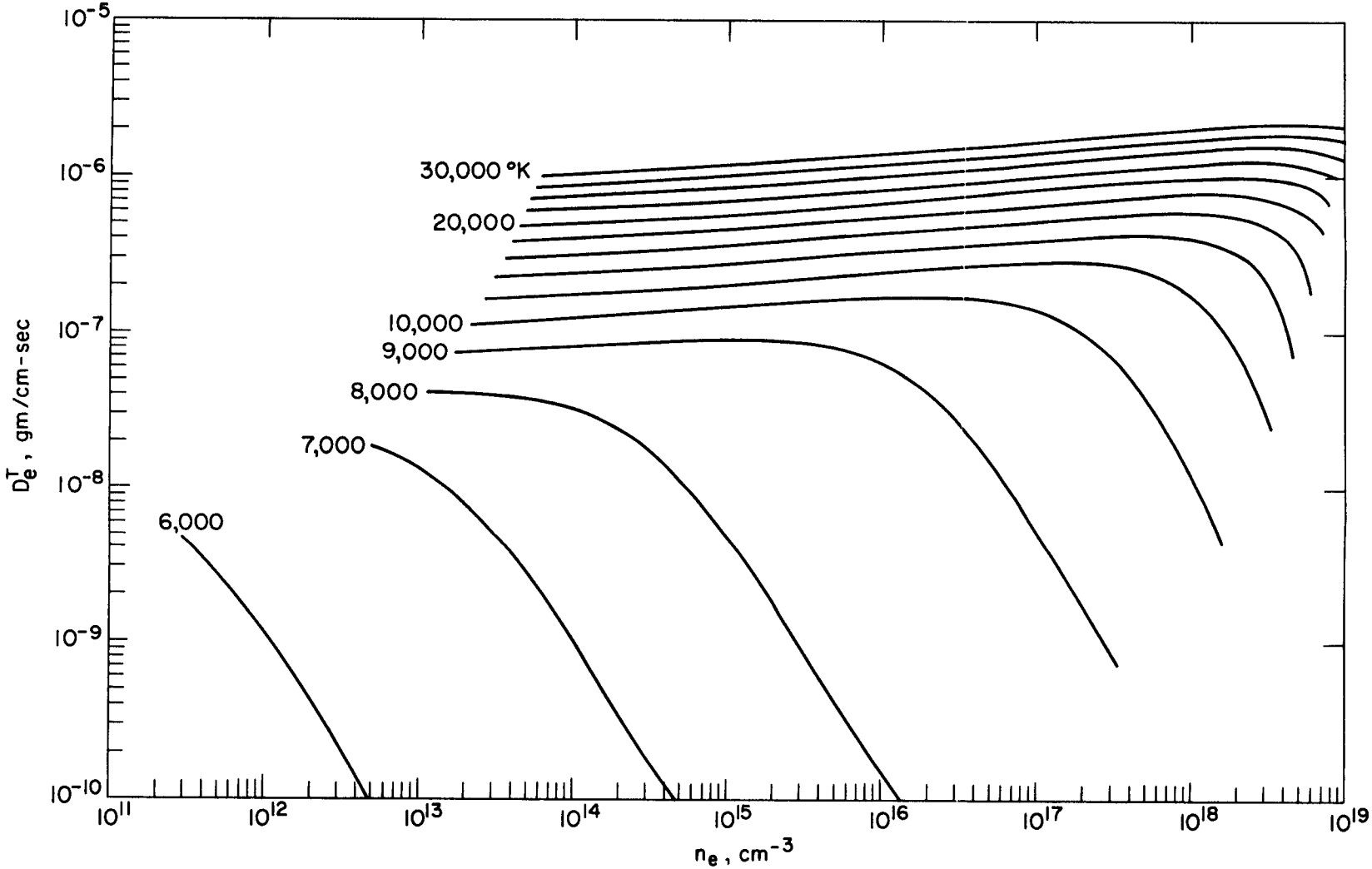

Figure 10.- Electron thermal diffusion coefficients as a function of temperature.

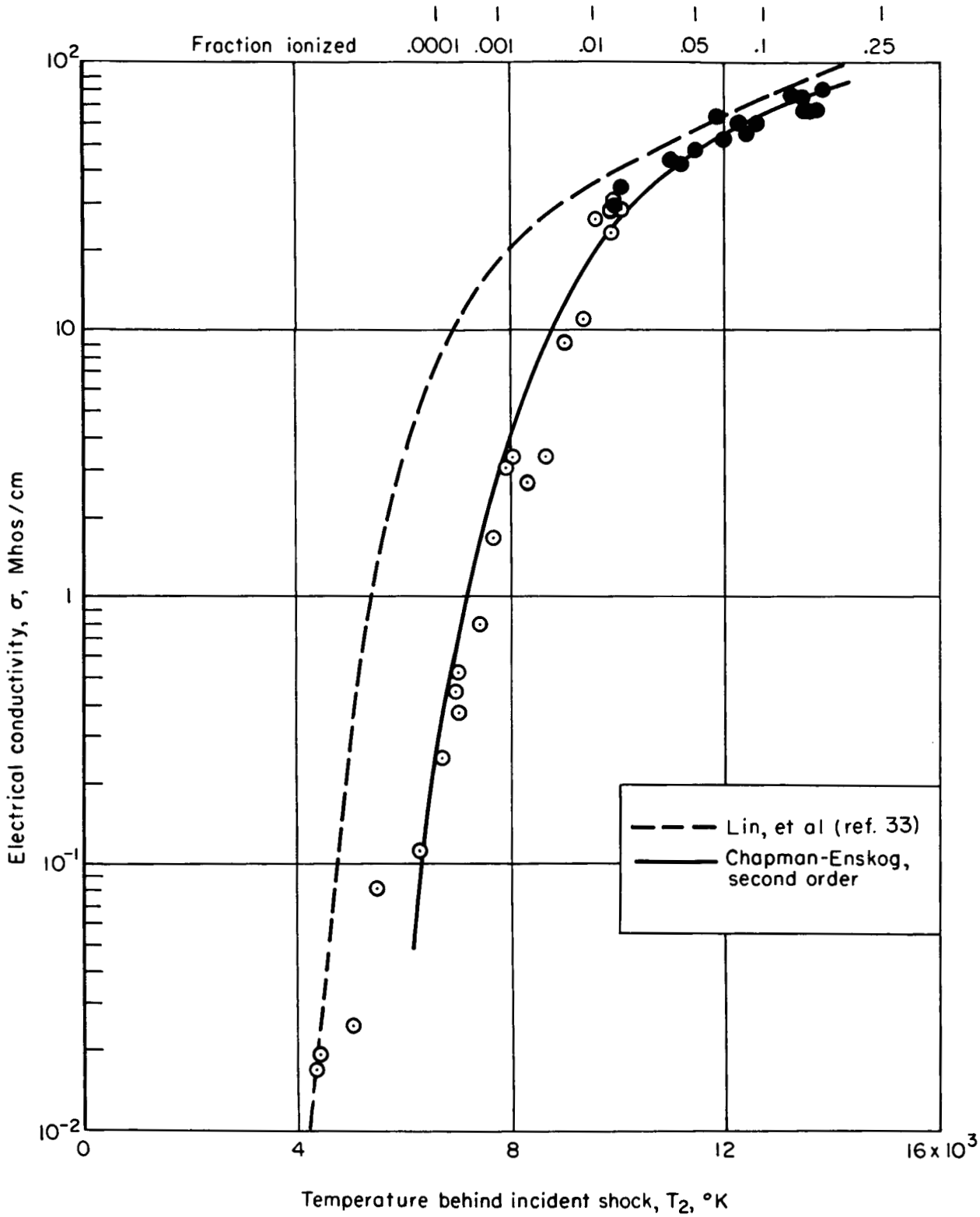

Figure 11.- Comparison of experimental and theoretical electrical conductivities for argon.

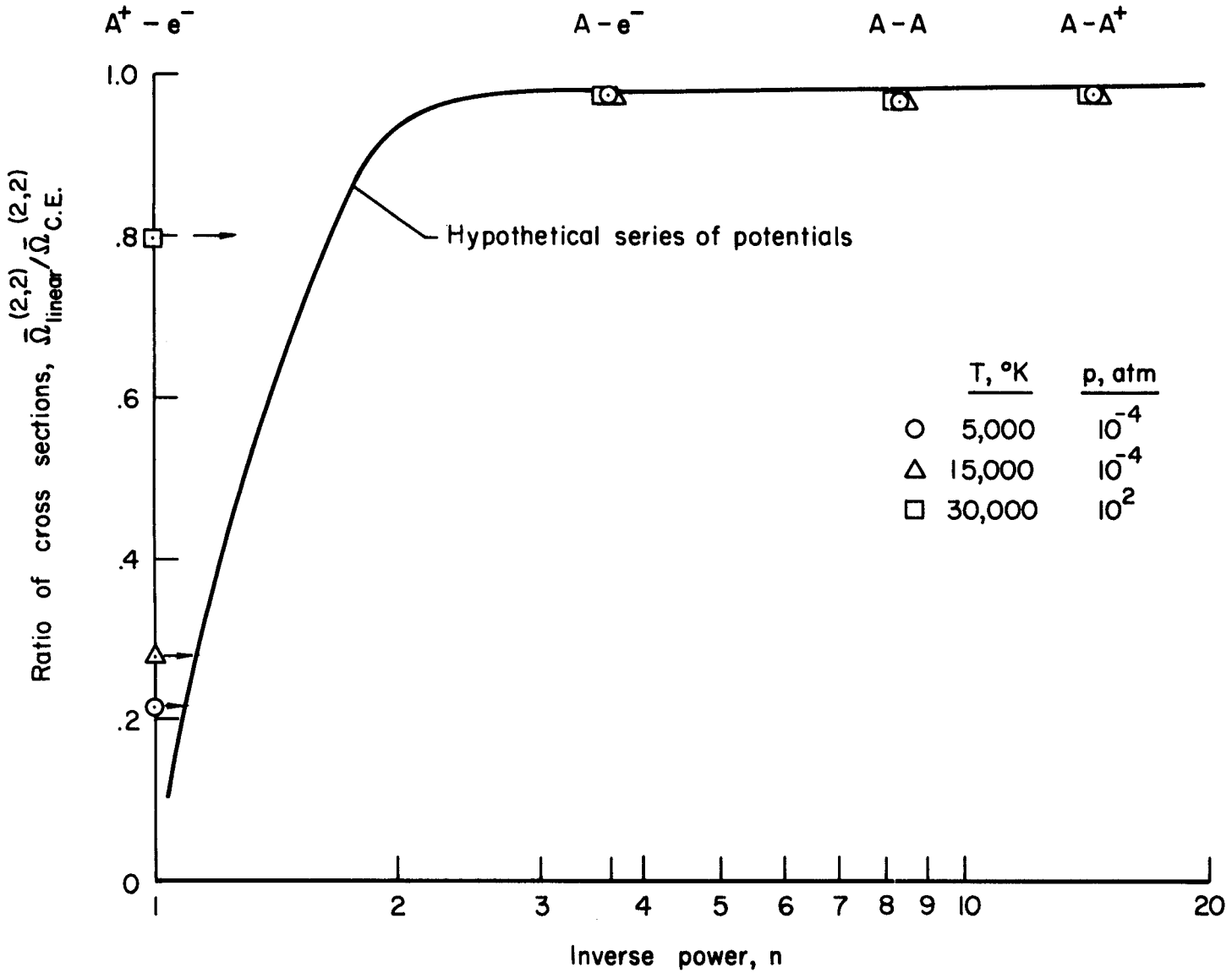

(a) Viscosity cross sections.

Figure 12.- Ratio of cross sections for various inverse power potentials.

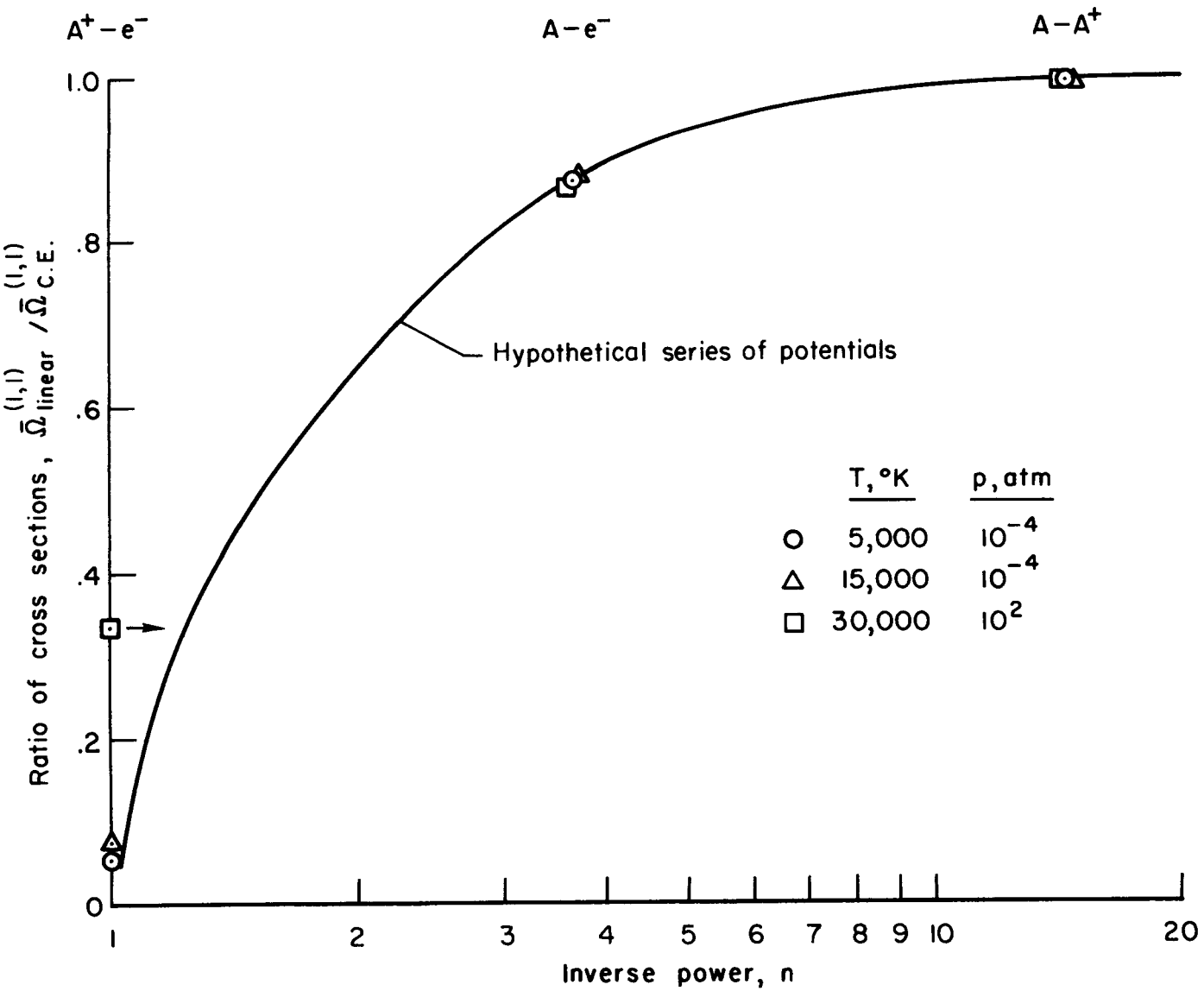

(b) Diffusion cross sections.

Figure 12.- Concluded.

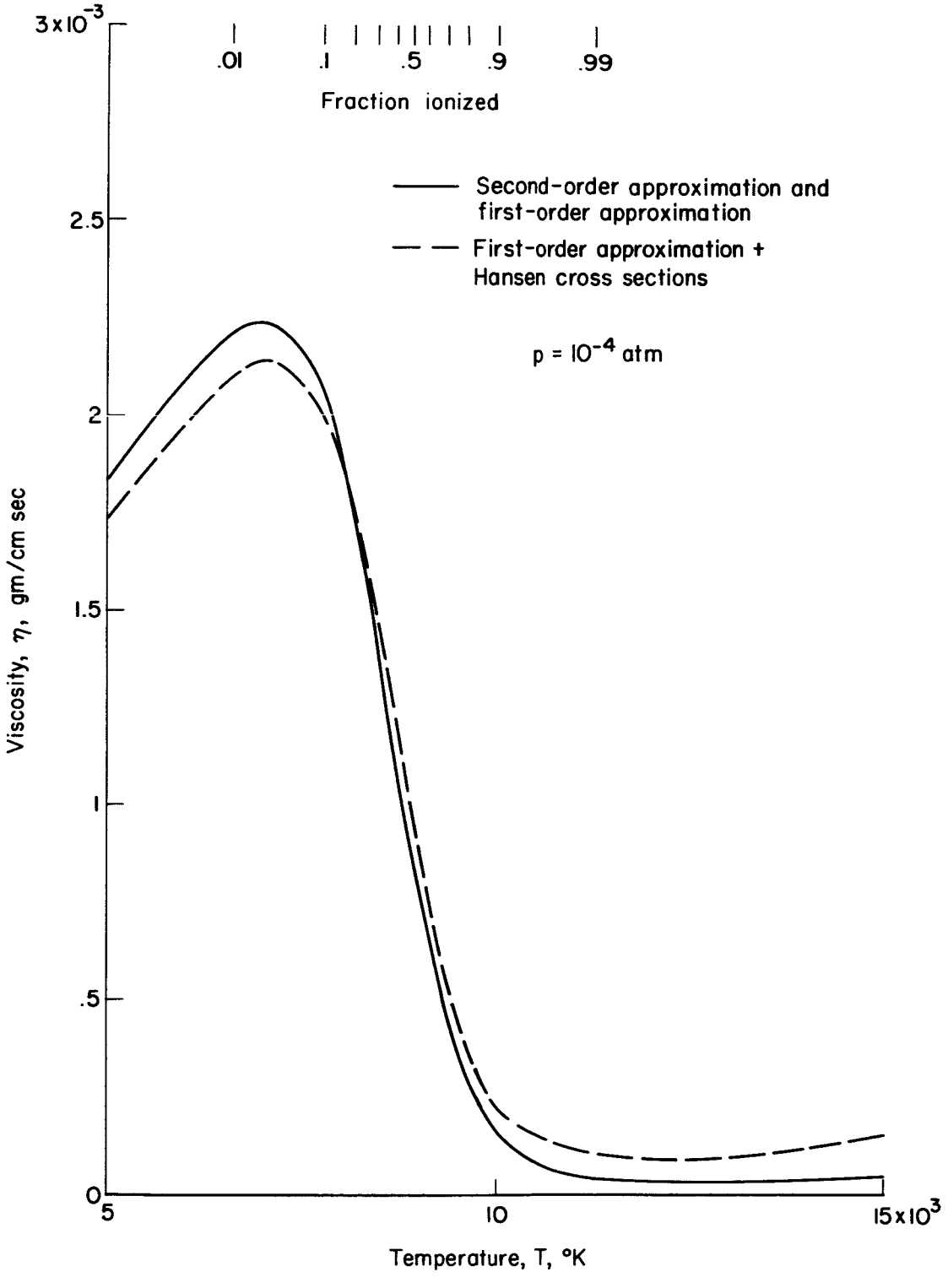

(a) $p = 10^{-4}$ atm

Figure 13.- Comparison of methods for calculating the viscosity.

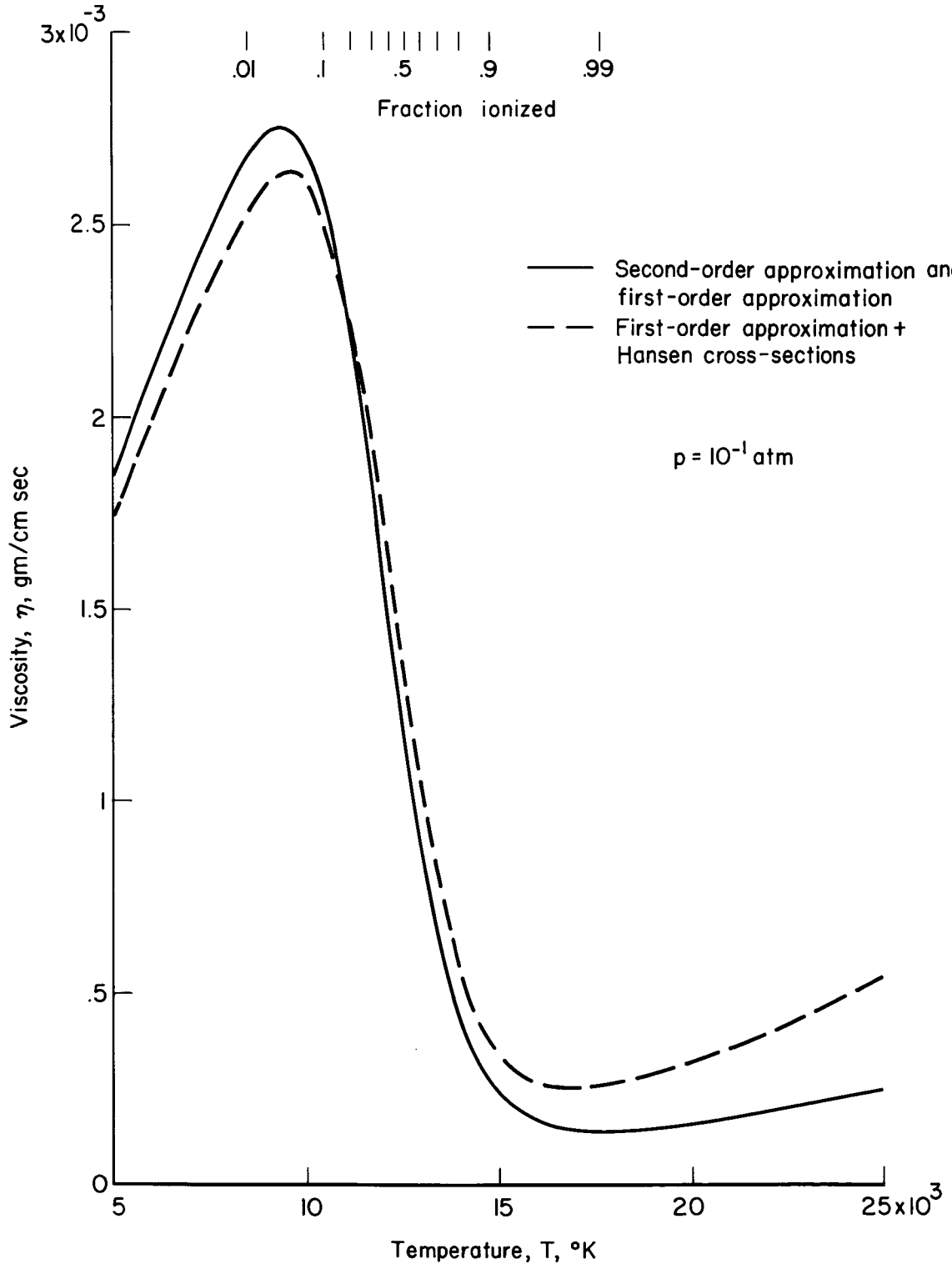

(b) $p = 10^{-1}$ atm

Figure 13.- Continued.

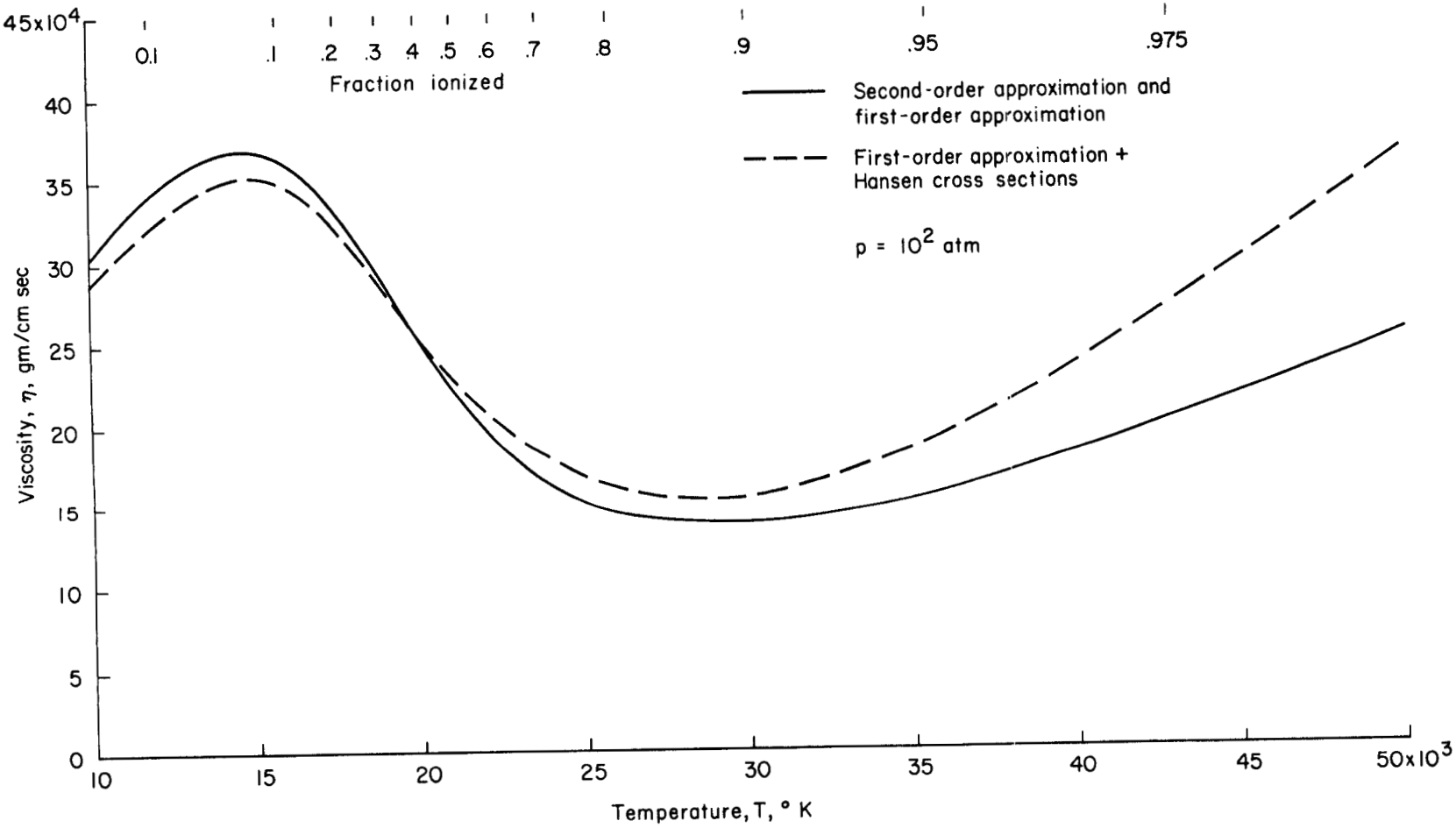

(c) $p = 10^2$ atm

Figure 13.- Concluded.

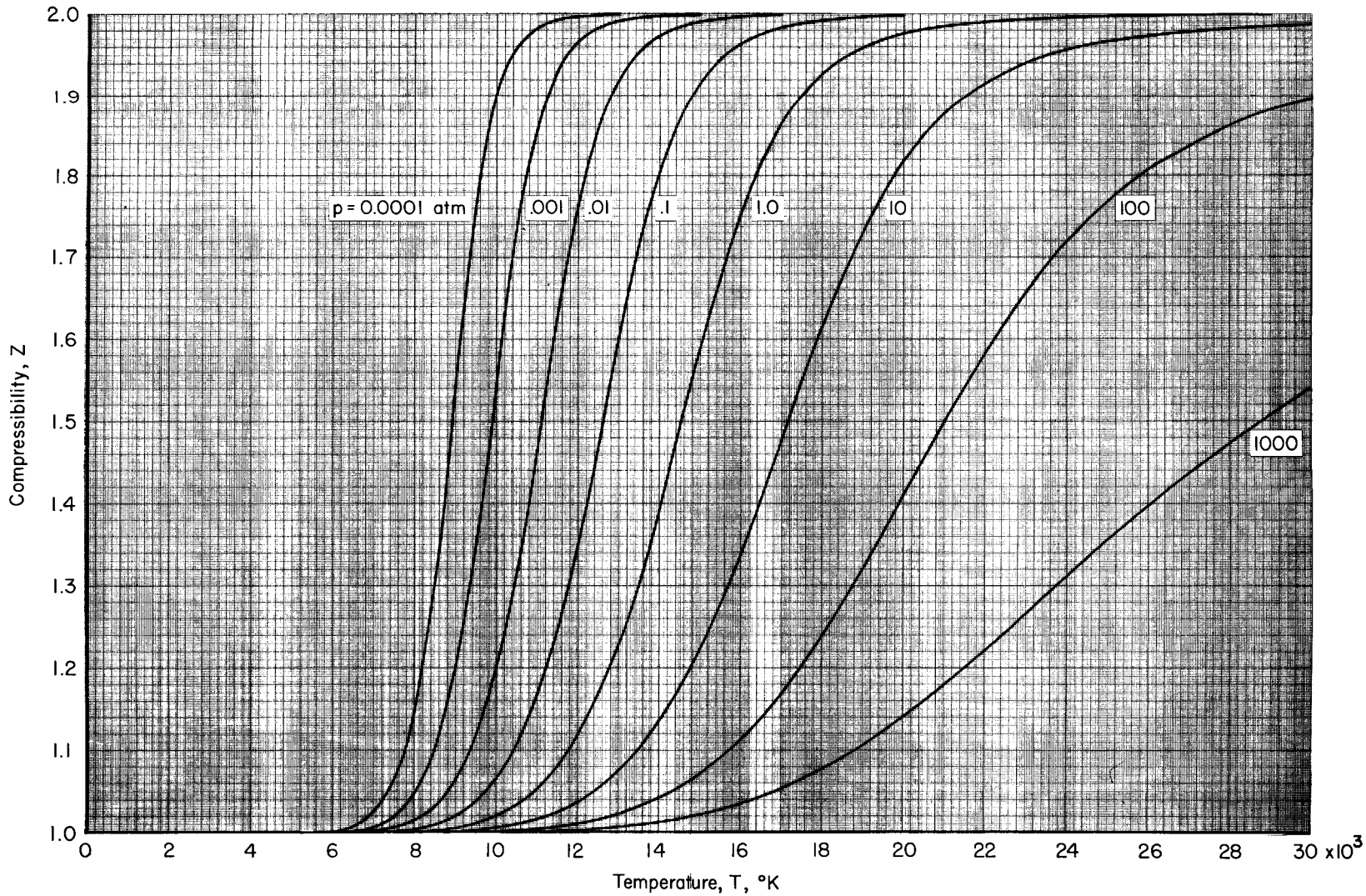

Figure 14.- Compressibility of argon as a function of temperature.

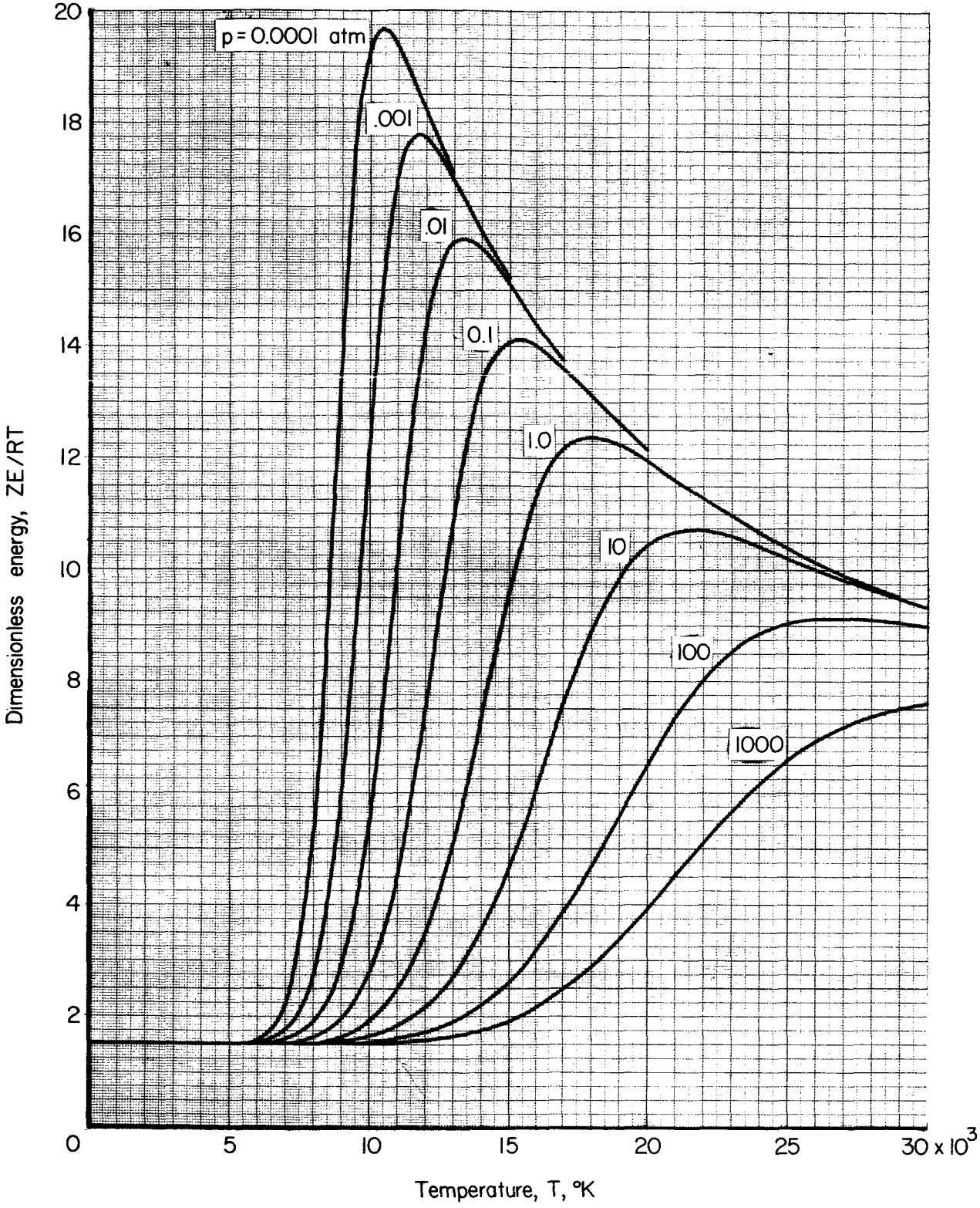

Figure 15.- Energy of argon as a function of temperature.

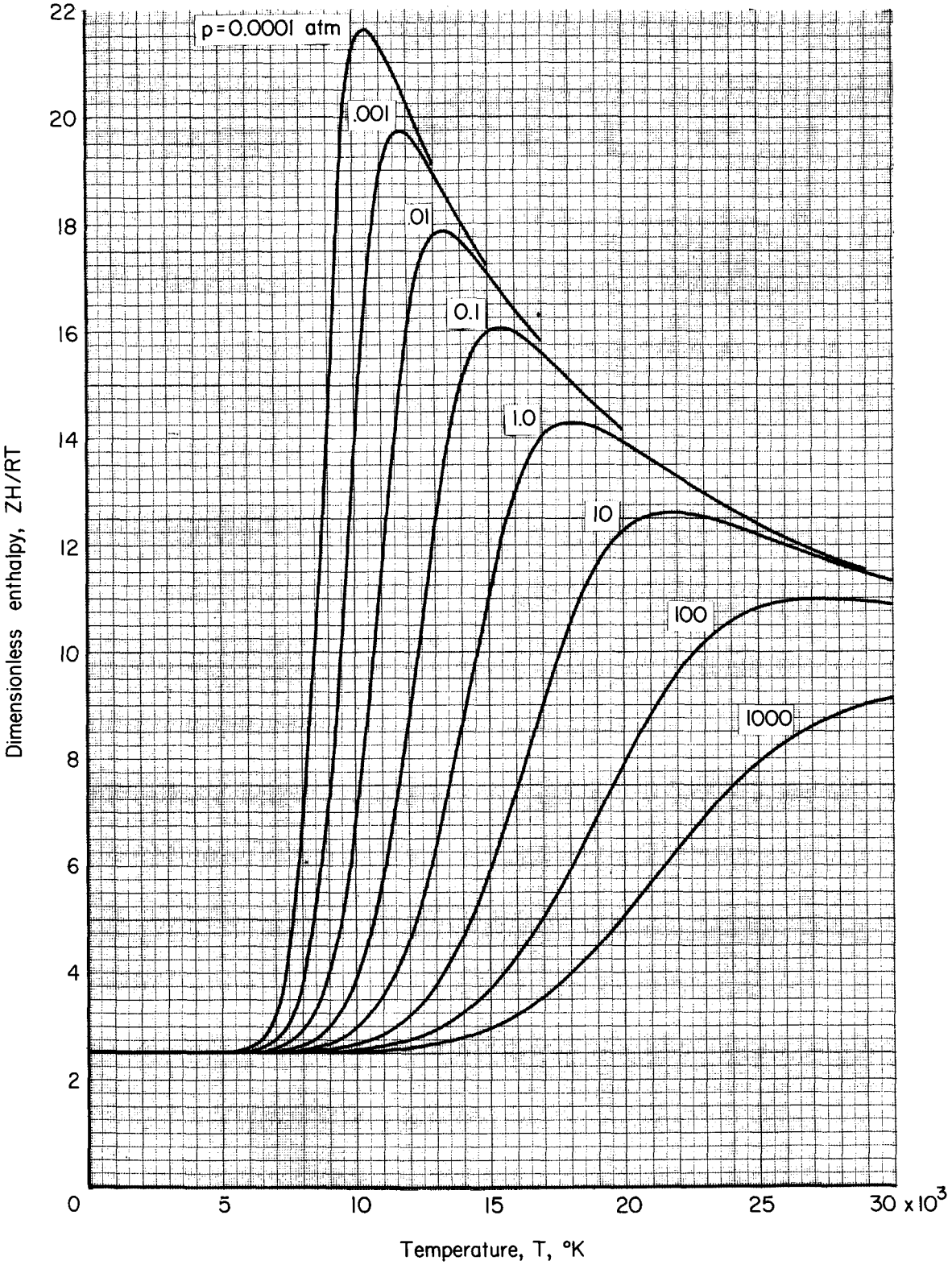

Figure 16.- Enthalpy of argon as a function of temperature.

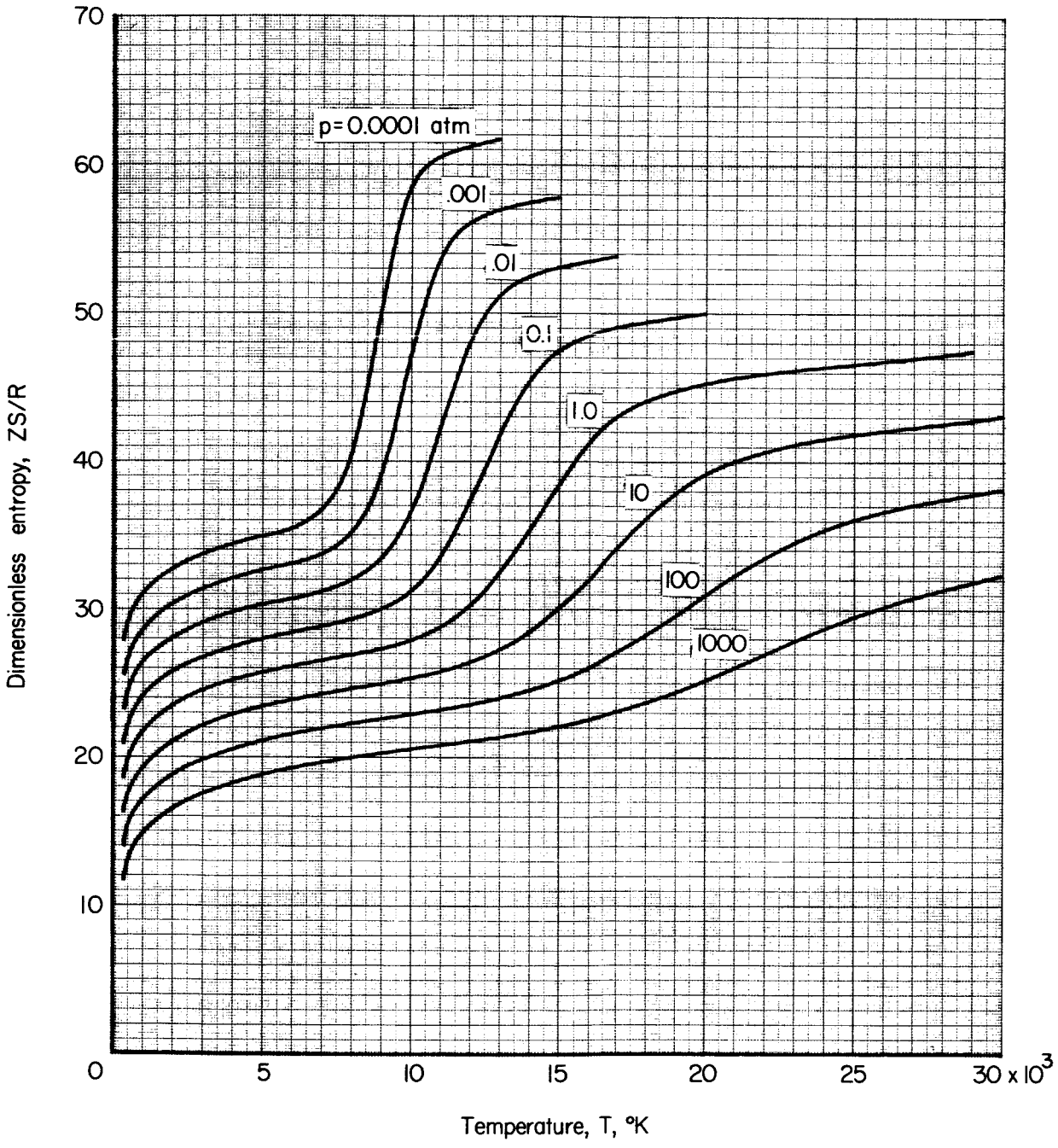

Figure 17.- Entropy of argon as a function of temperature.

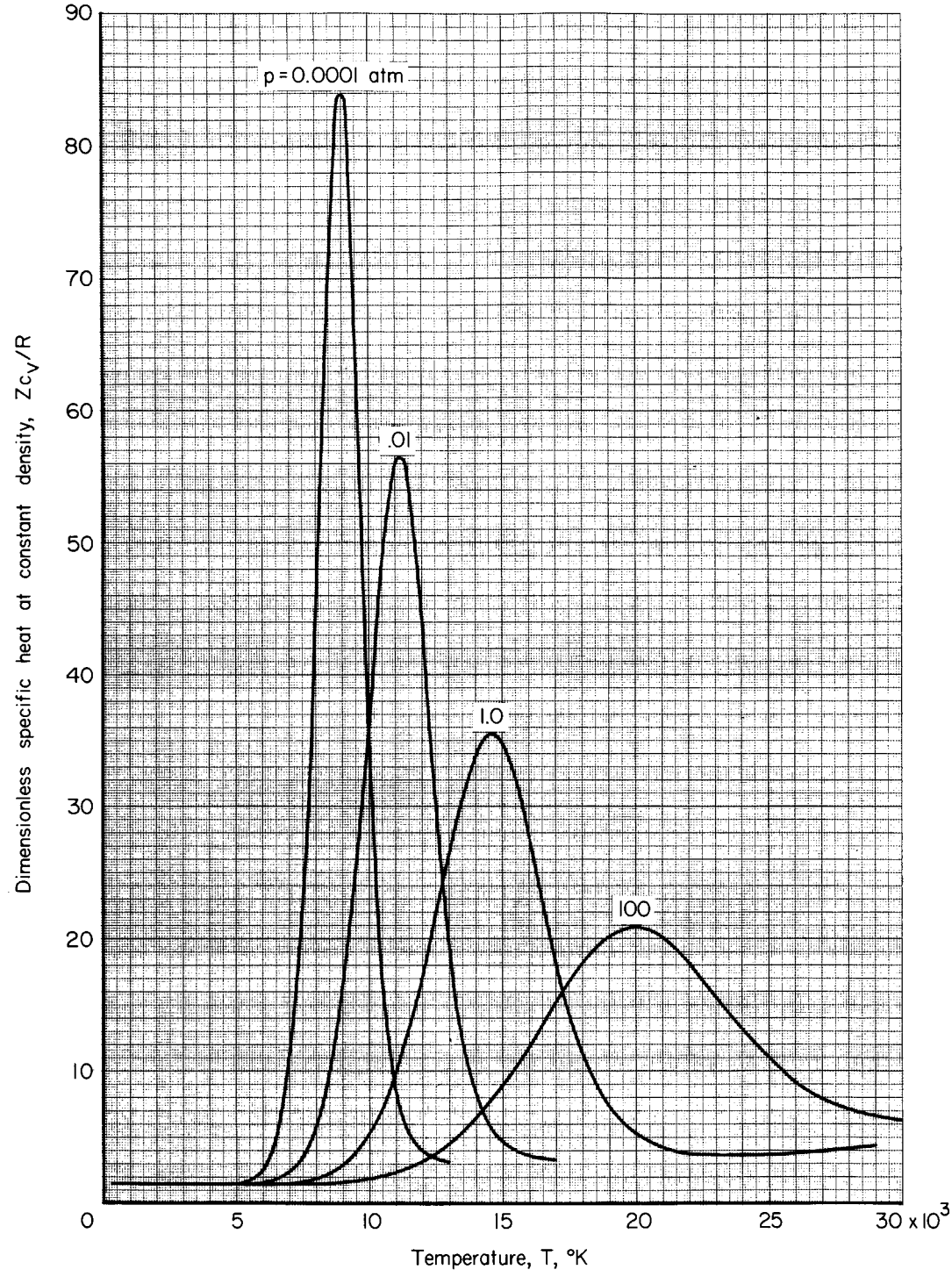

(a) Even powers of pressure.

Figure 18.- Specific heat of argon at constant density as a function of temperature.

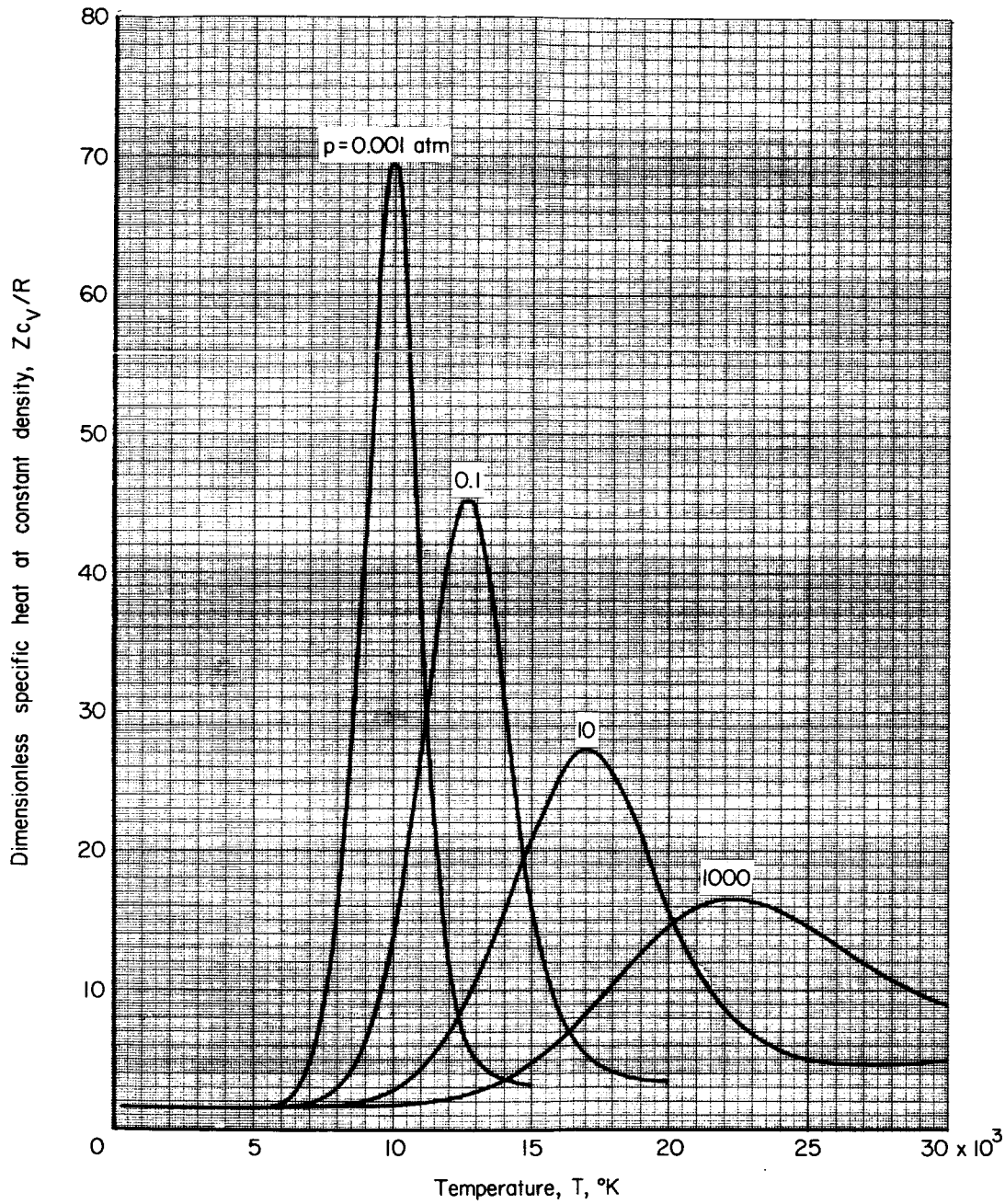

(b) Odd powers of pressure.

Figure 18.- Concluded.

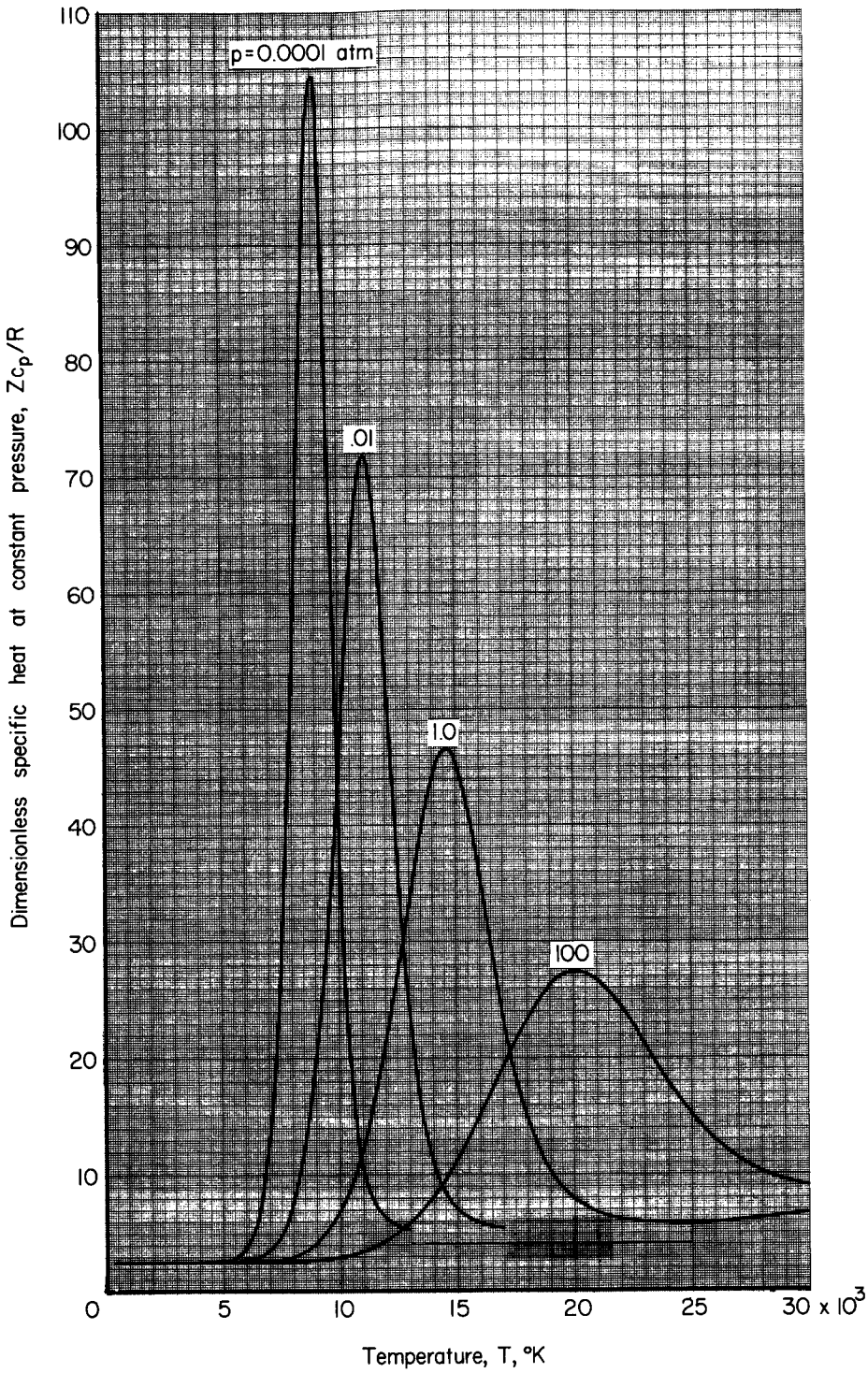

(a) Even powers of pressure.

Figure 19.- Specific heat of argon at constant pressure as a function of temperature.

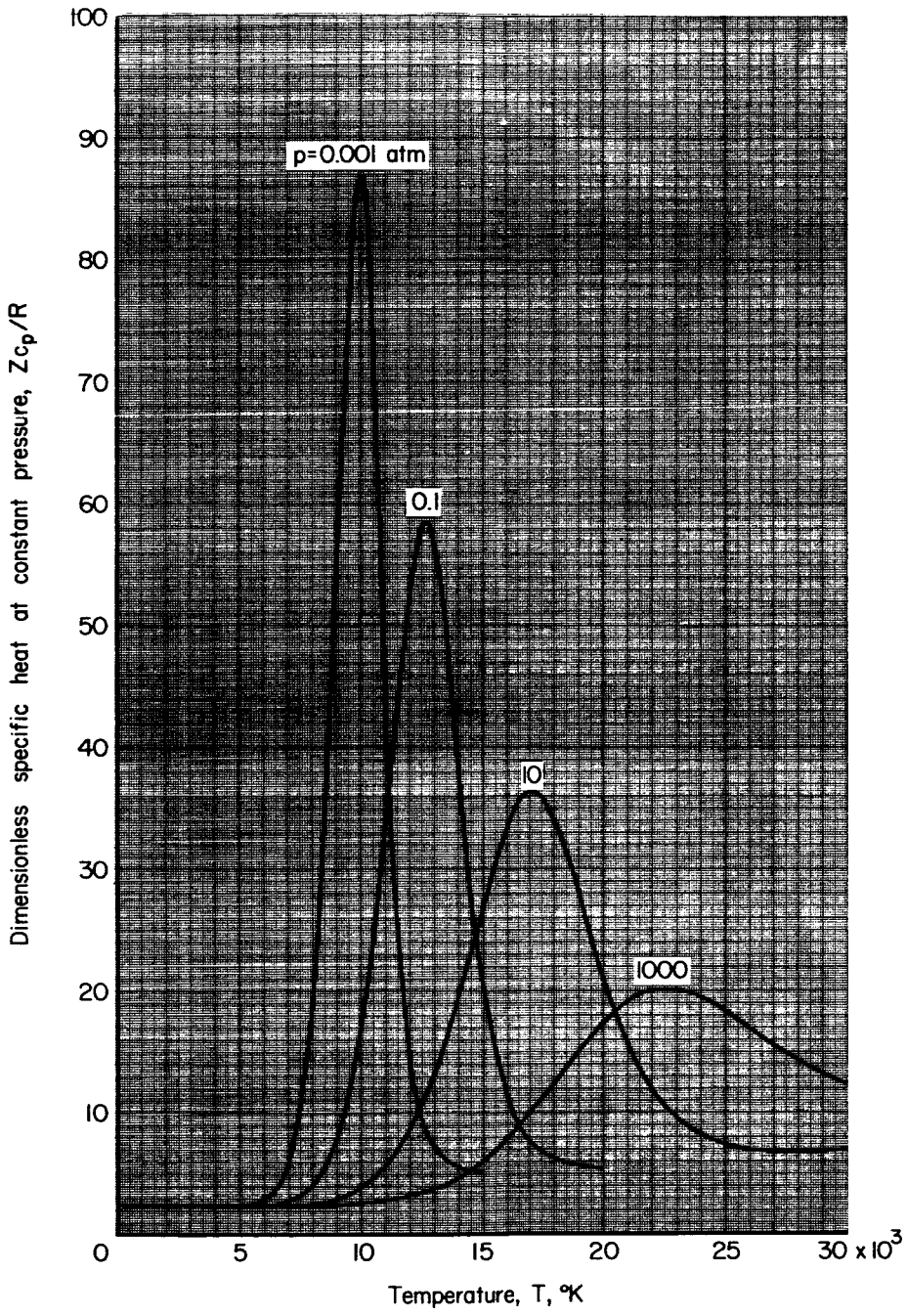

(b) Odd powers of pressure.

Figure 19.- Concluded.

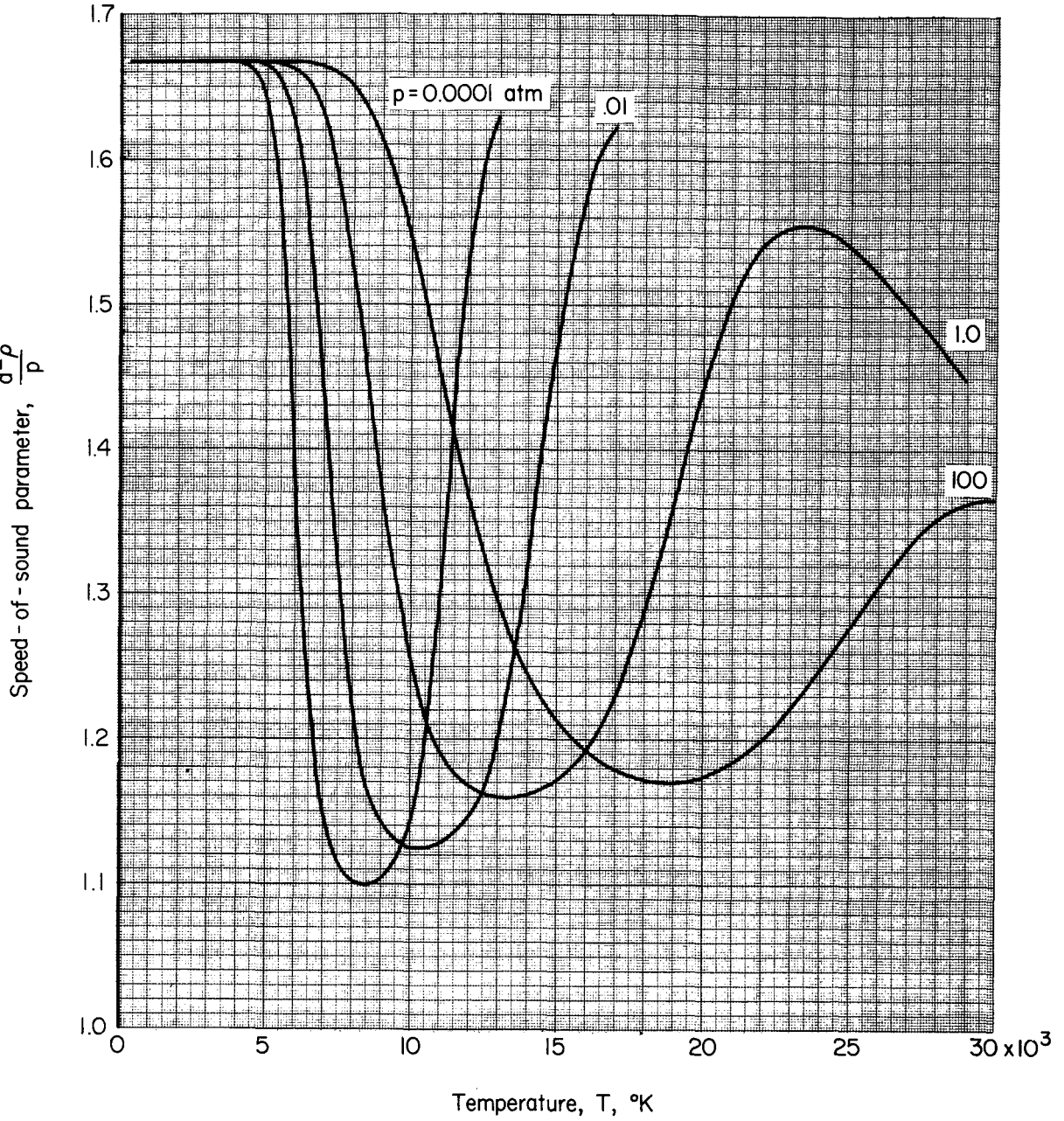

(a) Even powers of pressure.

Figure 20.- Zero frequency speed-of-sound parameter of argon as a function of temperature.

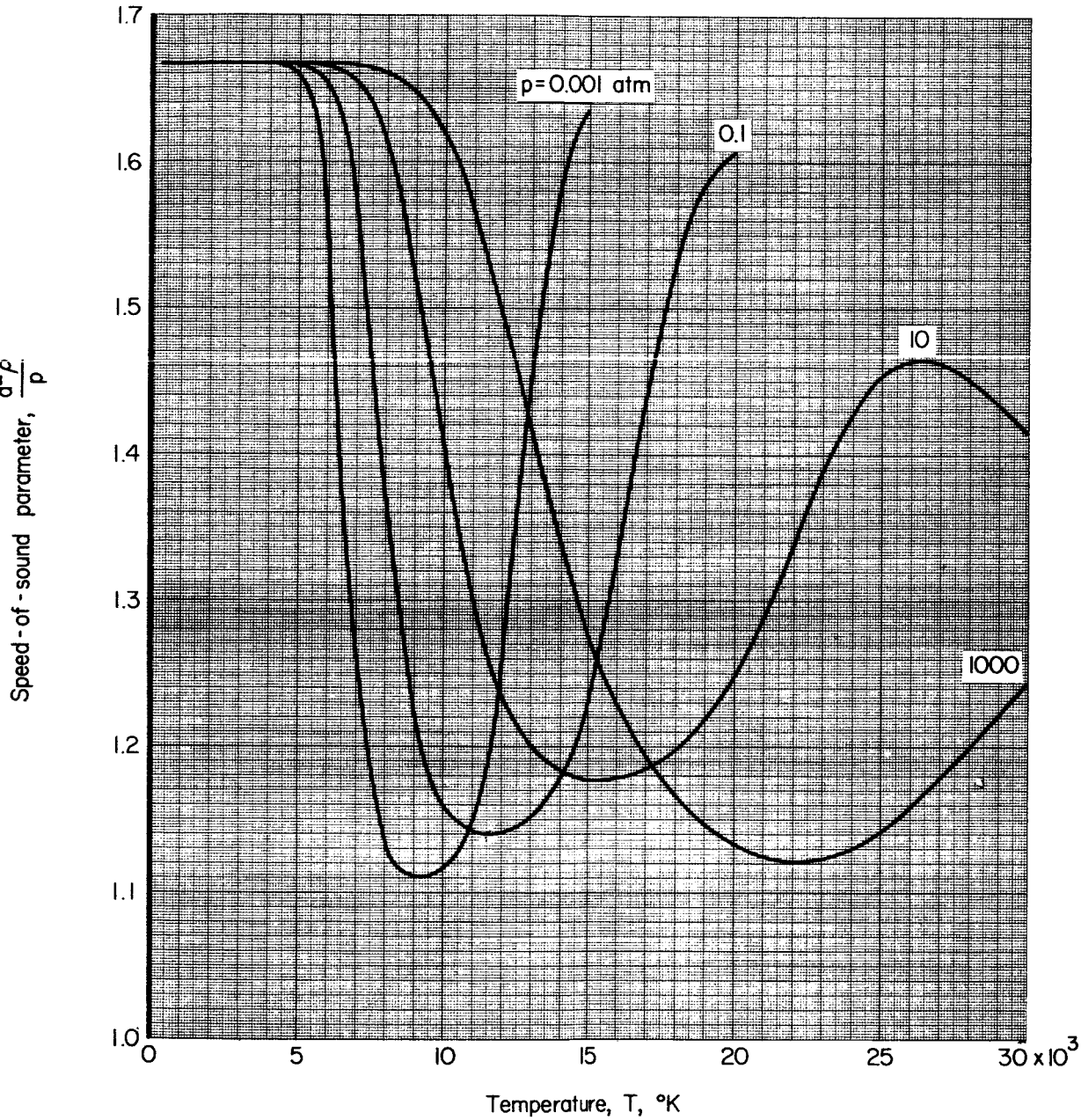

(b) Odd powers of pressure.

Figure 20.- Concluded.

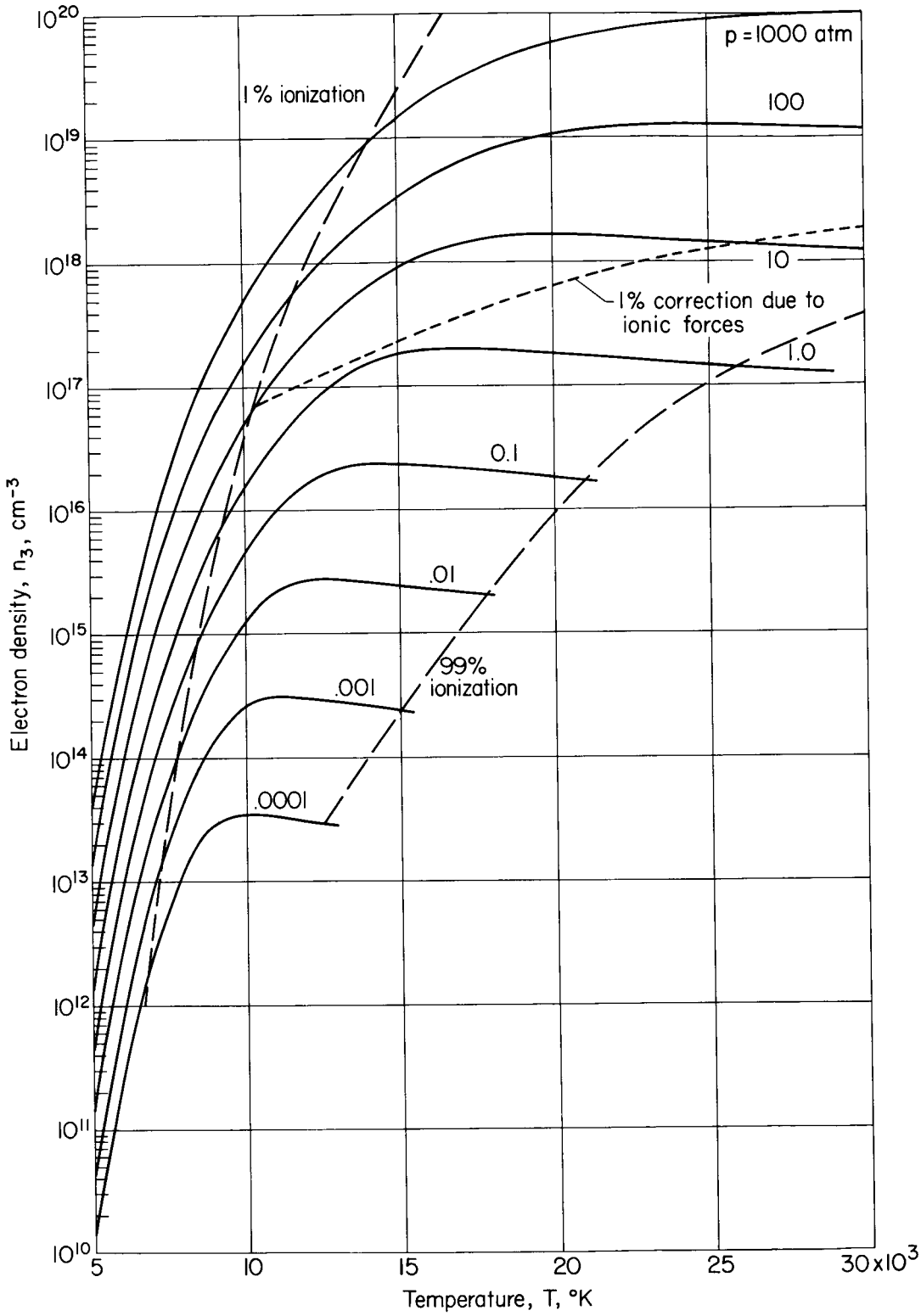

Figure 21.- Real gas corrections in the equation of state.

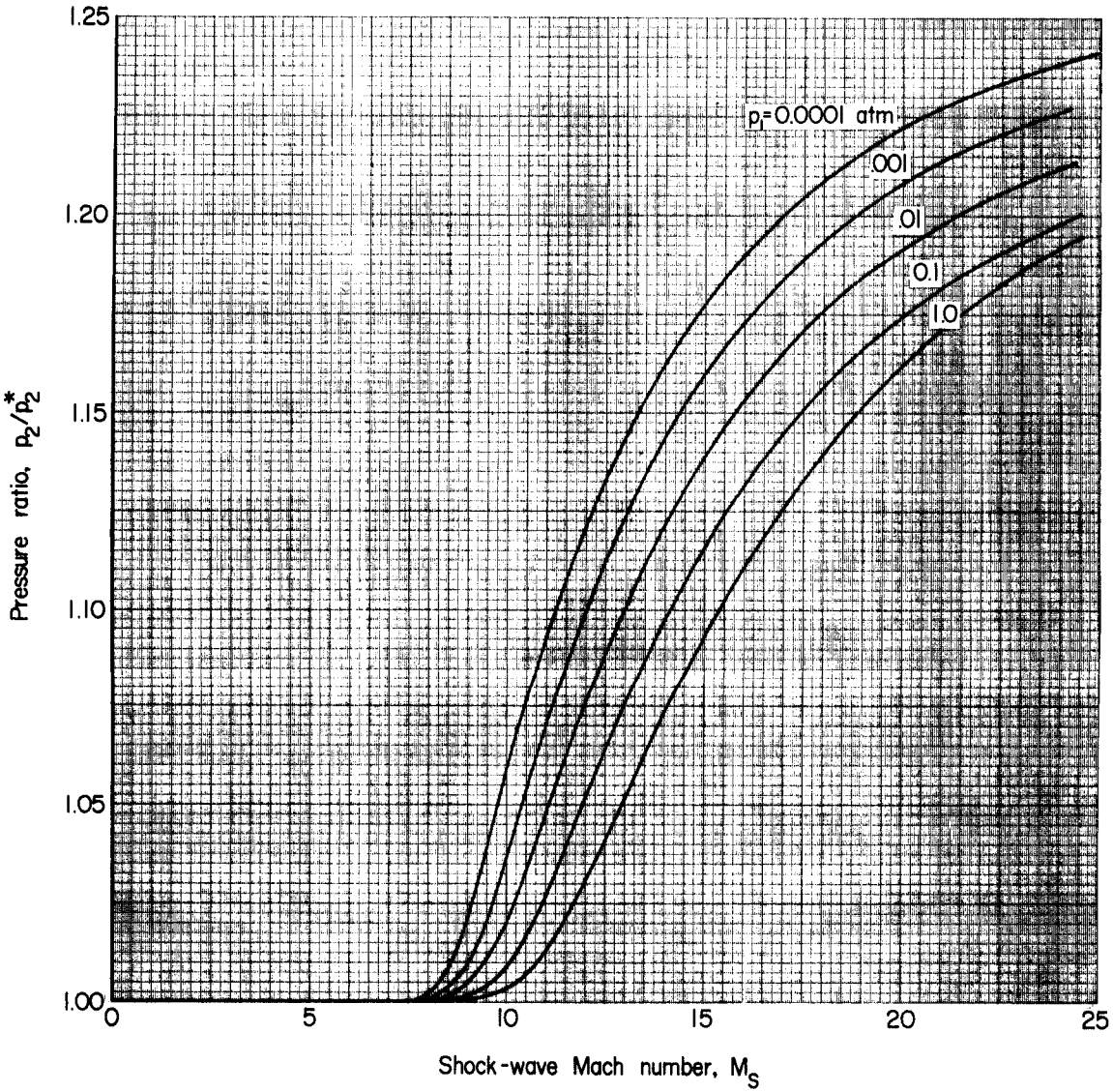

(a) Pressure ratio.

Figure 22.- Equilibrium thermodynamic properties behind incident shock for initial temperature of 293° K.

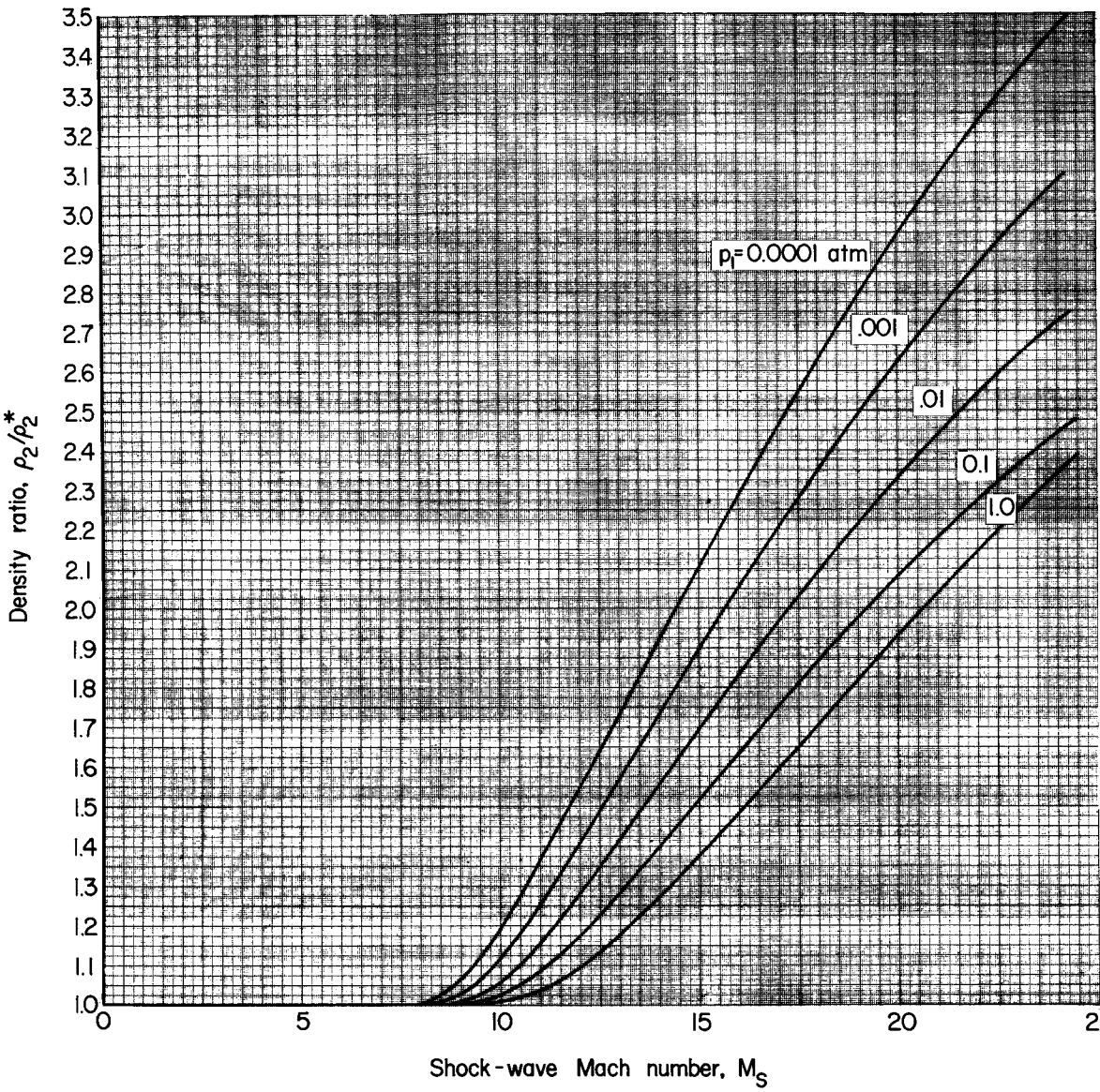

(b) Density ratio.

Figure 22.- Continued.

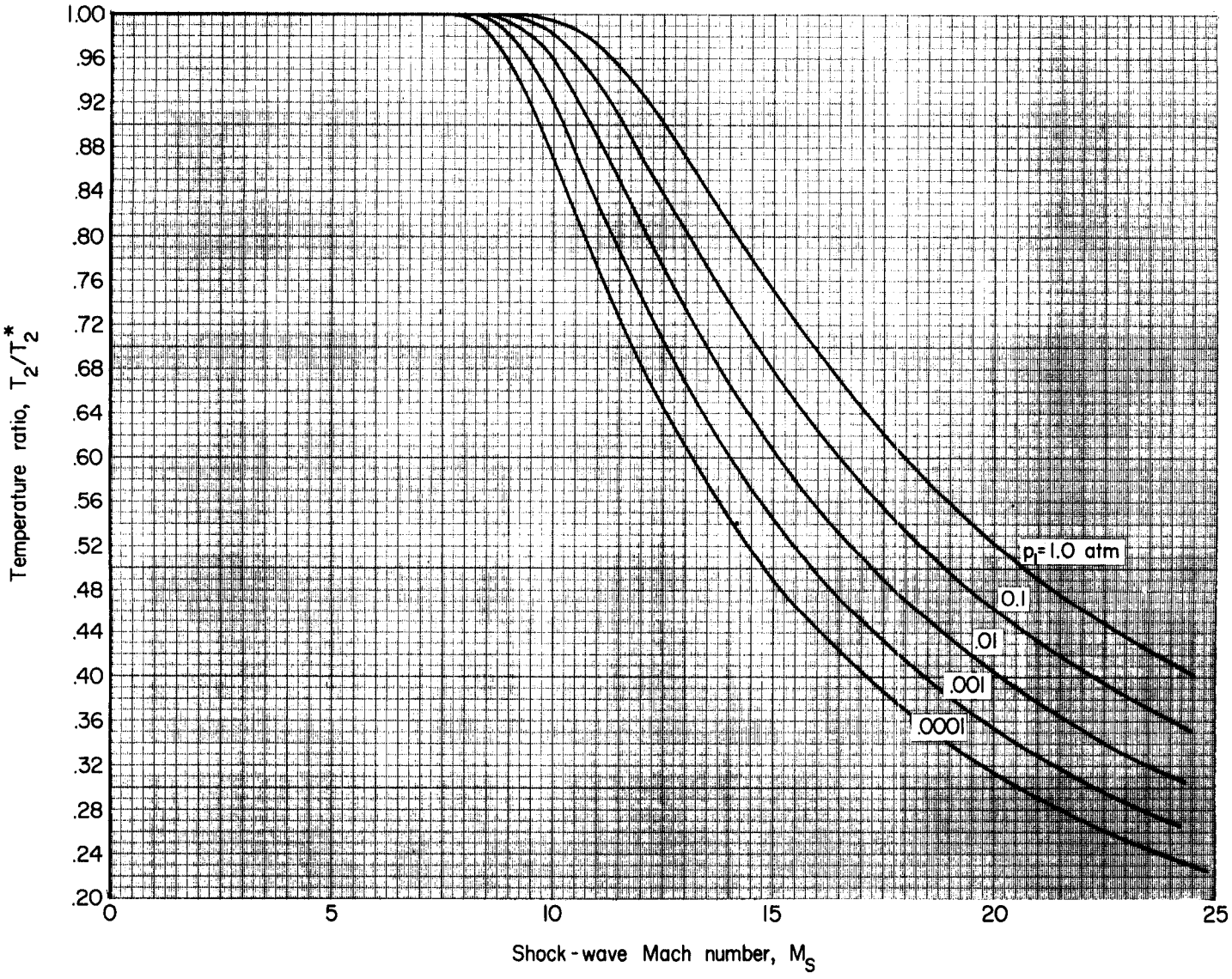

(c) Temperature ratio.

Figure 22.- Continued.

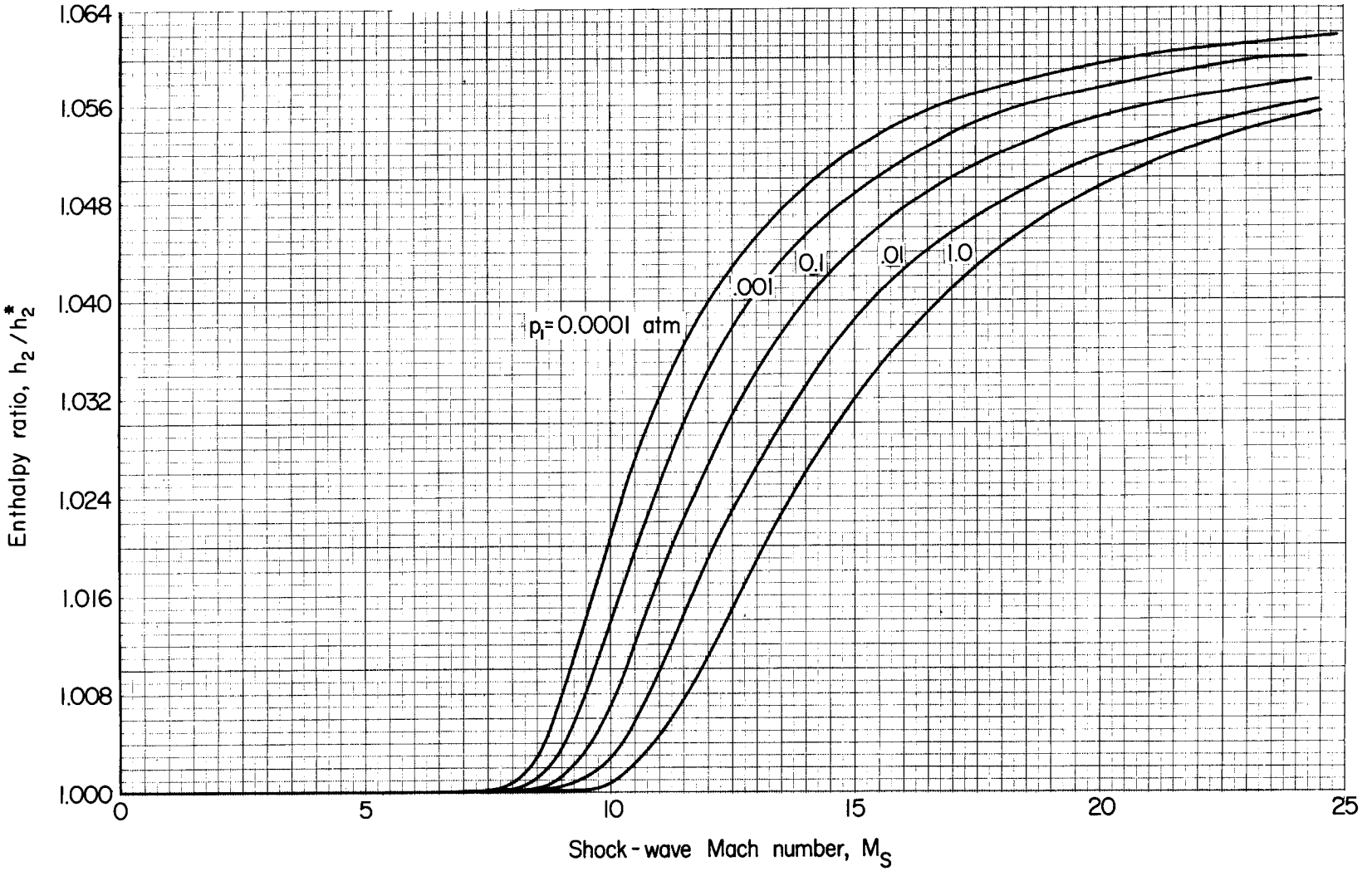

(d) Enthalpy ratio.

Figure 22.- Continued.

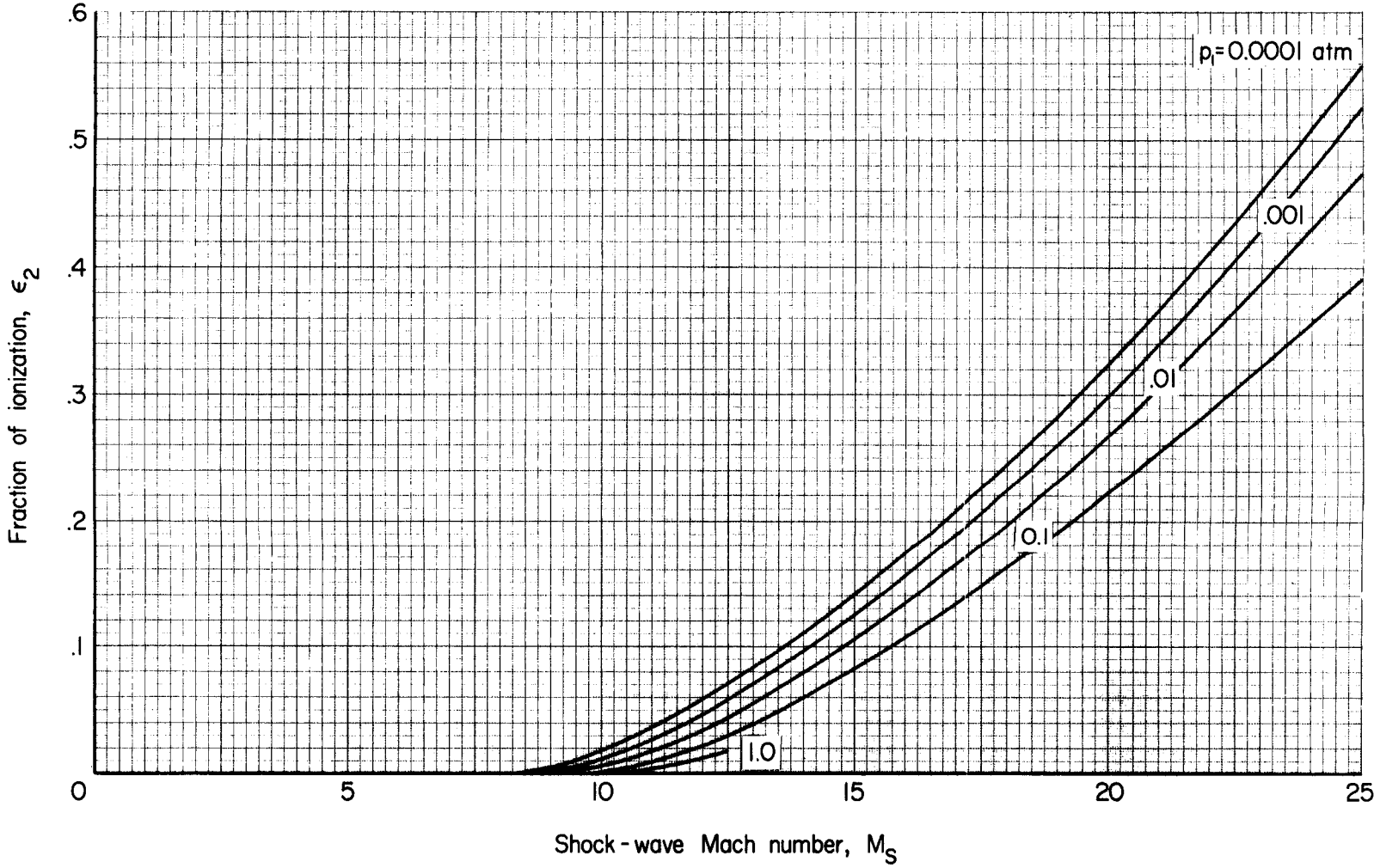

(e) Fraction of ionization.

Figure 22. - Concluded.

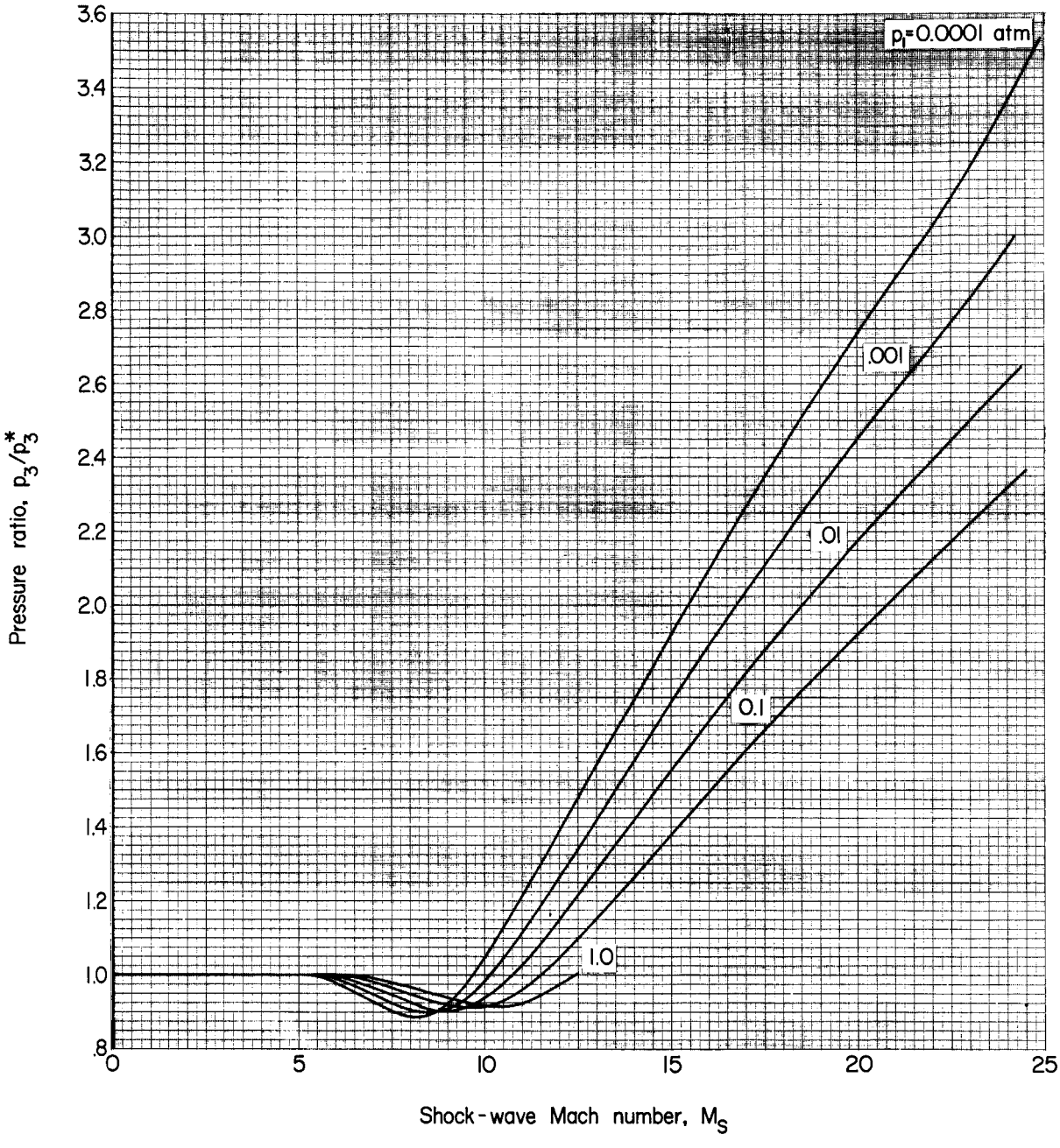

(a) Pressure ratio.

Figure 23.- Equilibrium thermodynamic properties behind reflected shock for initial temperature of 293° K.

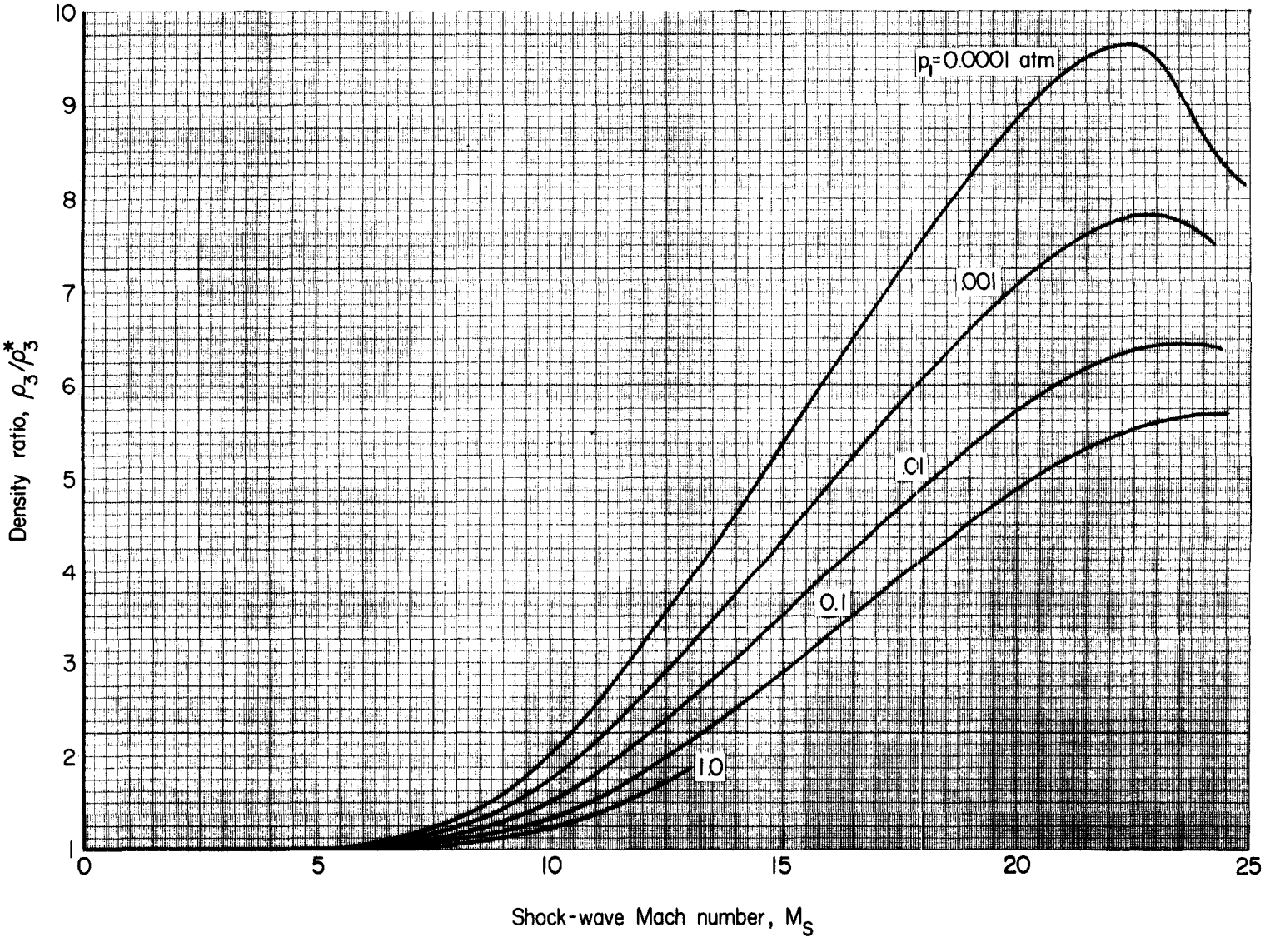

(b) Density ratio.

Figure 23.- Continued.

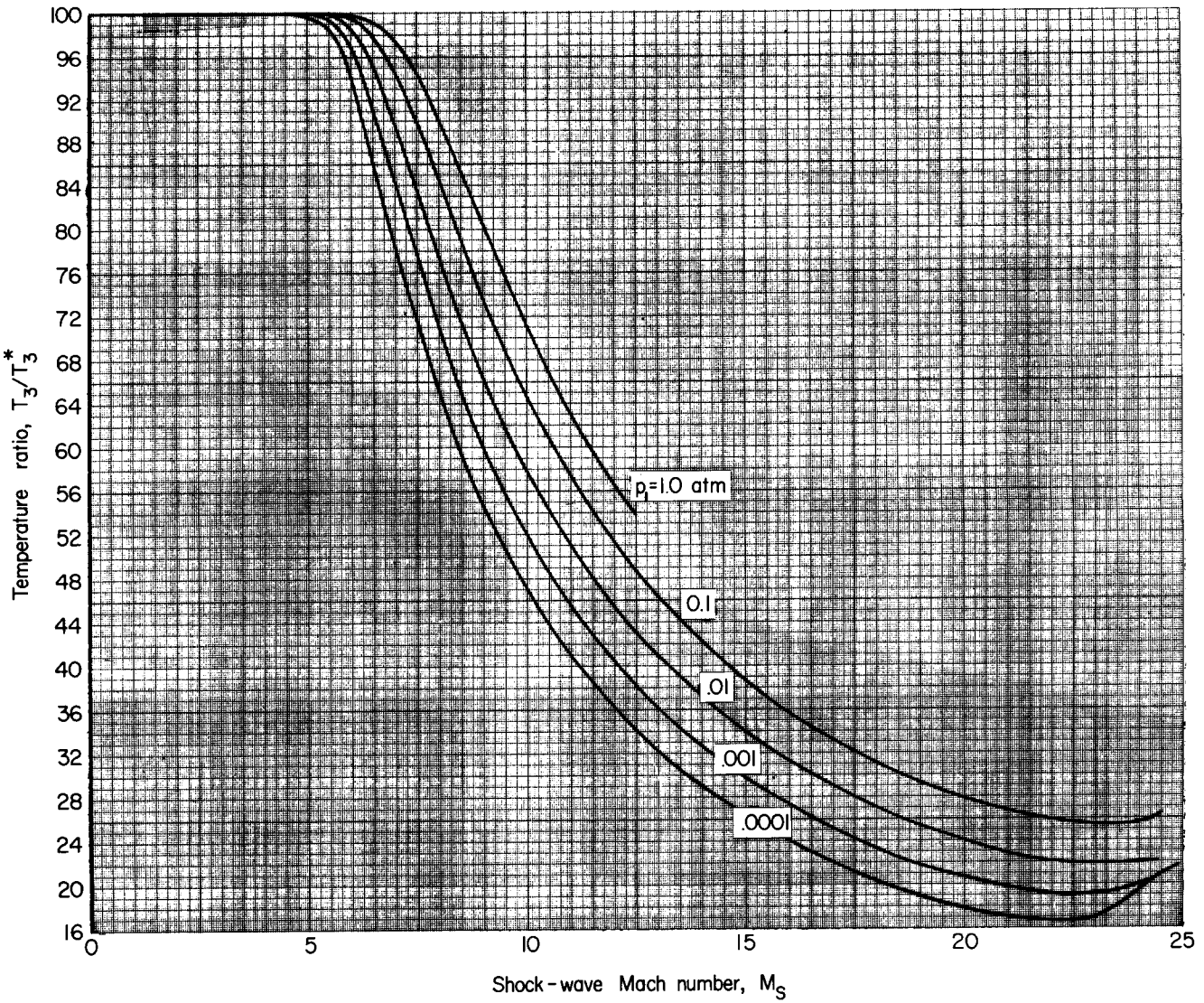

(c) Temperature ratio.

Figure 23.- Continued.

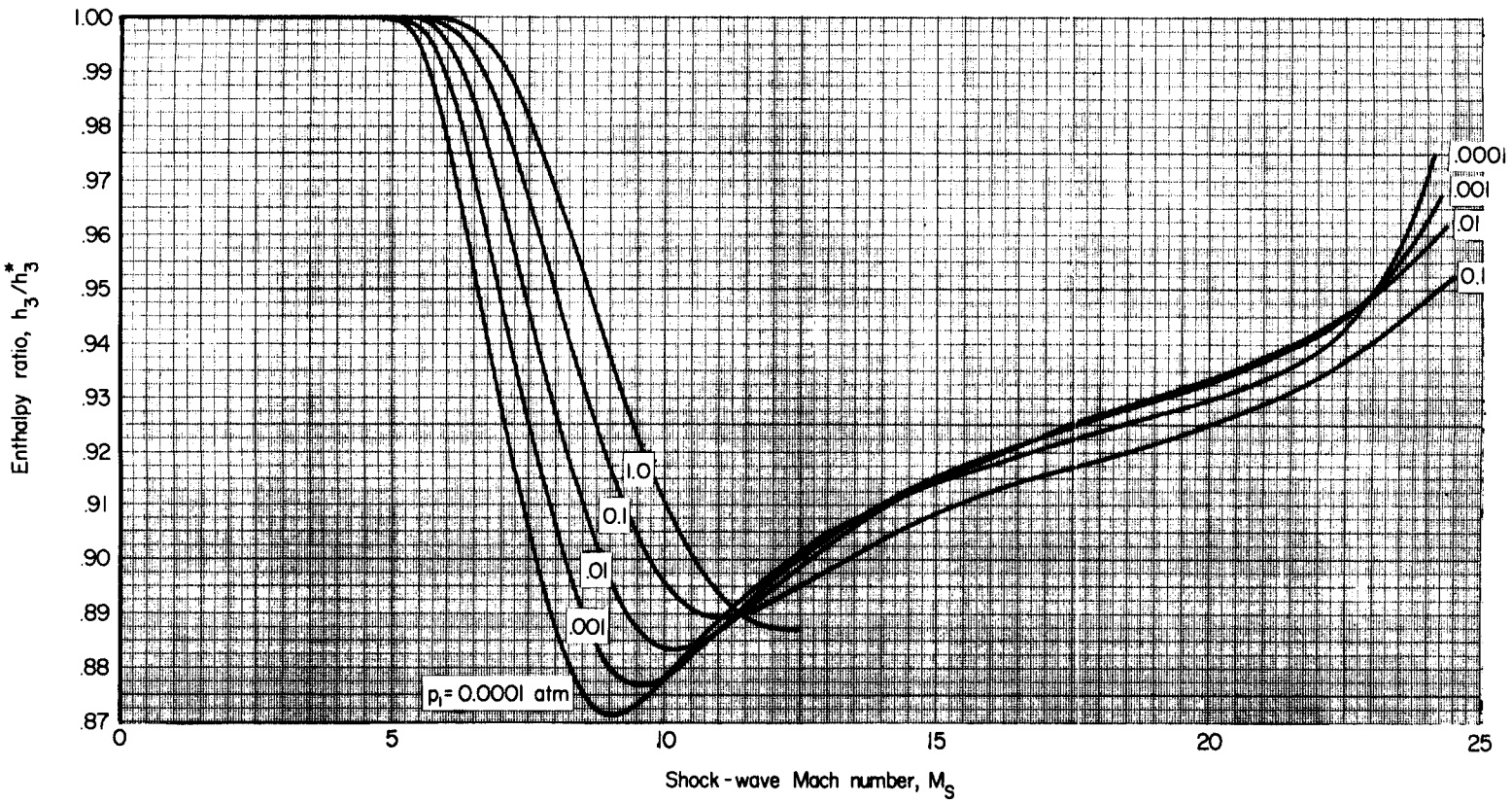

(d) Enthalpy ratio.

Figure 23.- Continued.

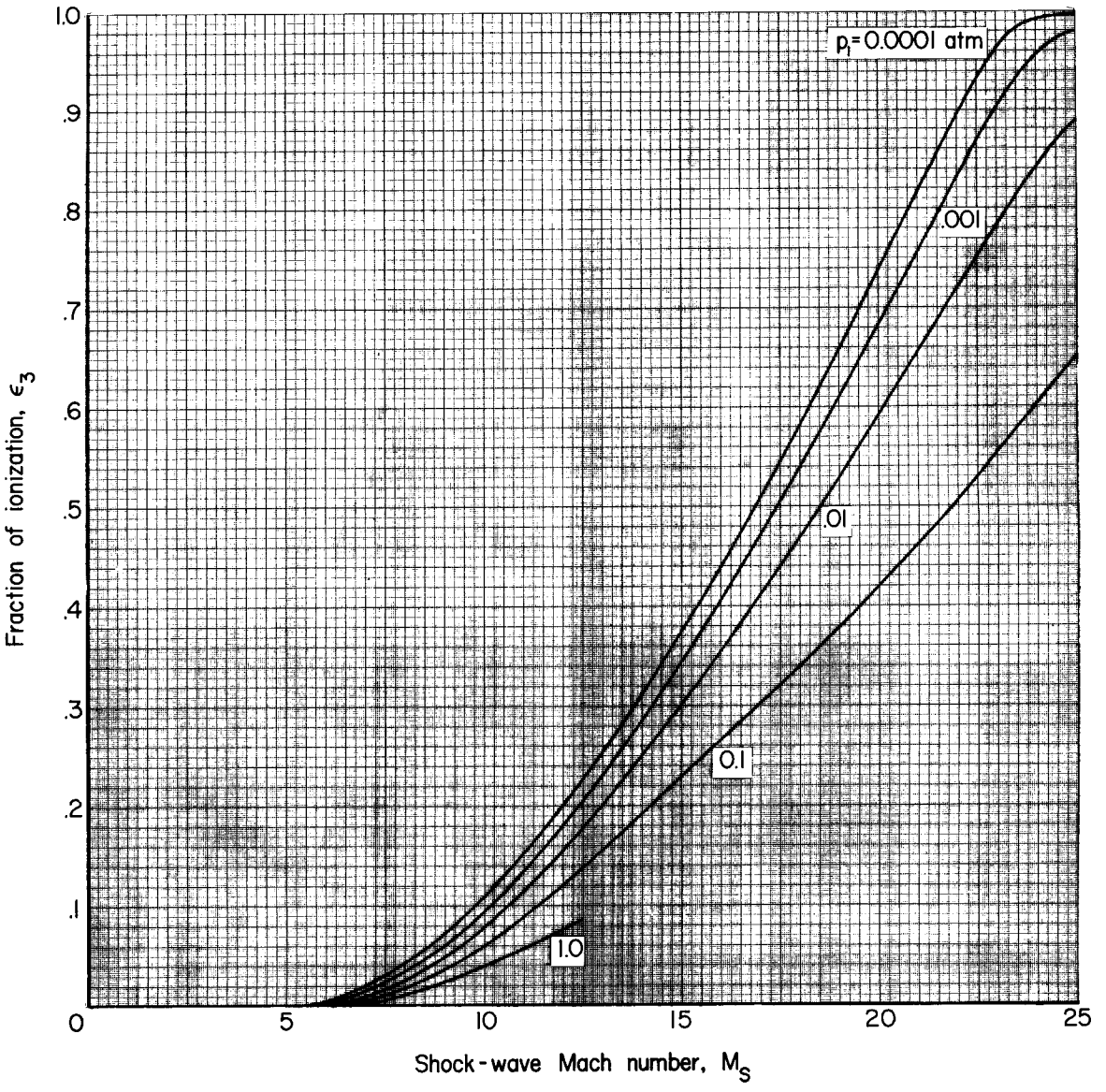

(e) Fraction of ionization.

Figure 23.- Concluded.